Dense Quantum Chromodynamics & Hard Thermal Loops

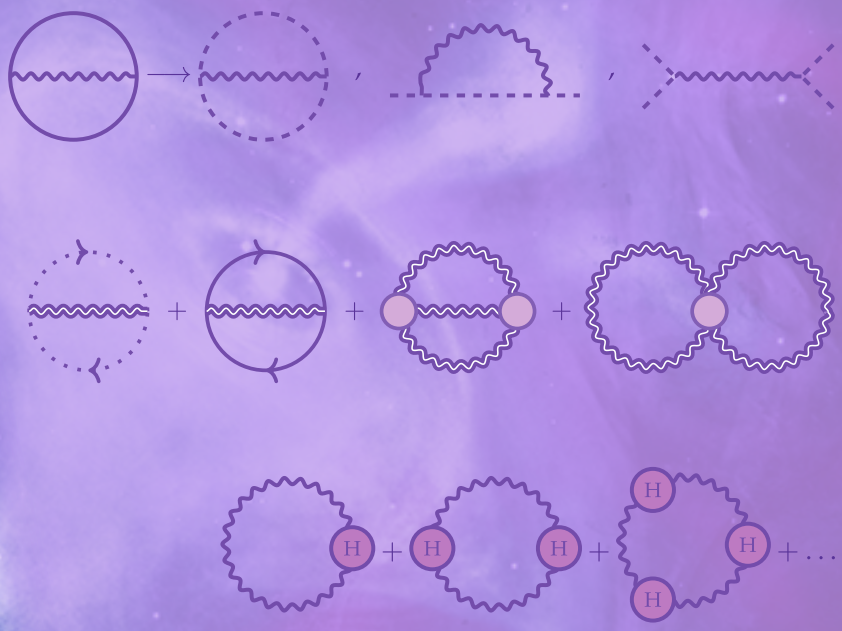

Saga Säppi

Dense Quantum Chromodynamics and Hard Thermal Loops

Saga Säppi

Department of Physics
University of Helsinki
Finland

DOCTORAL DISSERTATION

To be presented for public discussion with the permission of the Faculty of Science of the University of Helsinki, in Auditorium D101, Physicum, on the 6th of October, 2020 at 10 o'clock.

Helsinki 2020

ISBN 978-951-51-6521-3 (print)
ISBN 978-951-51-6522-0 (online)
http://ethesis.helsinki.fi
Unigrafia
Helsinki 2020

Abstract

This Thesis covers research conducted at the University of Helsinki in the field of thermal field theory, a framework for describing quantum fields in a medium, in particular at finite temperature and chemical potential. In the included Publications, there is a strong emphasis on describing field theories in a dense medium, at large chemical potentials, as well as on thermal resummation methods.

The central focus and inspiration for the research is the study of elementary particle physics, in the realm of relativistic quantum fields. Specific motivations include the desire to better understand the behaviour of dense, strongly interacting matter possibly present in the cores of neutron stars, push forward high-order perturbative calculations in thermal field theory, as well as to gain some analytic insight on nonperturbative physics by studying a simple low-dimensional model.

The main results emerging from the research carried out for this Thesis include a method for reducing zero-temperature finite-density Feynman loop integrals into a sum of vacuum integrals and its proof, the determination of a new high-order contribution to the weak-coupling perturbative expansion of the pressure of cold and dense Quantum Chromodynamics, as well as a study of a three-dimensional thermal quantum field theory using a novel nonperturbative method. The research also paved the way for future determination of the full next-to-next-to-next-to leading order pressure, which is currently well under way. All of this research was theoretical, and involved primarily analytic and in some cases numerical calculation methods.

In addition to peer-reviewed Publications, the Thesis contains an Introduction that builds the foundation of some key concepts — gauge theory and eventually Quantum Chromodynamics as well as thermal field theory, in particular in the imaginary-time formalism — required for understanding the included research. It also includes a more focussed Chapter on Quantum Chromodynamics at finite density, also covering Hard Thermal Loop theory.

Acknowledgements

As my years of studying at the University of Helsinki are nearing their end, I want to thank those that have made it such an enjoyable time.

First, of course, are my supervisors, the two Aleksis. Aleksi V. has been my 'local supervisor' for the past four and a half years and always had time for questions and has been incredibly helpful in immeasurably many ways, while Aleksi K. has helped me gain so much physical insight during our conversations, in particular during my two visits to CERN.

The rest of my collaborators also deserve many thanks: In addition to Ioan, Tyler, and Paul, who are co-authors in the papers included in this Thesis and whom I have greatly enjoyed collaborating with, I want to add Risto — our paper did not quite make it into the thesis, but I am confident it will be out soon! I also want to vocalise my appreciation towards all the teachers and course assistants who taught me over the years, including Kari Rummukainen, who was my first academic supervisor during my early undergraduate years.

Likewise, I greatly appreciate the efforts of Kirill Boguslavksi and my pre-examiners, Mikko Laine and Anton Rebhan, who have checked this work and been very helpful with suggestions, as well as Guy Moore for agreeing to be the opponent in my defense.

The University of Helsinki Research Foundation was kind enough to fund my doctoral studies, which saved me from plenty of grant-applying stress, and enough trust has been placed on me by Fondazione Bruno Kessler to hire me as a postdoc at ECT*, which has been an excellent motivation to finish this Thesis and has given me more self-confidence in my ability to hopefully continue further in academia.

I have also been fortunate enough to participate in many excellent conferences and school all over the world, sating my wanderlust and serving as the highlights of my studies, and am thankful for their organisers (Aleksi V. also deserves thanks for this, as I believe he recommended every single one to me and often helped fund them).

The environment on the third floor of Physicum is wonderful, and the University has been an excellent workplace. I am tempted to start listing names, but the list is too long. If I talked with you during lunches, ~~coffee~~ tea breaks, or whenever, you have made my time better, thank you. I do

want give a special mention to all those who strive to support equality and inclusion at the department.

At some point during the past eight or so years, I finally realised that sometimes one needs a semblance of life outside physics. I am very grateful to my parents and brothers. Especially my parents have always supported me, and have been confident I would be a scientist since I was a young child. Äiti, isä, Miro, Miika: Kiitos paljon.

Nonphysicist friends are likewise vital. The people at SMOK and LGC have helped me through some occasionally very rough patches, and I am truly thankful for all my friends: in particular River, Kimberly, Wolfie, and of course Naomi Hirasaki. Thank you all so much.

Next stop, Trento!

Included Publications

The following peer-reviewed Publications — each co-authored by the Doctoral Candidate — are included in the printed version of this Thesis, reprinted in their original form:

- Ghisoiu et al. (2016), On high-order perturbative calculations at finite density. *Nucl. Phys.* B915:102–118. Also available as an arXiv pre-print hep-ph/1609.04339.
- Gorda et al. (2018), Next-to-Next-to-Next-to-Leading Order Pressure of Cold Quark Matter: Leading Logarithm. *Phys. Rev. Lett.* 121, 202701. Also available as an arXiv pre-print hep-ph/1807.04120.
- Romatschke et al. (2019), Thermal free energy of large Nf QED in 2+1 dimensions from weak to strong coupling. *Phys. Rev.* D100, 073009. Also available as an arXiv pre-print hep-th/1908.09835.

They are also listed in the References of the Thesis in the above order [1, 2, 3]. The authors are listed in alphabetical order in accordance with the convention used in particle physics.

The Author's Contributions

Each of the three Publications was most certainly a product of collaboration, but the author of the Thesis was mainly responsible for analytical calculations in each of the Publications.

Some parts where the author's work is particularly well-represented are as follows: In the first paper, the overall structure of the proof was initially devised by the author and her supervisor, Aleksi Vuorinen. The author was also responsible for the technical details related to the low-temperature limit. In the second paper, the extraction of the main result, the $\mathcal{O}(g_s^6 \ln^2 g_s)$ term of the pressure was performed independently by Tyler Gorda and the author. In the last paper, the author again performed analytic computations, in particular the ones relating to the self-energy.

The writing process of each Publication was a collaborative effort.

Contents

Chapter 1

Quantum Chromodynamics

In this Chapter, a general overview of the Quantum Field Theory of strong interactions, *Quantum Chromodynamics* (QCD) is given. We start by considering gauge theories and Yang–Mills theories in general. This is followed with a historical review of strong interactions, a construction of the QCD path integral and associated Feynman rules. Lastly, some important properties of QCD are reviewed. Concepts such as gauge invariance and the Yang–Mills action are introduced using the language of differential geometry, with notation following the book by Baez & Muniain [4]. Readers unfamiliar with the formalism should not fret, as a switch to local coordinates will be made soon, and after the Feynman rules are introduced, they will be used almost exclusively. Sign conventions, notation for local coordinates, such as the Feynman rules of Sec. 1.7, and such largely follow the recent textbook on thermal field theory by Laine & Vuorinen [5].

1.1 Gauge Theories

Modern gauge theories, developed over the 20th century, have solidified their position as one of the most important building blocks of Quantum Field Theories (QFTs), being used not only in the high-energy context of elementary particle physics where they were initially developed [6], but also in pure mathematics and as effective field theories in a variety of applications. As such, before reviewing the details of QCD, we shall

set up the general framework of gauge theories, focussing in particular on Yang–Mills theories describing the dynamics of non-Abelian gauge fields. Concepts such as the action and gauge invariance are introduced using differential geometry.

The distinguishing feature needed to define a gauge theory is the choice of a *gauge group* G, also known as the *symmetry group* of the theory. A second piece of information necessary is the *base space* M, the physical space where the fields of the theory live in. In continuum QFT, this is typically a smooth manifold, most commonly an n-dimensional flat space of either Lorentzian ($\mathbb{M}^{1,n-1}$) or Euclidean ($\mathbb{R}^n$) signature. Important exceptions are lattice field theory, where a discrete space is used instead, and the imaginary time formalism of thermal field theory vital for this Thesis. In the latter, the time direction will be compactified to a circle, and the base space of choice is $S^1 \times \mathbb{R}^{n-1}$.

The base space and the gauge group can be combined into a (principal) G-fiber bundle $\mathcal{E} \xrightarrow{\pi} M$, a space that locally looks like $G \times M$ and is compatible with the group action. This provides us with the last necessary ingredient: The dynamical degrees of freedom of the theory themselves, which are connections on the bundle. They are usually identified with the connection coefficients that are commonly denoted by A and called the *gauge fields* of the theory. The definition can be generalised to general fiber bundles with fibers F, where the connection encodes additional information.

A useful result when working with connections tells us that an arbitrary connection D can at least locally in a neighbourhood of any point on the bundle be split as $D = d + C$ [4], where d is a *flat* (curvature-free) connection and C appears as a spacetime one-form taking values on the tangent space of the fibers, encoding the generalised curvature. For notational purposes, we assume that C can further be split into the gauge field part A and a part corresponding to the Riemannian curvature of the base space θ as $C = A + \theta$. Generalising the assumption is very straightforward, but makes the notation considerably more cumbersome.

While elegant and very general, the above definition is of little practical use in calculations, where one will have to specify the above ingredients in more detail. A first step towards concrete computations is giving a *Lagrangian* definition of a gauge theory. This is achieved by introduc-

ing an *action (functional)* S, a functional of the fields Φ, including gauge fields A and any possible additional *matter fields*. Actions are commonly represented in an integral form as

$$S[\Phi] = \int_M \mathrm{vol}_M \mathcal{L}(\Phi), \tag{1.1}$$

where vol_M is a volume form on M and $\mathcal{L}$ is a scalar-valued *Lagrangian (density)* of the theory dependent of the fields (and their derivatives), which themselves depend on the location in the base space. By varying the action with respect to the fields, one obtains the (classical) *equations of motion* of the fields as the standard Euler–Lagrange equations.

A gauge theory is set apart from other Lagrangian field theories by associating a representation R_ϕ of the gauge group G with each of the fields $\phi \in \Phi$, as well as a corresponding (left) action ℓ_ϕ of G on the field space F_ϕ with local dependence on the base space point, that is, locally mapping $G \times M \times F_\phi \to F_\phi$ and given by[1] $\ell_\phi : (\gamma, x, \phi) \mapsto \ell_\phi(\gamma, \phi(x))$. This defines a *local gauge transformation* $\ell_\Phi^{\gamma,x}$ of any function f of the fields, $\ell_\Phi^{\gamma,x} : (\gamma, f(\Phi(x))) \mapsto f(\{\ell_\phi(\gamma, \phi(x)) | \phi \in \Phi\})$ A given action functional S is a proper action of a gauge theory if it remains unchanged under such transformations for any $\gamma \in G$ and $x \in M$:

$$S[\Phi] = \int_M \mathrm{vol}_M \mathcal{L}(\Phi) \mapsto \int_M \mathrm{vol}_M(x) \mathcal{L}(\{\ell_\phi(\gamma, \phi(x)) | \phi \in \Phi\}) = S[\Phi]. \tag{1.2}$$

An action, and more generally any other quantity with this property, is said to be *(locally) gauge-invariant*. In contrast, later in this Thesis, *global* symmetries (independent of the base space point) will become central in the context of field theories finite density.

In principle, the Lagrangian formulation of a given gauge theory allows actual computations to be performed using a chosen framework, such as perturbation theory or lattice field theory. Having said that, there are often additional complications related to gauge theories after moving to the quantum theory. An example of this will be seen in the following discussion of Yang–Mills theory in the form of auxiliary *ghost fields* that will be added to the theory in Sec. 1.6.

[1] The standard choice of g for generic group elements is not used to avoid confusion with the coupling constant g in what follows.

1.2 Yang–Mills theory

As alluded to earlier in this Chapter, a particularly widely-used gauge theory is Yang–Mills theory. It can be constructed by defining a specific gauge-invariant action after imposing additional constraints on the gauge group G and its Lie algebra $\mathfrak{g}$ to ensure the action gives rise to a 'physically sensible' theory, making the action we will eventually define positive definite. Requiring G to be semisimple and compact is sufficient [7]. In order to define the action itself, we first establish some notation: Consider the Lie algebra $\mathfrak{g} \approx T_\gamma G \, \forall \gamma \in G$. Following [5], we take its generators T^a to be Hermitian and satisfy the algebra $[T^a, T^b] = i f^{abc} T_c$ where f^{abc} are the structure constants of $\mathfrak{g}$, and normalise them with $\mathrm{Tr}[T^a T^b] = \delta^{ab}/2$. From here through the rest of the Thesis, we will use the Einstein summation convention of summing over repeated indices. For bookkeeping reasons will also maintain a distinction between 'upper' and 'lower' indices even when dealing with positive-definite bilinear forms. As we start to slowly move towards more physical quantities, it is also worth mentioning that we will always use natural units, setting $c = k_B = \hbar = 1$

At this point, we can write down an explicit local parametrisation for the gauge field A: They are $\mathfrak{g}$-valued one-forms on the spacetime M, $A = A^a_\alpha T_a \mathrm{d}x^\alpha$. We are closer to writing down the action (using local coordinates if desired), but first, it will be useful to discuss how the gauge fields transform. In standard jargon, they are said to 'transform in the adjoint representation', that is, the local gauge transformations ℓ^γ_A (or rather, the one-parameter group of transformations $\omega_\gamma : \gamma = e^{ig\omega_\gamma}$) read

$$\ell^\gamma_A : A \mapsto A + \mathrm{D}\omega_\gamma(x) + \mathcal{O}(\omega^2_\gamma), \; D_\alpha \omega_\gamma(x) \equiv \omega_{\gamma;\alpha}(x) + ig[\omega_\gamma(x), A_\alpha]. \tag{1.3}$$

In Eqn. (1.3) $\omega_\gamma(x) = \omega_\gamma(x)^a T_a$ is a $\mathfrak{g}$-valued zero-form on M, g is the *coupling (constant)* of the theory indicating the strength of the interaction, and $\mathrm{D} \equiv \mathrm{d}_D$: the covariant derivative associated with the connection D, here acting on zero-forms. Lastly, we have introduced the comma notation for partial differentation: $_{,\alpha} \equiv \partial_\alpha$, $_{;\alpha} \equiv \boldsymbol{\nabla}_\alpha$, where $\boldsymbol{\nabla}$ is the covariant derivative associated with the metric part of the connection.

Generally speaking, the *curvature* of a connection is encoded in a curvature two-form Γ obtained by formally 'differentiating the connection'

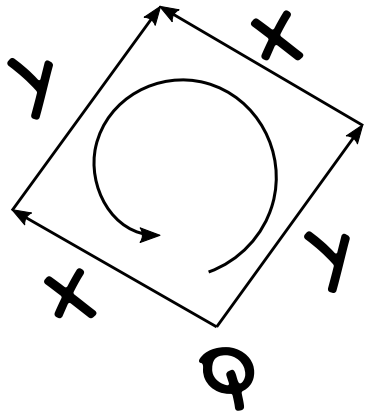

Figure 1.1: On a bundle with a curvature form Γ, the change in a quantity Q as it is parallel transported around the closed parallelogram characterised by vectors X, Y is given by $\Gamma(X, Y)Q$.

in some appropriate way. As before, we assume that the gauge part can be separated from the connection. For the gauge fields, the *field strength* $F = F^a_{\alpha\beta} T_a \mathrm{d}x^\alpha \wedge \mathrm{d}x^\beta$ is defined as the A-dependent part of Γ, with the covariant derivative now acting on one-forms

$$F \equiv \mathrm{D}A \implies F^a_{\alpha\beta} = A^a_{\beta;\alpha} - A^a_{\alpha;\beta} + g f^a_{bc} A^b_\alpha A^c_\beta. \tag{1.4}$$

With the remainder of the connection assumed to (largely for notational simplicity) describe the curvature of the base space, the A- independent parts of the curvature form are then encoded in the standard Cartan curvature form $\Omega = \mathrm{d}\theta + \theta \wedge \theta$. If the remaining connection furthermore corresponds to a metric connection, the components of Ω in a local frame are associated with those of the Riemann curvature tensor.

A commonly encountered expression for the curvature form in a local coordinate frame is as a Lie bracket or a commutator of covariant derivatives. This can be immediately obtained from Eqn. (1.4) by using the antisymmetry of the structure constants, which lets one cast the components of F into the appropriate form. However, this simple form holds only in a local coordinate frame; when acting on general sections one

must use the standard definition of a curvature form from differential geometry, subtracting the derivative along the Lie bracket of the sections. For readers familiar with classical Riemannian geometry or general relativity, this provides an intuitive picture. In the purely metric setting, connections are defined in order to shift (tangent) vectors between points on the base space — to parallel transport them. Connections on fiber bundles are entirely analogous, transporting quantities between fibers over different points on the base space. Following this analogy, we can build intuition on the curvature: The curvature form (the Riemann curvature tensor, to be precise) of the tangent bundle admits a simple interpretation in local coordinates. With the metric connection, curvature is often depicted as parallel transporting a vector along the sides of an infinitesimal parallelogram using covariant derivatives. As the curvature is given by the commutator of covariant derivatives, over the sides of the parallelogram its action on a tangent vector yields the change in the vector transported over the loop. The curvature serves the exact same purpose on more complicated bundles, the quantities it transports simply become more abstract. The idea is illustrated in Fig. 1.1.

Before moving on to the Yang–Mills action, we make one last comment on geometry: With the concept of parallel transport fresh in mind, we are able to also talk about *holonomy*: Intuitively, it measures the failure for objects to be preserved under parallel transport around loops. This is somewhat related to many other mathematical notions, such as categorising distinct loops or surfaces by means of homotopy, or the difference of local and global triviality in cohomology. While this may appear abstract and within the scope of this Thesis we are unfortunately unable to give it a precise definition or the attention it deserves, holonomy has an important place in physics. In Sec. 3.1, we shall very briefly recall how it relates to the phase structure of Yang–Mills theories.

With F defined, the Yang–Mills action can be defined as[2]

$$S_{\mathrm{YM}}[A] \equiv \frac{1}{2}\int_M \mathrm{Tr} F \wedge \star F = \frac{1}{4}\int_M \mathrm{vol}_M F^a_{\alpha\beta} F_a^{\alpha\beta}. \tag{1.5}$$

[2]As all the Publications included in this Thesis deal with base spaces of Euclidean signature exclusively, we will implicitly assume this when it comes to sign factors. These can easily be compensated, for example the action obtains a minus sign from moving to Euclidean space as well as from changing to anti-Hermitian generators of the algebra.

Here, we denote by Tr a trace in the Lie algebra indices, and $\star$ is the Hodge star of differential geometry. The second equality follows immediately from the defining property of the Hodge star as well as from the normalisation of the trace. The action is invariant under gauge transformations, which is easiest to see in a local frame by using full gauge transformations as opposed to the one-parameter group of transformations in Eqn. (1.3). Given a transformation ℓ, D transforms in a local coordinate frame as $\ell_D^{\gamma,x} : D_\alpha \mapsto \gamma(x) D_\alpha \gamma(x)^{-1}$, and from the alternative expression of F as a commutator of covariant derivatives, we see that it, too, transforms as $F \mapsto \gamma(x) F \gamma^{-1}(x)$, with juxtaposition denoting the natural action of the gauge group. As the notation indicates, the transformation matrices γ are thought of as spacetime zero-forms, so that the action stays invariant.

The definition of F as a curvature form, a commutator of covariant derivatives, leads to another identity: F satisfies the Bianchi identity $\mathrm{D}F = 0$. While it seems natural since F is defined as a derivative, the identity is not entirely trivial, as the connection may not be flat. Regardless, it follows in a straightforward manner locally by splitting the connection (and therefore the covariant derivative) as explained in Sec. 1.1 into a flat connection d and the curvature parts Ω and F defined earlier. In terms of the derivatives, d is therefore nilpotent, $\mathrm{d}^2 = 0$. The identity then follows by acting with D on the curvature form — from classical Riemannian geometry, we know that the Cartan part of the curvature Ω fulfills the Bianchi identity on its own. Alternatively, it follows from the definition of F as a commutator and the Jacobi identity of the Lie bracket. In the absence of matter fields minimising the Yang–Mills action leads to a second relation, $\mathrm{D}\star F = 0$. Together, these are the *Yang–Mills equations*, the equations of motion of the gauge fields, and essentially the non-Abelian generalisations of Maxwell's equations of 19th century electrodynamics in vacuum, the electrodynamical setting turning the connection D into, at least in flat space, a flat connection.

The pure Yang–Mills theory can be extended by adding *matter fields* to the action, and the gauge connection provides a particularly suitable way of generating interaction terms between the Yang–Mills and matter terms: If the complete action is desired to be locally gauge-invariant, naïve kinetic terms involving only spacetime derivatives must be changed

to gauge-invariant quantities. The simplest possible replacement is to exchange them with covariant derivatives appropriate to the representation these matter fields transform in. For QCD, we shall see the concept in action as we perform this 'gauging' process for a set of massive Dirac fermion fields in Sec. 1.4.

However, before moving on to QCD, it is worth noting that, as usual, definitions vary. In particular, there are different conventions for the placement of the coupling g — a commonly seen variant is obtained by scaling the gauge fields $A \mapsto gA$ and moving the coupling in front of the action in Eqn. (1.5) — as well as signs and factors of i when explicitly expanding out the components. In addition, the technical definition of a Yang–Mills theory given above excludes an important case of $G = \mathrm{U}(1)$. However, this Abelian theory relevant for (Quantum) Electrodynamics (QED) is a natural extension of the above discussion.

Of more fundamental importance is the explicit form of the action given in Eqn. (1.1). Of course, in principle one is free to study the consequences of an arbitrary action. In a physical theory, a question often arises whether additional terms can or should be added to the action. Their form is typically governed by overarching physical symmetries or the goal of specific renormalisability properties. In relativistic theories, these usually include Lorentz-invariance and invariance under a combined Charge – Parity – Time (CPT)-transformation, and the whole construction of Lagrangian gauge theories relies on a local gauge symmetry of the action. Nevertheless, possible additions are numerous. Thankfully, with a physical theory expected to be valid to an energy scale Λ, terms whose mass dimension is greater than the dimensionality of the spacetime ought to be suppressed by powers of Λ. As such, in theories such as QCD that we expect to describe nature well up to very large energy scales, leaving out these terms is a good approximation in most situations.

However, an a priori unsuppressed term obeying the relevant physical symmetries can be added in the form of $S_{\mathrm{CP}} \propto \theta_s F \wedge F$, where θ_s is some proportionality constant indicating the relative impact of this term in comparison to S_{YM}. This additional term is of topological nature: Integrated over a manifold, it is a topological invariant known as the *second Chern class*. As such, it has an interpretation as a boundary term and it

vanishes classically when working with compactly supported fields. Regardless, the term has physical consequences arising at the quantum level [8] and a priori, there is no reason to discard it. However, experiments have confirmed that in the case of QCD, the proportionality constant θ_s appears to be either zero or vanishingly small [9]. To contrast this, in the Standard Model the 'θ_s-angle' of weak interactions does not affect physics even at the quantum level [10]. For QCD, the conundrum of why θ_s is so small is the essence of the so-called *strong CP problem* of particle physics: While S_{CP} preserves the apparently fundamental CPT symmetry, it does not preserve P, or indeed CP. While an intriguing topic in its own, a more in-depth discussion is unfortunately beyond the scope of this Thesis, and the term will be discarded in what follows. An interested reader is advised to read any of the number of related publications such as [11].

1.3 History of QCD

Depending on the perspective, the roots of QCD can be traced to a number of different points along the 20^{th} century. The long-lived strongly interacting subatomic particles — protons and neutrons — were discovered before the second world war [12, 13, 14]. The lightest mesons, pions, were first observed in 1947 in cosmic ray events [15], with the discovery of kaons following later the same year, using the same method [16]. However, at this time there was no indication that these or any other subatomic particles were non-elementary. For the leptons discovered during the same time frame, the viewpoint has held: They are still thought to be elementary.

By the 1960s, some cracks had started to appear in the paradigm of viewing all subatomic particles as indivisible and elementary. At this point, the number of known strongly interacting particles increased dramatically as particle accelerator technology developed (discoveries included Λ [17], Δ [18] and others, as well as the charged or uncharged variants of them and other previously discovered particles), with no clearly discernible pattern to explain their properties. A method of 'organising' them based on the representation theory of the matrix group $\mathrm{SU}(3)$ was proposed in 1961 [19, 20]. It refined an earlier characterisation based on the $\mathrm{SU}(2)$ isospin symmetry, and explained the properties of numerous

of these newly discovered particles, but turned out to be incomplete. A few years later, a proposal was finally made [21, 22] that the many newly-found particles were not elementary after all, but rather composite, formed of an SU(3) triplet of elementary particles dubbed *quarks* (from [23]). While the same symmetry group had already been used before, this step was fundamentally important in recognising what to our current best knowledge are some of the elementary degrees of freedom of strong interactions. Many further hadronic resonances have since been observed, but their properties are now better understood within the context of QCD.

At first, the quark model only included three types or *flavours* of quarks: The u(p), d(own), and s(trange) quarks. While protons, neutrons and pions could be explained with just the first two, the last one was required to explain the properties of kaons that turned out to be the first known 'strange' particles — although this was of course not obvious at the time of their discovery. Understanding the properties of weak interactions lead to a proposal of a fourth flavour [24], the c(harm) quark, and experimental evidence was obtained not long after this [25, 26]. Subsequent theoretical development, again in the study of the weak sector, led to the addition of two additional quarks [27]. The fields were now split into three families of two quarks, a model that survives to date. The 70s did not end before the first particle containing the b(ottom) quark was observed [28], but the final and heaviest t(op) quark was not seen experimentally until 1995 [29, 30]. Some of the properties of the six quarks are shown in Fig. 1.2. The value of the top quark has not fully converged to a method-independent value, and in the Figure it is taken to be the value from direct measurements in the sense of [31], as opposed to cross section measurements. Finally, the column labelled 'others' describes miscellaneous quantum numbers which vanish for flavours unless explicitly listed.

As the flavours were being discovered, the quark model was a resounding success in other aspects as well. On the theoretical front, the discovery of *asymptotic freedom* of non-Abelian Yang–Mills theory [32, 33] in 1973 finally allowed for a well-defined QFT of quarks and gluons, now using SU(3) as a local gauge symmetry — we will have more to say about asymptotic freedom both at the end of the next Section as well

Flavour	Mass	Charge	Other
up	$2.16^{+0.49}_{-0.26}$ MeV	$2/3$	isospin $1/2$
down	$4.67^{+0.48}_{-0.17}$ MeV	$-1/3$	isospin $-1/2$
strange	93^{+11}_{-5} MeV	$-1/3$	strangeness -1
charm	$1.27^{+0.02}_{-0.02}$ GeV	$2/3$	charmness 1
bottom	$4.18^{+0.03}_{-0.02}$ GeV	$-1/3$	bottomness -1
top	$172.9^{+0.4}_{-0.4}$ GeV	$2/3$	topness 1

Figure 1.2: Properties of quarks (values from [31])

as in Sec. 1.8. This QFT became known as Quantum Chromodynamics due to its resemblance with the corresponding theory of the electromagnetic interactions, Quantum Electrodynamics. Some of the most remarkable early experimental results were studies of deep inelastic scattering at the Stanford Linear Accelerator Center showing that nucleons did indeed have substructure [34] in 1969; as well as the observation of 3-jet events, indicating the existence of gluons, the force carriers of the strong interaction at Deutsches Elektronen-Synchrotron [35] in 1979. Lastly, the deconfined phase of matter whose true degrees of freedom were quarks and gluons — the *quark-gluon plasma* — was finally discovered in 2000 [36].

For a review of recent developments, see the relevant parts of [31].

1.4 Strong Interactions and the QCD Lagrangian

The previous Section is a very brief history of how QCD became the accepted field theory for describing strong interactions. In modern terms, it is a Yang–Mills theory with gauge group $\mathrm{SU}(N_c)$, minimally coupled to N_f massive fermions, with a coupling g_s. The values of N_c and N_f realised in nature are 3 and 6 respectively, but in computations it is often convenient to treat these as arbitrary parameters — in particular, different fermion fields might be 'active' as effective dynamical degrees of freedom in different systems, and limiting values of large numbers of fermions or colours might allow one to examine otherwise intractable systems. This

approach, known as the *large-N limit* in general settings, is a key ingredient for many nonperturbative studies. A well-known example is the AdS/CFT-duality, where the relevant limit is $N_c \to \infty$. For this Thesis, the general method is relevant for the paper [3], discussed also in Sec. 2.10, where the limit of a large number of *fermions* is taken instead.

The gauge fields, gluons, transform in the adjoint representation of $\mathrm{SU(N_c)}$ and there are therefore $d_A \equiv \dim \mathfrak{ad}\mathrm{SU}(N_c) = N_c^2 - 1 \overset{N_c=3}{=} 8$ different varieties of them under the gauge group charge. The fermionic fields, quarks and antiquarks, are split into N_f 'flavours' each of which transforms in the (anti)fundamental representation of $\mathrm{SU(N_c)}$, so that their charge under the gauge group can be any of the N_c 'colours'. As already mentioned, the flavours are known as *u*(p), *d*(own), *s*(trange), *c*(harm), *b*(ottom), and *t*(op); the colours are called red, green, and blue.

Furthermore, the quarks are Dirac spinor fields[3], that is in $3+1$ spacetime dimensions, they transform in the representation $(0, 1/2) \oplus (1/2, 0)$ of the Lorentz group $\mathrm{SO}(1,3)$. In the path integral formalism used across the Thesis, they must be taken as Grassmannian (anticommuting) fields in order to maintain the correct statistics. This is the minimal choice for quarks when working within the Standard Model of particle physics, but higher-dimensional representations are required in a number of situations, ranging from studying bound states [37] to extensions of the Standard Model. To mention a few, the latter include many technicolor models, where fermions often transform in extended representations [38] or Grand Unified Theories where the whole QCD gauge group is (together with the electroweak $\mathrm{SU}(2) \times \mathrm{U}(1)$) embedded onto a higher-dimensional group [39].

There is a standard, and in a certain sense minimal, way of adding quark fields to a QFT. This can be summarised as the QCD Lagrangian, which is commonly written down in the flavour eigenbasis that renders the mass matrix diagonal:

$$\begin{aligned} \mathcal{L}_{\mathrm{QCD}}(A, \psi, \overline{\psi}) &\equiv \frac{1}{4} F^2 + \overline{\psi}(\not{D} + m)\psi \\ &= \frac{1}{4} F^a_{\alpha\beta} F_a^{\alpha\beta} + \sum_{f=1}^{N_f} \overline{\psi}_f (\gamma_\alpha D^\alpha + m_f \mathbb{1}) \psi_f . \end{aligned} \tag{1.6}$$

[3] As mentioned, the CP-violating term discussed at the end of Sec.1.2 is set to zero.

In Eqn. (1.6), $\mathbb{1}$ represents the identity matrix in both colour and spinor indices and D^α is now the covariant derivative associated with the gluon fields A that has nontrivial indices in colour space stemming from the generators T^a appearing in $A_\alpha = A^a_\alpha T_a$ acting on spinors. The γ_α are the generators of the Clifford algebra appropriate for the spacetime, with nontrivial indices in spinor space, that is to say, they obey the algebra $\{\gamma_\alpha, \gamma_\beta\} = 2g_{\alpha\beta}$, where g is the metric. In a $3+1$-dimensional Minkowski space they are the famous γ matrices that generate $\mathcal{C}\ell(1,3)$ associated with the Lorentz group. The choice that the gauge field part of D^α corresponds precisely to the standard covariant derivative of the $\mathrm{SU}(N_c)$-bundle connection, whose coefficients are $-g_s A^a_\alpha T^{ij}_a$, is the choice of *minimal coupling* (between the Dirac fields and the gauge fields), following the gauging procedure described in the previous Section.

Note that if the connection is nontrivial beyond the presence of the gauge terms, the covariant derivative must be modified to be appropriate for fermions, in particular using the spin connection for the Riemannian connection. Adding other types of fields, such as scalars fields, to the Lagrangian follows a completely analogous procedure. This becomes relevant in theories such as dimensionally reduced QCD (see Sec. 2.7 for a brief discussion) or the full Standard Model of particle physics containing the Higgs field, but for QCD itself fermions are sufficient. Having mentioned the Standard Model and the Higgs, it should also be noted that the Lagrangian in Eqn. (1.6) only contains information about strong interactions, not from the electroweak sector. In particular, the masses present in the Dirac terms are not truly static in the context of the full Standard Model, but rather dynamically generated by the spontaneous breaking of the electroweak symmetry via the Yukawa interactions between quarks and the Higgs.

With a working definition of the Lagrangian, one may in principle use the standard QFT toolbox to perform calculations, predict experimental results, and infer general properties of the theory. In practice, this is difficult. For example, a vital property of the theory of strong interactions is that it exhibits a property known as *confinement*: The fundamental fermionic degrees of freedom, quarks, are not observed individually in experiments, but instead seen combined into bound states, *hadrons*. One might hope to show this from the Lagrangian, but this is not a trivial

statement, and in fact has no known analytic proof. However, numerical lattice field theory simulations suggest that systems based on the QCD Lagrangian do in fact exhibit confinement, and are able to accurately measure related properties of hadrons such as their mass spectra [40].

Problems also arise when attempting to understand *chiral symmetry breaking*. In addition to the local $\mathrm{SU}(N_c)$ symmetry, the massless Dirac Lagrangian exhibits a global $\mathrm{SU}_L(N_f) \times \mathrm{SU}_R(N_f)$ flavour symmetry under spinor rotations. To see the way this symmetry manifests itself, let $j \in \{R, L\}$. We define left- and right-handed projection operators in spinor space $\mathbb{P}_j \equiv \frac{1}{2}(\mathbb{1} \pm \gamma_5)$ where $\gamma_5 = i\prod_{n=0}^{n=3}\gamma^n$ in $3+1$ dimensions. The symmetry acts on the field components $\psi_j \equiv \mathbb{P}_j\psi$ in the natural way, $\psi_j \mapsto U_j\psi_j$, with $(U_L, U_R) \in \mathrm{SU}_L(N_f) \times \mathrm{SU}_R(N_f)$. The symmetry is known to break spontaneously — we will discuss the consequences in Sec. 3.1, but for the purposes of the current topic the most important aspect is that it has proven very difficult to show this symmetry breaking directly from the QCD Lagrangian. It should be noted that the chiral symmetry originates from a greater $U(N_f) \times U(N_f)$ symmetry, of which a global $\mathrm{U}(1)$ phase symmetry remains unbroken, and corresponds to the conserved quantity of baryon number, which will be important later in the Thesis when discussing chemical potential in Sec. 2.3.

A failure to show such fundamental properties could spell doom to any analytic efforts to understand strong interactions from first principles, but thankfully, there is a saving grace in another vital property of QCD: asymptotic freedom, the discovery of which was mentioned as a milestone in the development of QCD earlier in this Section. To understand why, one has to realise that the main challenge in performing QCD computations is the fact that the QCD Yang–Mills coupling g_s is large at the relatively low energies encountered in ordinary situations and laboratory settings. This is to be expected from a theory describing strong interactions, but presents a great obstacle to the analytic treatment of the theory: Unlike in, say, QED, at low energies quantities cannot be reliably organised as a perturbative series in the coupling, and well-understood methods of perturbation theory cease to apply. However, it turns out that in QCD, the coupling *decreases with the energy scale* [32, 33]: The strong interaction becomes weaker as the energy scale decreases, whereas the op-

posite happens in QED. The reasons for this behaviour will be discussed later in Sec. 1.8. However, it justifies the use of perturbation theory in the study of extremely energetic — for example, very dense or hot — QCD systems and shows that quarks are, indeed, asymptotically free. Asymptotic freedom also has strong implications regarding the qualitative nature of QCD matter, as first noted by Collins & Perry soon after the discovery of asymptotic freedom [41, 42].

1.5 Fundamentals of Functional Integration

Due to the important role perturbation theory plays in the Publications included in this Thesis, the next step is to derive the QCD Feynman rules. In order to present this in a sensible and mostly self-contained manner, as well as for future reference, we will first perform the path integral quantisation of QCD. In this process, we add gauge-fixing auxiliary ghost fields with the usual Faddeev-Popov trick, and are then able to derive the Feynman rules.

In this Thesis, familiarity with the general formalism of functional integral methods in non-Abelian gauge theories as presented in standard textbooks such as [43, 44] is assumed, but for completeness, and to establish notation, we will review some basic definitions.

The starting point to a functional integral formulation of a Lagrangian quantum field theory is the *partition function* Z. As with nearly every other formula of the Thesis, we fix the spacetime to be Euclidean for simplicity of the formulae. In the next Chapter, this will be seen to be especially important when considering thermal field theory in Sec. 2.1, but even in vacuum formally performing a Wick rotation $t \mapsto \tau = it$ often helps with practical calculations. With this convention established, Z is given by

$$Z = \int\limits_{\mathcal{F}} \mathcal{D}\Phi \exp\Big(- S[\Phi] \Big), \tag{1.7}$$

where S is the (Euclidean) action obtained by integrating over the Lagrangian (for QCD, given in Eqn. (1.6)), Φ are the elementary fields (for QCD, $\overline{\psi}, \psi, A$), $\mathcal{F}$ is function space appropriate for fields Φ, and $\mathcal{D}$ is the associated, somewhat ambiguous, functional integration measure. We

will remain ambivalent about the nature of $\mathcal{F}$ for now, and drop it from the notation, but will have more to say about it after fixing the base space M when constructing the imaginary-time formalism of thermal field theory.

Later, the partition function Z is of fundamental importance when computing thermodynamic quantities such as the pressure p or the free energy[4] Ω in equilibrium thermal field theory. In many situations, it alone is not sufficient. In addition to the partition function, one often considers *correlation functions* of operators built from the elementary fields. Given such a composite operator $\mathcal{O}$, the associated correlation function is given by the quotient

$$\langle \mathcal{O} \rangle = \frac{\int \mathcal{D}\Phi \exp\Big(- S[\Phi] \Big) \mathcal{O}[\Phi]}{\int \mathcal{D}\Phi \exp\Big(- S[\Phi] \Big)}. \tag{1.8}$$

Correlation functions are the fundamental building blocks of a QFT. While they can be interpreted as true statistical correlation functions also in QFTs, some physical intuition on what they represent can be achieved by looking at specific examples. The prototypical example of a correlation function is the aptly-named *propagator*, given by the correlation function of a field at two different points in the base space with desired causal properties. It describes the transition amplitude of a field between the two points, while higher-order correlation functions describe interactions between fields. While we work almost exclusively with Euclidean quantities, in vacuum QFT in Minkowski spacetime, the very important LSZ reduction formula allows one to relate measurable cross sections with time-ordered correlation functions [44]. In QFTs, correlation functions are often called n-point functions, with n referring to the number of external fields — for example, the propagator is an example of a two-point function.

Relations such as Eqn. (1.8) show that any constant coefficients in the functional integrals cancel in physical quantities, which alleviates the trouble associated with defining the functional integration measure. In-

[4] As these two quantities are nearly interchangeable, we will rarely make a distinction between them in future.

deed, we will routinely identify functional integrals up to (typically infinite) normalisation factors.

With slight abuse of notation, we can denote $(\phi, j_\phi) = \int_M \mathrm{vol}_M \phi_a j_\phi^a$ for a *source term* j_ϕ associated with $\phi \in \Phi$, and use it to conveniently compute correlation functions by taking functional derivatives of the *generating functional*

$$Z[j_\Phi] = \int \mathcal{D}\Phi \exp\Big(- S[\Phi] + \sum_{\phi\in\Phi} (\phi, j_\phi)\Big). \tag{1.9}$$

An often more convenient quantity particularly relevant for thermal field theory is the *generating functional of connected correlation functions* $W[j_\Phi] = \ln Z[j_\Phi]$, defined in analogy with the Gibbs free energy of classical statistical mechanics. The 'connectedness' property of W has an intuitive interpretation in terms of the diagrammatic small-coupling expansion of a QFT by the standard method of *Feynman graphs*; the correlation functions it generates consist exclusively of graph-theoretically connected diagrams. A particular consequence is that the perturbative expansion of the free energy — essentially W at vanishing source, $\Omega \sim \ln Z$ — can (at least naïvely) be obtained by summing together connected Feynman diagrams contributing to a given order in the coupling. The free energy is an exception to the rule that physical observables are obtained as ratios, but it can be rendered finite by subtracting the corresponding quantity in vacuum.

While W is of particular interest in thermal field theory, other similarly defined generating functions can also be of interest; for example the generating function of one-particle irreducible (strongly connected, in graph-theoretical terms) diagrams, the *effective action*, is defined as a formal Legendre transformation $E[\Phi_c] = W[j_\Phi] - \sum_{\phi\in\Phi}(\phi, j_\phi)$ [5].

As mentioned, this Section is intended merely as an overview. For proofs of the listed properties and in general for a more thorough overview of the topic the reader is advised to turn to standard textbooks, such as the comprehensive tome by Zinn-Justin [43].

[5] The effective action is also commonly denoted as Γ.

1.6 Functional Integral for QCD

When building a perturbation theory of a QFT, the standard method is to extract quadratic terms from the action, treat them as the 'free action' that can be dealt with exactly by identifying the quadratic functional integrals as extensions of finite-dimensional Gaussian integrals, and expanding the exponential containing the nonquadratic terms in some hopefully small parameter. In the case of the QCD Lagrangian of Eqn. (1.6), this parameter is the coupling g_s. However, the Yang–Mills action contains a problematic element: The differential operator associated with the quadratic term is not properly invertible, and the situation cannot be ameliorated by introducing a naïve mass term, as that would break gauge invariance. The issue can be resolved by restricting the integration to only the equivalence classes of gauge field configurations not related by a local gauge transformation, the so-called *gauge orbits*. A standard way of removing the redundant 'overcounted' gauge configurations goes by the name of the of the *Faddeev–Popov trick* [45]. The derivation presented here follows [46] to an extent.

To begin with, we observe that one may insert a unity in the functional integral in the form

$$1 = \int \mathcal{D}\gamma \delta[X[A^\gamma]]\mathcal{J}[X[A]], \tag{1.10}$$

where $\delta, \mathcal{D}\gamma, \mathcal{J}$ are the functional generalisations of the Dirac δ, the Haar measure[6] of the gauge group, and the Jacobian determinant respectively, and $X[A]$ is some gauge fixing condition, set to zero by the Dirac δ. It turns out that the form of X calls for a careful treatment. It is generally not sufficient for fixing the representative of a gauge orbit uniquely, leading to the generation of so-called *Gribov copies*. The copies do not affect perturbative calculations, and as such are yet another topic we will not cover fully, with the reader advised to turn to review articles such as [47].

At least formally, the identity in Eqn. (1.10) is trivial, and we may proceed by noting that as the original integrand is gauge-invariant as a physical quantity, the same holds after inserting the RHS of Eqn. (1.10),

[6]The Haar measure is a left-invariant measure of a group, finite for compact subsets and unique for (locally) compact (Lie) groups.

and furthermore for the Jacobian determinant itself. Therefore a constant factor of $\int \mathcal{D}\gamma$ can be extracted and subsequently ignored, resulting in a gauge-invariant expression with the gauge-fixing condition $X[A] = 0$ enforced by an explicit Dirac δ.

Two more modifications will be made in order to express the gauge-fixed functional integral in the form of a standard functional integral over a modified action.

Step one is to observe that integrals over Grassmannian variables have the property

$$\det K = \int \mathcal{D}\overline{\eta}\eta \exp(-K[\overline{\eta}, \eta]), \tag{1.11}$$

with K a suitable matrix (or generally a linear operator) and $\overline{\eta}, \eta$ a conjugate pair of Grassmannian variables. This can be used to turn the functional Jacobian determinant present in Eqn. (1.10) into an integral over a pair of Grassmannian auxiliary variables. In this case, these are commonly known as Faddeev–Popov ghosts. Note that while they are Grassmannian in nature, they are not 'true' fermions, and for example will obey bosonic statistics in a thermal system (see Sec. 2.1).

The next step is to similarly convert the Dirac δ into an integral. For both convenience and concreteness, we will do this by fixing the form of the gauge-fixing condition X to what is known as the family of *(ξ-)covariant gauges*. This reads $X = -\star \mathrm{d} \star A$, or component-wise for M of constant curvature $X_a = -A^{\alpha}_{a,\alpha}$. Furthermore, we note that since the actual integrand over the gauge orbits does *not* depend on the form of the constraint, we can shift the argument of δ by a newly-introduced field Ξ independent of the existing fields, and multiply the whole expression by $\int \mathcal{D}\Xi \exp(-\frac{1}{\xi}\int_M \mathrm{vol}_M \mathrm{Tr}\Xi^2)$, with $\xi \in \mathbb{R}$ an arbitrary constant. Changing the order of integration then lets us exchange Ξ with X in this expression due to the Dirac δ.

Writing the steps outlined above out, and recalling that we identify

functional integrals up to a constant coefficient,

$$\begin{aligned} Z_{\mathrm{QCD}} &= \int \mathcal{D}A\overline{\psi}\psi \exp(-S_{\mathrm{QCD}}) \\ &= \int \mathcal{D}\gamma A\overline{\psi}\psi\delta[X[A^{\gamma}]]\mathcal{J}[X[A]] \exp(-S_{\mathrm{QCD}}) \\ &= \Big(\int \mathcal{D}\gamma\Big) \int \mathcal{D}A\overline{\psi}\psi\delta[X[A]]\mathcal{J}[X[A]] \exp(-S_{\mathrm{QCD}}) \\ &= \int \mathcal{D}A\overline{\psi}\psi\overline{\eta}\eta[X[A]-\Xi] \exp(-J[\overline{\eta},\eta;X]) \exp(-S_{\mathrm{QCD}}) \\ \Longrightarrow\ Z_{\mathrm{QCD}} &= \int \mathcal{D}\Xi \exp\left(-\frac{1}{\xi}\int\limits_{M} \mathrm{vol}_M \mathrm{Tr}\Xi^2\right) Z_{\mathrm{QCD}} \\ &= \int \mathcal{D}A\overline{\psi}\psi\overline{\eta}\eta \exp\left(-S_{\mathrm{QCD}} - J[\overline{\eta},\eta;X] - \frac{1}{\xi}\int\limits_{M} \mathrm{Tr}X\wedge\star X\right). \end{aligned} \tag{1.12}$$

We are now ready to write down the complete gauge-fixed generalisation of the QCD action in a ξ-covariant gauge corresponding to Eqn. (1.6):

$$\begin{aligned} S_{\mathrm{gf-QCD}}(A,\psi,\overline{\psi},\overline{\eta},\eta) \equiv &\int\limits_{M} \mathrm{Tr}\left(\frac{1}{2}F\wedge\star F + \frac{1}{\xi}\mathrm{d}\star A\wedge\star\mathrm{d}\star A\right) \\ &+ \int\limits_{M} \mathrm{vol}_M\left(\overline{\psi}(\not{D}+m)\psi + \langle\boldsymbol{\nabla}\overline{\eta}, D\eta\rangle\right), \end{aligned} \tag{1.13}$$

with $\langle , \rangle$ denoting a metric-induced inner product, and where the explicit form of the Jacobian has been worked out for $X = -\star\mathrm{d}\star A$. Note that the last term includes only one gauge-covariant derivative, and that working in a space of non-Euclidean signature one would have to keep track of some additional sign factors. In the next Section we will write the distinct terms in a more explicit form in flat space in the process of extracting the Feynman rules.

As a last point of note, the Faddeev–Popov trick described in this Section is not the only possible method of fixing the gauge of Yang–Mills theory. A more generally applicable framework is known as *BRST quantisation*. In it, one builds an algebraic complex using a nilpotent transformation operator that acts on the fields. Then, physical states can be

extracted from a larger 'initial' Hilbert space as cohomology groups of the said complex constructed in the standard way.

1.7 QCD Feynman Rules

As mentioned briefly in Sec. 1.5, a common way of organising the weak-coupling expansion of QFT is by means of a diagrammatic expansion in terms of Feynman diagrams. To summarise the building blocks of the expansion, the graphical notation can be linked with the functional expressions by relating the edges, or lines, of a graph to propagators of fields, with each distinct field being represented by a line with a distinct appearance, and likewise associating the vertices with interactions between the fields. In this Section, we will give a concise summary of this correspondence — the *Feynman rules* — in the case of QCD.

The propagators are obtained by computing each of the 2-point functions of the fields to leading order (LO). For QCD, in flat Euclidean space $\mathbb{R}^d$, and momentum space[7], we can look at each such correlation function one by one: Starting with the gauge field contribution

$$\begin{aligned}
S|_{AA} &= \int_{\mathbb{R}^d} \Big[\frac{1}{2}\mathrm{Tr} dA \wedge \star dA + \frac{1}{\xi}\mathrm{Tr} d\star A \wedge \star d\star A\Big] \\
&= \frac{1}{2}\int_{\mathbb{R}^d} \mathrm{d}^d X \Big[A^a_{\beta,\alpha}(X)A^{\beta,\alpha}_a(X) - A^a_{\beta,\alpha}(X)A^{\alpha,\beta}_a(X) + \frac{1}{\xi}A^{a,\alpha}_\alpha(X)A^\beta_{a,\beta}(X)\Big] \\
&= \frac{1}{2}\int_{\mathbb{R}^d} \mathrm{d}^d X A^a_\alpha(X)\Big[-\delta^\alpha_\beta\Delta + (1-\xi^{-1})\partial^\alpha\partial_\beta\Big]\delta^b_a A^\beta_b(X) \\
&= \frac{1}{2}\int_{KP}\int_{\mathbb{R}^d} \mathrm{d}^d X e^{iX\cdot(K+P)} A^a_\alpha(K)\Big[\delta^\alpha_\beta P^2 - (1-\xi^{-1})P^\alpha P_\beta\Big]\delta^b_a A^\beta_b(P) \\
&= \frac{1}{2}\int_{KP} \delta(K+P)A^a_\alpha(K)\Big[\delta^\alpha_\beta P^2 - (1-\xi^{-1})P^\alpha P_\beta\Big]\delta^b_a A^\beta_b(P),
\end{aligned} \tag{1.14}$$

[7]Note that we abuse notation by using the same symbol for a function and its Fourier transform, distinguishing them by arguments alone.

where we integrated by parts, discarding boundary terms, and moved to momentum space. The quadratic functional integral will simply give the inverse of the kernel

$$
\begin{aligned}
G^{ab}_{\alpha\beta}(P) &\equiv \left\langle A^a_\alpha(K) A^b_\beta(P) \right\rangle \\
&= \frac{1}{Z_{\text{QCD}}} \int \mathcal{D}A\overline{\psi}\psi\overline{\eta}\eta e^{-S|_{AA}+\cdots} A^a_\alpha(K) A^b_\beta(P) \\
&= \left(\delta_{\alpha\beta}\frac{1}{P^2} - (1-\xi)\frac{P_\alpha P_\beta}{P^4}\right)\delta^{ab}\delta(K+P) =
\end{aligned}
$$

(1.15)

In above and what follows, '...' denotes the irrelevant parts of the action. Proceeding with the quarks, noting that having conjugate fields will change one of the signs in the argument of the Dirac δ,

$$
\begin{aligned}
S|_{\overline{\psi}\psi} &= \int_{\mathbb{R}^d} \text{vol}_{\mathbb{R}^d} \overline{\psi}(\partial\!\!\!/ + m)\psi \\
&= \sum_{f,f'} \int_{\mathbb{R}^d} \mathrm{d}^d X \overline{\psi}^I_f(X)\left[\partial\!\!\!/ + m_f\right]\delta^{f,f'}\delta_{IJ}\psi^J_{f'}(X) \\
&= \sum_{f,f'} \int_{KP} \int_{\mathbb{R}^d} \mathrm{d}^d X e^{iX\cdot(-K+P)}\overline{\psi}^I_f(K)\left[iP\!\!\!/ + m_f\right]\delta^{f,f'}\delta_{IJ}\psi^J_{f'}(P) \\
&= \sum_{f,f'} \int_{KP} \delta(P-K)\overline{\psi}^I_f(K)\left[iP\!\!\!/ + m_f\right]\delta^{f,f'}\delta_{IJ}\psi^J_{f'}(P),
\end{aligned}
\tag{1.16}
$$

where we wrote $m = \text{diag}(m_1, \ldots m_{N_f})$ for the diagonal quark mass matrix m, and with the correlation function being

$$
S^{f,f'}_{IJ}(P) \equiv \left\langle \overline{\psi}^f_I(K)\psi^{f'}_J(P) \right\rangle = \frac{\delta^{f,f'}\delta_{IJ}\delta(P-K)}{iP\!\!\!/ + m_f} =
$$

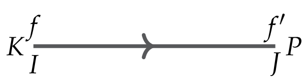

(1.17)

The remaining ghost propagator is perhaps the most straightforward

to compute:

$$\begin{aligned} S|_{\overline{\eta}\eta} &= \int_{\mathbb{R}^d} \mathrm{vol}_{\mathbb{R}^d} \langle \partial\overline{\eta}, \partial\eta \rangle \\ &= \int_{\mathbb{R}^d} \mathrm{d}^d X \overline{\eta}^a(X) \delta_{ab}(-\Delta) \eta^b(X) \\ &= \int_{KP} \int_{\mathbb{R}^d} \mathrm{d}^d X e^{iX\cdot(-K+P)} \overline{\eta}^a(K) \delta_{ab} P^2 \eta^b(P) \\ &= \int_{KP} \delta(P-K) \overline{\eta}^a(K) \delta_{ab} P^2 \eta^b(P), \end{aligned} \tag{1.18}$$

$$C^{ab}(P) \equiv \left\langle \overline{\eta}^a(K) \eta^b(P) \right\rangle = \frac{\delta^{ab}\delta(P-K)}{P^2} = \; K^{a} \cdots\cdots\rangle \cdots\cdots {}^{b}\, P \tag{1.19}$$

Vertex terms are related to the interacting parts of the action. In perturbation theory, these terms can be expanded in the limit of small but nonvanishing coupling, which results in the computation of field correlation functions in the sense of Eqn. (1.8) after changing the order of the expansion and integration, with the action replaced by its quadratic terms S_0. The Feynman rules, denoted here by Γ_Φ for a vertex of fields Φ, are obtained simply as the leading-order expansions of the action. Note that in the graphical rules factors of $1/n!$ are removed from the gluon n-point vertices after enforcing the fact that the n fields are each identical. Again, starting with the gauge contributions, we have, with normalised symmetrisation brackets, and writing $\overline{\mathrm{D}} = D - \boldsymbol{\nabla}$ for the gauge-field

dependent part of the covariant derivative

$$
\begin{aligned}
S|_{AAA} &= \frac{2}{2}\int\limits_{\mathbb{R}^d} \mathrm{Tr}\overline{\mathrm{D}}A \wedge \star \mathrm{d}A \\
&= g f^a_{bc} \int\limits_{\mathbb{R}^d} \mathrm{d}^d X A_a^{[\alpha,\beta]}(X) A^b_\alpha(X) A^c_\beta(X) \\
&= ig f^a_{bc} \int\limits_{KPQ}\int\limits_{\mathbb{R}^d} \mathrm{d}^d X e^{iX\cdot(K+P+Q)} K^{[\alpha} A_a^{\beta]}(K) A^b_\alpha(P) A^c_\beta(Q) \\
&= \frac{1}{2} ig f_{abc} \int\limits_{KPQ} \delta(K+P+Q)(\delta^{\alpha\gamma}K^\beta - \delta^{\alpha\beta}K^\gamma) A^a_\alpha(K) A^b_\beta(P) A^c_\gamma(Q) \\
&= \frac{1}{3!} ig f_{abc} \int\limits_{KPQ} \delta(K+P+Q) A^a_\alpha(K) A^b_\beta(P) A^c_\gamma(Q) \times \\
&\times \Big[\delta^{\alpha\beta}(P^\gamma - K^\gamma) + \delta^{\beta\gamma}(Q^\alpha - P^\alpha) + \delta^{\gamma\alpha}(K^\beta - Q^\beta)\Big],
\end{aligned}
\tag{1.20}
$$

$$
(\Gamma_{AAA})^{\alpha\beta\gamma}_{abc}(K,P,Q) = ig f_{abc}\Big[\delta^{\alpha\beta}(P^\gamma - K^\gamma) + \delta^{\beta\gamma}(Q^\alpha - P^\alpha) +
$$

$$
+ \delta^{\gamma\alpha}(K^\beta - Q^\beta)\Big] =
$$

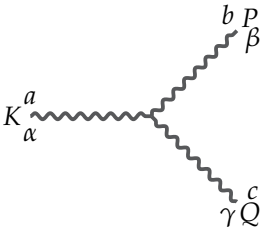

(1.21)

$$
\begin{aligned}
S|_{AAAA} &= \frac{1}{2}\int\limits_{\mathrm{R}^d} \mathrm{Tr}\overline{\mathrm{D}}A \wedge \star\overline{\mathrm{D}}A = \\
&= \frac{1}{4}g^2 f_{eab}f^{ecd}\int\limits_{\mathrm{R}^d} \mathrm{d}^d X A^a_\alpha(X)A^b_\beta(X)A^\alpha_c(X)A^\beta_d(X) \\
&= \frac{1}{2}\times\frac{1}{4}g^2(f_{eab}f^{ecd}-f_{eab}f^{edc})\int\limits_{KPQR}\int\limits_{\mathrm{R}^d}\mathrm{d}^d X e^{iX\cdot(K+P+Q+R)}\times \\
&\times A^a_\alpha(K)A^b_\beta(P)A^\alpha_c(Q)A^\beta_d(R) \\
&= \frac{3}{4!}g^2 f_{eab}f^{ecd}(\delta^\alpha_\gamma\delta^\beta_\delta-\delta^\alpha_\delta\delta^\beta_\gamma)\int\limits_{KPQR}\delta(K+P+Q+R)\times \\
&\times A^a_\alpha(K)A^b_\beta(P)A^\gamma_c(Q)A^\delta_d(R) \\
&= \frac{1}{4!}g^2\Big[f_{eab}f^e_{cd}(\delta^{\alpha\gamma}\delta^{\beta\delta}-\delta^{\alpha\delta}\delta^{\beta\gamma})+f_{eac}f^e_{bd}(\delta^{\alpha\beta}\delta^{\gamma\delta}-\delta^{\alpha\delta}\delta^{\gamma\beta}) \\
&+ f_{ead}f^e_{bc}(\delta^{\alpha\beta}\delta^{\delta\gamma}-\delta^{\alpha\gamma}\delta^{\delta\beta})\Big]\int\limits_{KPQR}\delta(K+P+Q+R)\times \\
&\times A^a_\alpha(K)A^b_\beta(P)A^c_\gamma(Q)A^d_\delta(R),
\end{aligned}
\tag{1.22}
$$

$$
\begin{aligned}
&(\Gamma_{AAAA})^{abcd}_{\alpha\beta\gamma\delta}(K,P,Q,R) \\
&\quad= g^2\Big[f_{eab}f^e_{cd}(\delta^{\alpha\gamma}\delta^{\beta\delta}-\delta^{\alpha\delta}\delta^{\beta\gamma})+f_{eac}f^e_{bd}(\delta^{\alpha\beta}\delta^{\gamma\delta}-\delta^{\alpha\delta}\delta^{\gamma\beta}) \\
&\quad+f_{ead}f^e_{bc}(\delta^{\alpha\beta}\delta^{\delta\gamma}-\delta^{\alpha\gamma}\delta^{\delta\beta})\Big] =
\end{aligned}
$$

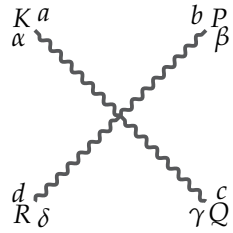

(1.23)

In the quark-gluon vertex one must note that the γ-matrix must be

placed in the appropriate position

$$\begin{aligned} S|_{\overline{\psi}A\psi} &= \int_{\mathbb{R}^d} \mathrm{vol}_{\mathbb{R}^d} \overline{\psi}\overline{\not{D}}\psi \\ &= -igT^a_{IJ}\delta^{f,f'} \int_{\mathbb{R}^d} \mathrm{d}^d X \overline{\psi}^I_f(X) \not{A}^a(X) \psi^J_{f'}(X) \\ &= -igT^a_{IJ}\delta^{f,f'} \int_{\mathbb{R}^d} \mathrm{d}^d X \int_{KPQ} e^{iX\cdot(-K+P+Q)} \overline{\psi}^I_f(K)\gamma_\alpha A^\alpha_a(P)\psi^J_{f'}(Q) \\ &= -igT^a_{IJ}\delta^{f,f'} \int_{KPQ} \delta(P+Q-K)\overline{\psi}^I_f(K)\gamma_\alpha A^\alpha_a(P)\psi^J_{f'}(Q), \end{aligned} \tag{1.24}$$

$$(\Gamma_{\overline{\psi}A\psi})^{ff'a}_{IJ\alpha}(K,P,Q) = -igT^a_{IJ}\delta^{f,f'}\gamma_\alpha\delta(P+Q-K) =$$

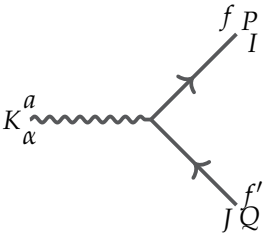

(1.25)

Once again, the ghost-gluon vertex causes no significant complications.

$$\begin{aligned} S|_{\overline{\eta}A\eta} &= \int_{\mathbb{R}^d} \mathrm{vol}_{\mathbb{R}^d} \left\langle \partial\overline{\eta}, \overline{\mathrm{D}}\eta \right\rangle \\ &= gf^{abc} \int_{\mathbb{R}^d} \mathrm{d}^d X \overline{\eta}_{a,\alpha}(X) A^\alpha_b(X)\eta_c(X) \\ &= -igf^{abc} \int_{\mathbb{R}^d} \mathrm{d}^d X \int_{KPQ} e^{iX\cdot(-K+P+Q)} K_\alpha \overline{\eta}_a(K) A^\alpha_b(P)\eta_c(Q) \\ &= -igf^{abc} \int_{KPQ} \delta(P+Q-K) K_\alpha \overline{\eta}_a(K) A^\alpha_b(P)\eta_c(Q), \end{aligned} \tag{1.26}$$

$$(\Gamma_{\overline{\eta}A\eta})_{\alpha}^{abc}(K,P,Q) = -igf^{abc}P_{\alpha}\delta(P+Q-K) =$$

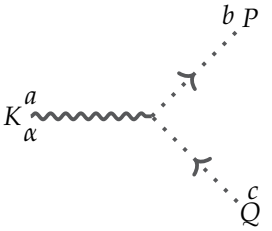

(1.27)

Lastly, one should keep in mind the generic rules associated with a Feynman diagram expansion:

- In each loop, continuous (momentum) variables are integrated over,
- In each loop, discrete indices are traced over,
- For each Grassmannian loop, a factor of -1 is inserted,
- For each graph, an appropriate *symmetry factor* is inserted.

As for the last point, the symmetry factors essentially account the number of times a diagram appears in the path integral and its order of expansion. They can be obtained by carefully expanding the functional integrals and performing them using *Wick's theorem* [48], but often it is convenient to simply compute them using the symmetry properties of graphs. Note that momentum conservation at each vertex is automatically enforced by the vertices presented in this Section.

1.8 QCD β Function and Asymptotic Freedom

With the QCD Feynman rules derived, we are in principle ready to proceed with calculations. However, a priori, it is not clear how much sense perturbative calculations make in a strongly coupled theory. As alluded to in Sec. 1.4, the question is answered at least partially by studying the way the coupling changes with energy scale, or equivalently, the β function of the theory.

Before discussing the details, it is sensible at this point to make a brief foray into the conventions related to renormalisation and regularisation

used in the Thesis. Over the 20th century, dealing with the emergence of seemingly infinite quantities became an everyday chore in field theory. Today, the standard approach to handling them can be split into two parts: The apparently infinite quantities are associated with finite ones by using *regularisation*, with a subsequent *renormalisation* of the action rendering it and related quantities finite, and allowing for the determination of finite physical quantities.

The modern choice for the former is usually *dimensional regularisation*, where divergent integrals encountered in field theoretical calculations are analytically continued to (a sufficiently large open set of) the complex plane. The divergences are then associated with the poles of the analytically continued expressions at integer dimensions, usually in $3+1$ spacetime dimensions. The behaviour near them is extracted by expanding them in, conventionally, $D = 4 - 2\epsilon$ dimensions for small ϵ. However, occasionally other regularisation methods are useful. In fact, an example of this is in the determination of the logarithmic terms of the cold dense QCD pressure, where the logarithmic dependence on the coupling can be obtained by formally regularising integrals with a *cutoff* [2] (see also Sec. 3.5), by which one essentially restricts the application of the used description to certain scales.

As for renormalisation, continuum field theories commonly use subtractive renormalisation, where physical quantities are obtained by subtracting *counterterms* from the Lagrangian. In this process, the parameters and fields of the Lagrangian are scaled by appropriate renormalisation constants. The counterterms and renormalisation constants are obtained by evaluating specific diagrams associated with the different parameters and fields of the Lagrangian at a specific *renormalisation scale*, and their form depends also on the choice of the exact *renormalisation scheme*. Commonly used subtractive schemes in continuum are the minimal subtraction (MS) and the modified minimal subtraction ($\overline{\text{MS}}$) schemes, with the former removing only the divergences and the latter also a commonly occurring constant. The renormalisation scale also plays an important role when estimating the magnitude of perturbative corrections in calculations. Aside from subtractive renormalisation, alternative renormalisation methods are also in use. Most prominent of these are Wilsonian renormalisation group methods, which are particularly useful in lattice

field theory, where the lattice spacing acts as a regulator — as lattice field theory will only be mentioned very occasionally, we will not cover this further.

Returning to the question of the sensibility of pQCD, we define the β function as the variation of the coupling g of a QFT with the energy scale Λ,

$$\beta(g) \equiv \frac{\partial g}{\partial \ln \Lambda} = \Lambda \frac{\partial g}{\partial \Lambda}. \tag{1.28}$$

To give some context, in order to renormalise a theory, in addition to such β functions β_i of any couplings g_i, one must generally consider the *anomalous dimensions of the fields* γ_i for each field ϕ_i. They are defined in an analogous way to the β function. Defining the renormalisation constant Z_i between the renormalised and bare fields ϕ_i^r, ϕ_i^b respectively as $Z_i^{1/2}\phi_i^r = \phi_i^b$, we define

$$\gamma_i \equiv -\frac{\Lambda}{2}\frac{\partial \ln Z_i}{\partial \Lambda} = -\frac{\Lambda}{2Z_i}\frac{\partial Z_i}{\partial \Lambda}. \tag{1.29}$$

Together, the anomalous dimensions and beta functions appear in the fundamental relation of renormalisation theory, the *Callan-Symanzik* or *Renormalisation group equation*, which, written for an n-point function $\Gamma^{(n)}$ at the scale Λ reads

$$\frac{\mathrm{d}}{\mathrm{d}\Lambda}\Gamma^{(n)} = \Big(\Lambda\frac{\partial}{\partial \Lambda} + \sum_i \beta_i \frac{\partial}{\partial g_i} + n\sum_j \gamma_j\Big)\Gamma^{(n)} = 0. \tag{1.30}$$

Measurements of physical quantities always occur at some reference scale Λ. The quantities can then be evolved according to the renormalisation group equations, allowing one to evaluate them at different scales. However, the β functions are, by construction, sufficient for examining the behaviour of the couplings themselves.

In QCD, the β function is one of the most accurately-known quantities in perturbation theory. The evaluation of successive terms has progressed with a steady pace since the discovery of asymptotic freedom, the current state-of-the-art result being a five-loop calculation due to Herzog et al. [49]. For qualitative purposes, the first nontrivial order suffices, and for reasons of convention we move from the coupling g_s to a rescaled

coupling $\alpha_s \equiv g_s^2/4\pi$:

$$\beta_{\mathrm{QCD}}(\alpha_s) = -\Big(\frac{11}{3}C_A - \frac{4}{3}T_F N_f\Big)\frac{\alpha_s^2}{4\pi} + \mathcal{O}(\alpha_s^3) \equiv \beta_0\alpha_s^2 + \mathcal{O}(\alpha_s^3), \quad (1.31)$$

with $C_A = N_c$ and $T_F = 1/2$ being group invariants and N_f the number of active quarks at the scale under consideration. This result has striking implications: For $N_c = 3$, it is negative as long as $N_f < 17$, in particular remaining so with the physically established values of N_c, N_f. This implies that the coupling *decreases*. We may obtain the explicit behaviour of the coupling simply by integrating the β function from a known scale Λ to Λ'. To LO, this yields

$$\alpha_s(\Lambda') = \frac{\alpha_s(\Lambda)}{1 - 2\beta_0\alpha_s(\Lambda)\ln(\Lambda'/\Lambda)}. \quad (1.32)$$

It is due to the behaviour seen in Eqn. (1.32) that the asymptotic freedom discussed in Sec. 1.4 arises: The coupling can be made arbitrarily small at a sufficiently large scale. Unfortunately for applications of pQCD, it does not decrease very rapidly, and at the Z-boson mass of $M_Z \approx 91\,\mathrm{GeV}$ has been measured to still be $\alpha_s(M_Z) \approx 0.12$ [31] – in comparison, the QED coupling α_e at the same scale is much smaller, $\alpha_e(M_Z) \approx 7.8 \times 10^{-3}$ [50]. Regardless, the qualitative behaviour is absolutely vital for justifying the use of weak-coupling perturbation theory.

The evolution equation portrayed in Eqn. (1.32) is generic for any field theory with a quadratic LO coefficient of the β function. Examining it, we see a peculiar behaviour appearing at the scale $\Lambda_L = \Lambda e^{\frac{1}{2}\beta_0^{-1}\alpha_s^{-1}(\Lambda)}$: The coupling seems to diverge based on this calculation, and this even happens at a *finite* scale. Substituting the results from the previous paragraph to Eqn. (1.32), we obtain a value of $\Lambda_L \sim \mathcal{O}(10^{-1})$ GeV. While the value should be taken with a grain of salt — even at $\Lambda = M_Z$ the coupling is sizable — this indicates that pQCD breaks down well before vanishingly small energies. Indeed, it is a sign of the change from QCD degrees of freedom to hadrons, the so-called (de)confinement transition, which is discussed in more detail in the context of the phase diagram in Sec. 3.1. In QED and other theories where the coupling increases with the energy scale, and the high-energy limit of the theory is not protected by asymptotic freedom, such a breakdown occurs at high energies instead, and is

known as a *Landau pole*. In QED, or generally electroweak theory, it is often taken to indicate that the theory must be replaced by a different description far in the ultraviolet.

It is interesting to consider a different behaviour: theories where the couplings do *not* vary with the scale, that is, ones with vanishing β functions. In the absence of Landau poles, such theories can be defined at arbitrary small or large scales, and as such provide a tool for understanding QFTs beyond the weakly coupled limit. Typically used scale-invariant theories are Conformal Field Theories (CFTs), which can in fact be characterised as those with vanishing (generalised) β functions of *all* operators. CFTs are used widely in physics, from many-body physics to the (suggestively named) AdS–CFT conjecture, and also in mathematics, particularly in two dimensions. In the latter context, they serve as one of the few examples of rigorously well-defined QFTs. The relevance of CFTs for this Thesis is mainly related to the Publication [3] (see also Sec. 2.10), where a specific CFT is used in a nonperturbative study of the thermal pressure, and the scale-invariant nature of the theory plays an important role in studying its properties.

Chapter 2

Thermal Field Theory

At this point, it is time to introduce a *medium* to a QFT. In particular, we formulate an equilibrium QFT at finite temperature in the *imaginary-time formalism* used extensively in the Publications included in this Thesis, and discuss its implications. Afterwards, we add finite chemical potentials as manifestations of *global* symmetries of the action, incorporating this in the thermal field theory formalism. Following this, some standard computation techniques and related results used in perturbation theory are covered. Next, the infrared problems plaguing thermal QFTs are considered, with a focus on QCD, and some solutions are briefly discussed, with a proper treatment left for the following Chapter. The Chapter finishes with introduction of the results of two of the Publications included in the Thesis, the first concerning calculation methods at finite density, and the second some nonperturbative results from conformal low-dimensional QFTs, in particular from QED in $2+1$ dimensions and at finite temperature.

2.1 Thermal QFT in Equilibrium

In order to construct a QFT at finite temperature, we can follow the well-established foundation of (classical or quantum) statistical mechanics and generalise it from the point-particle setting to a quantum field theory. As a starting point, we consider the *temperature* T of the system under study not as a dynamical quantity, but rather as an intrinsic property of the

background. In other words, we take the system to be in a *thermal bath*. The quantities of interest in a statistical setting are correlation functions. Then, in analogy with the *canonical ensemble* treatment of statistical mechanics, the correlation function of an observable is obtained by tracing it against the *Boltzmann measure* $e^{-\beta H}$, where H is the Hamiltonian of the system and β the inverse temperature

$$\langle \mathcal{O} \rangle = \frac{\mathrm{Tr} e^{-\beta H} \mathcal{O}}{\mathrm{Tr} e^{-\beta H}}. \tag{2.1}$$

This is, of course, very reminiscent of the corresponding formula in the functional integral formalism, Eqn. (1.8). Indeed, even the functional notation is borrowed from statistical mechanics, compare for example Eqn. (1.7) with the partition function of statistical mechanics in the canonical ensemble, $Z = \mathrm{Tr} e^{-\beta H}$. This close correspondence between the formalisms is one of the main reasons for using functional integrals in this Thesis, along with the quantisation of non-Abelian gauge theories they make manageable. Given a relationship of this form, the field-theoretical generalisation of the statistical correlation functions should be achieved by identifying the Euclidean action S with βH and the functional integral with the trace.

The latter is an intuitively obvious thing to do: Identifying the trace with an *integral* is already natural and a commonplace procedure in both classical statistical systems with continuous degrees of freedom as well as in quantum statistics. Meanwhile, functional integrals can, at least when neglecting mathematical rigour, be constructed with a limiting process of a sequence of ordinary high-dimensional integrals, corresponding to the quantum field at different points in the base space.

Identifying S and βH is somewhat more involved. To realise why making such an identification is a sensible course of action, we note that $e^{-\beta H}$ is nothing but the analytic continuation of the unitary time evolution operator $e^{iH(t_2 - t_1)}$ familiar from point-particle quantum mechanics to *imaginary time* on the time interval $(0, \beta)$. On the other hand, in a field theory context the (Euclidean, but vacuum) matrix element of an operator between states at different times can be represented as a functional integral against the action e^{-S}. This immediately extends to our analytically continued evolution operator: the matrix element between states at

(imaginary) times 0 and β can be represented in the same way, over the fields with boundary values set by the field values at 0 and β. Hence, the identification of the expectation values $\mathrm{Tr} e^{-\beta H}\mathcal{O}$ with functional integrals $\int \mathcal{D}\Phi e^{-S}\mathcal{O}$ is correct; the only step left is to specify how the functional integration behaves in more detail.

To do so, let us consider the nature of this new auxiliary time variable a bit more. In vacuum, the time variable typically ranges through $\mathbb{R}$: Matrix elements are computed between *asymptotic* states. In a thermal medium, the whole real axis is to be replaced with an imaginary time variable that only takes values on $(0, \beta)$. The imaginary nature corresponds to rotating a physical Lorentzian path integral to Euclidean signature, in a way that is usually known as a *Wick rotation*, but more interestingly, the time dimension has been turned into a line segment. To determine the boundary conditions, we recall that the boundary conditions in vacuum are vanishing — the fields ought to have compact support. Now requiring the functional integral to behave as a trace sets them to be periodic or antiperiodic, changing not only the domain of the integration for the action, but also for the functional integral. It is due to the (anti)periodic nature that one commonly says that the time direction is *compactified into a circle*, replacing the standard Euclidean spacetime $\mathbb{R}$ with $S^1 \times \mathbb{R}^3$. Another important consequence is that singling out the temporal direction reduces the symmetries of the system, as will be discussed in more detail in Sec. 2.5.

In making this identification with the Euclidean time variable and an auxiliary imaginary time describing thermal properties, we have, of course, made an important assumption: Time itself ought not to play a role in any quantities computed in this way, since imaginary time is needed solely for a thermal description. As such, this *imaginary-time formalism*, also known as *Matsubara formalism* [51], only describes time-independent quantities in *equilibrium*. A brief discussion of the formalism for time-dependent and/or nonequilibrium quantities will follow in the next Section. However, even the simpler imaginary-time formalism allows one to compute many quantities of practical interest, such as free energies and their derivatives.

Another way to see the periodic nature arise, as well as to further motivate the term imaginary time, is to construct a so-called *KMS* (Kubo–

Martin–Schwinger) *relation* [52, 53] for a correlation function of two (possibly composite) operators $\mathcal{O}_1, \mathcal{O}_2$. Making an exception to the usual assumptions of this Thesis, we begin in *Minkowskian* spacetime, with the two operators evaluated at spacetime points $(t_1, x_1), (t_2, x_2)$

$$\left\langle \mathcal{O}_1^M(t_1, x_1)\mathcal{O}_2^M(t_2, x_2) \right\rangle = \frac{1}{Z}\mathrm{Tr}\Big(\mathcal{O}_1^M(t_1, x_1)\mathcal{O}_2^M(t_2, x_2)e^{-\beta H} \Big). \tag{2.2}$$

The next step is to write the time evolution of the second operator explicitly in the Heisenberg picture, assuming H to be time-independent

$$\begin{aligned} \langle \mathcal{O}_1^M(t_1, x_1)\mathcal{O}_2^M(t_2, x_2) \rangle &= \frac{1}{Z}\mathrm{Tr}\Big(\mathcal{O}_1^M(t_1, x_1)e^{it_2 H}\mathcal{O}_2^M(0, x_2)e^{-it_2 H - \beta H} \Big) \\ &= \frac{1}{Z}\mathrm{Tr}\Big(\mathcal{O}_1^M(t_1, x_1)e^{-\beta H}e^{i(t_2 - i\beta)H}\mathcal{O}_2^M(0, x_2)e^{-i(t_2 H - i\beta)H} \Big). \end{aligned} \tag{2.3}$$

Finally, we interpret $e^{i(t_2 - i\beta)H}$ as a formal time evolution operator to *complex* time and obtain

$$\begin{aligned} \left\langle \mathcal{O}_1^M(t_1, x_1)\mathcal{O}_2^M(t_2, x_2) \right\rangle &= \frac{1}{Z}\mathrm{Tr}\Big(\mathcal{O}_2^M(t_2 - i\beta, x_2)\mathcal{O}_1^M e^{-\beta H} \Big) \\ &= \left\langle \mathcal{O}_2^M(t_2 - i\beta, x_2)\mathcal{O}_1^M(t_1, x_1) \right\rangle. \end{aligned} \tag{2.4}$$

After moving to Euclidean space $t_i \mapsto \tau_i = it_i$ and defining the Euclidean operators $\mathcal{O}_i^E(\tau_i) = \mathcal{O}_i^M(it_i)$ we see near-periodicity in the imaginary time direction:

$$\left\langle \mathcal{O}_1^E(\tau_1, x_1)\mathcal{O}_2^E(\tau_2, x_2) \right\rangle = \left\langle \mathcal{O}_2^E(\tau_2 + \beta, x_2)\mathcal{O}_1^E(\tau_1, x_1) \right\rangle. \tag{2.5}$$

In particular if $\mathcal{O}_i$ are fundamental fields with a shared *grading* — both either bosonic or fermionic — the correlator is exactly (anti)periodic.

While the Faddeev-Popov ghost fields discussed in Sec. 1.6 and Sec. 1.7 do not appear in physical observables, the (anti)periodicity appears also in the functional integrals as discussed earlier, and we note at this point that one must be careful with the ghost fields. Despite being Grassmannian, they arise from a *bosonic* Jacobian matrix as seen earlier, and as a result also obey periodic, not anti-periodic, boundary conditions.

In conclusion, the imaginary-time formalism of thermal field theory can be summarised in the following fundamental statement:

Time-independent correlation functions of Euclidean QFTs in an equilibrated thermal medium can be computed by compactifying the time direction of the associated Euclidean vacuum QFT into a circle of radius $\beta/2\pi$, and setting the fundamental fields to have either periodic or antiperiodic boundary conditions depending on their grading.

Lastly, a practical note. Particularly in a perturbative context, Fourier analysis is an invaluable tool, as computations are often considerably more tractable in momentum space. There, the compactification of one of the spacetime directions has a striking consequence: elementary Fourier analysis tells us that the momenta p_0 along this direction are *discretised*, taking only values $\omega_n = 2n\pi T$ for periodic boundary conditions and $\omega_n = (2n+1)\pi T$ for antiperiodic boundary conditions, with $n \in \mathbb{Z}$. The discretised momentum variables are commonly known as (bosonic or fermionic) *Matsubara modes*. Similar replacements must be made elsewhere, with for example integrals transforming to appropriately scaled discrete summations, which is covered in more detail in Sec. 2.4.

2.2 Moving Beyond the Imaginary-Time Formalism

It is evident from the construction of the basic imaginary-time formalism that it is restricted to computing time-independent quantities. The physical time is left out when identifying the auxiliary imaginary parameter with an imaginary time in the formal evolution operator. While, as mentioned, still useful for the study of many problems, the formalism is not capable of directly probing the properties of time-dependent quantities in out-of-equilibrium systems. At least in some specific cases, this problem can be solved by analytically continuing the Euclidean expressions to Minkowski space.

Regardless, one has to wonder how a therma field theory describing the time-dependence from the start could be formulated. A way to solve the issue is to, instead of taking the 'time' variable to be purely imaginary, fully *complexifying* it. Then, in essence, the imaginary part of the complex time evolution corresponds to the thermal part of the operator on a compact interval as in the imaginary-time formalism, but there is still a physi-

cal time variable in the real part of the complexified time. This formalism is known as the *real-time formalism* or the *Schwinger–Keldysh formalism*.

The most commonly encountered form of the Schwinger–Kelydish formalism, constructed using a contour extending by $-i\beta$ on the lower half-plane, still requires us to use the tools of classical thermodynamics — ensembles, a well-defined temperature, and so on. Consequently, it leaves out the possibility of studying truly nonequilibrium quantities. However, slight deviations from equilibrium are allowed, enabling the computation of important time-sensitive quantities such as decay rates of particles, useful in studies of Beyond Standard Model physics; properties of bubble nucleation, needed in the study of cosmological phase transitions; and the details of transport phenomena, essential when examining heavy-ion collisions. However, the formalism also admits a more general description using arbitrary density operators, allowing the study of fully nonequilibrium phenomena.

The extended range of applicability makes one question why bother with the imaginary-time formalism to begin with, but unfortunately the Schwinger-Keldysh method comes with its own downsides. Most notable of these is the fact that one has to double number of independent fields, which naturally makes computations more complicated. In addition, the more complicated causal structure requires one to consider a number of new correlation functions. Especially the introduction of new two-point functions with different analyticity properties is a standard chore in real time. The choice was made to omit a more thorough exposition on the formalism due to the added complexity: It is *not* used in any of the included Publications and fully deriving it would cause significant notational and conceptual sidetracking. As always, the interested reader is suggested to consult any of the comprehensive reviews and books available on the topic, such as [54, 55, 56].

2.3 QFTs at Finite Densities

While related to the presence of a medium, the details of introducing finite density to a QFT differs somewhat from the introduction of a finite temperature. However, as with finite temperature, our treatment starts from statistical mechanics, where the study of (quantum) particles can be

readily generalised to a field theory. To achieve this, we ought to replace the Boltzmann measure $e^{-\beta H}$ with the *Gibbs measure* $e^{-\beta(H-\mu Q)}$, or equivalently the canonical ensemble with the *grand-canonical ensemble*. Here Q and μ are the conjugate pair of a *number density (operator)* and the associated *chemical potential* respectively.

It turns out that the density is given by an integrated (zero-component of a) global *Noetherian symmetry current* j. For a symmetry transformation u parametrised by a variable θ, acting on fields ϕ^a and leaving the Lagrangian $\mathcal{L}$ invariant, the symmetry current is given by

$$j_\alpha = \sum_a \frac{\delta \mathcal{L}}{\delta \partial^\alpha \phi^a} \frac{\delta u_\theta^a(\phi^a)}{\delta \theta}. \tag{2.6}$$

At first sight, the above claim might seem puzzling: Why is a finite density, or eventually a chemical potential, so intimately related to the somewhat abstract Noether symmetry? However, in the proper context, this makes perfect sense: A chemical potential describes an excess of *something* — a type of particles, a quantum number, any similar property. However, as we are working strictly with equilibrium systems, this excess must be a constant in the base space, a conserved quantity. In terms of the current, it must be divergence-free. At this point, it becomes understandable why the excess must correspond to a (global) symmetry transformation acting on the fields of the Lagrangian, and the realisation opens up the powerful machinery of Noetherian symmetries and currents.

In principle, one can consider a number of different densities and associated symmetries, but their implementations often share similarities. For QCD, one is typically interested in some form of quark densities, and the associated symmetry is a $\mathrm{U}(1)^{N_f}$ symmetry acting nontrivially on each of the quark flavours. To be explicit, the one-parameter group of transformations reads

$$\overline{u} : \psi \mapsto (\mathbb{1} - i\Theta)\psi, \qquad u : \overline{\psi} \mapsto (\mathbb{1} + i\Theta)\overline{\psi}, \tag{2.7}$$

where Θ is some arbitrary constant real diagonal matrix in flavour space. The gauge field does not transform. This is evidently a symmetry of the Lagrangian Eqn. (1.6) for each quark flavour. In Eqn. (2.7) we have made

the choice of transforming the fields in the antifundamental representation and their conjugates in the fundamental representation; note that this is possible without loss of generality as any physical quantities involve summing over 'particles and antiparticles', that is, two chemical potentials with opposite signs.

We immediately obtain the symmetry current by substituting the transformation in Eqn. (2.7) to Eqn. (2.6), giving us $j_\alpha = \overline{\psi}\gamma_\alpha\psi$. In particular, the quark number charge is given by

$$Q = \int_{\Sigma_t} j_0 = \int_{\Sigma_t} \psi^\dagger\psi \tag{2.8}$$

where Σ_t represents a single time slice of a foliation of the base space. The Dirac fermions are particularly amenable to the addition of a finite chemical potential. According to the subtraction prescription, removing $-\mu Q$ from the Hamiltonian directly corresponds to modifying the standard Dirac Lagrangian of the fth quark flavour with chemical potential μ_f by changing the partial derivative according to

$$\overline{\psi}_f\partial\psi_f \mapsto \overline{\psi}_f\Big(\gamma^0(\partial_0+\mu_f)+\gamma^i\partial_i\Big)\psi_f. \tag{2.9}$$

Naturally, this immediately generalises to the covariant derivative appearing in the interacting Lagrangian of Eqn. (1.6) by linearity. It turns out that the replacement is also identical for other standard Lagrangians, an important example being a $\mathrm{U}(1)$-charged complex scalar field where showing this explicitly is slightly less trivial due to the form of the action, but can be accomplished by introducing a pair of auxiliary conjugate momentum fields [57, 5]. Thus, at least restricting to QFTs that the articles included in this Thesis are concerned with, we can make the following statement:

Time-independent correlation functions of Euclidean QFTs in an equilibriated dense medium can be computed by shifting the 0*-component of the derivatives of each field with a chemical potential μ by μ.*

Notably, this is completely compatible with the modifications needed to move to finite temperature.

As with finite temperature, it is important to observe the consequences of the modification in Eqn. (2.9) in momentum space. Since the chemical

potential μ is a constant, a simple Fourier transformation shows that the change corresponds to a shift[1] $p_0 \mapsto p_0 + i\mu$ in the zero-component of the momentum P, or equivalently the Matsubara modes ω_n.

Finally, we consider the specific example of QCD, where the relevant part is the Dirac Lagrangian present in Eqn. (1.6). As mentioned, each quark flavour has its own chemical potential. To be specific, we consider three active flavours so that the set of chemical potentials is $\{\mu_u, \mu_d, \mu_s\}$. Often a more convenient representation is to use conserved quantum numbers instead: The baryon number (B), electric charge (Q), and strangeness (S) constitute an equally good choice of symmetries. The linear map for the change of basis from $\{\mu_B, \mu_Q, \mu_S\}$ to $\{\mu_u, \mu_d, \mu_s\}$ can be read off simply from the quantum numbers of the quarks shown in Fig. 1.2 (with the addition of the baryon number, which is $1/3$ for each flavour), and by inverting it we get

$$L: \begin{pmatrix} \mu_u \\ \mu_d \\ \mu_s \end{pmatrix} \mapsto \begin{pmatrix} \mu_B \\ \mu_Q \\ \mu_S \end{pmatrix} = \begin{pmatrix} 1 & 2 & 0 \\ 1 & -1 & 0 \\ 0 & 1 & -1 \end{pmatrix} \begin{pmatrix} \mu_u \\ \mu_d \\ \mu_s \end{pmatrix}. \tag{2.10}$$

We will have more to say about the nature of the chemical potentials in concrete physical systems in Sec. 3.2. It turns out that in cool neutron stars constraining the chemical potentials results in only a single free parameter to a good approximation.

2.4 Evaluating Matsubara Sums

Following the developments of this Section so far, we have gathered the necessary tools to move from a vacuum QFT to an equilibrium QFT at finite temperature and density. Modifications occur only in quantities related to the 'temporal', or 0-component, direction in the Euclidean spacetime. For future reference, we need only the generalisations of the Feynman rules of Sec. 1.7. At finite temperature, they are modified by enforcing the zero-components of momenta p_0 to take values at Matsubara modes ω_n, fermionic (odd integer multiples of πT) for quarks, bosonic

[1] Note that the arbitrary choice of representations in Eqn. (2.7) determines this sign, and the opposite convention is also very commonly used.

(even integer multiples of πT) for gluons and ghosts; changing the zero-component integrals from $\int_{\mathbb{R}} \mathrm{d}p_0/(2\pi)$ to scaled sums $T\sum_{\omega_n}$; and changing all Dirac deltas with zero-component arguments $\delta(p^0)$ to scaled Kronecker deltas $\beta\delta_{p^0,0}$. At finite quark number densities μ^f, the zero-components of momenta p^0 of quarks are further shifted to $p^0 + i\mu^f$.

This leads to a change in practical computations, as instead of fully SO(4)-symmetric, often conveniently dimensionally regularised integrals one must compute sums over the Matsubara frequencies, alongside the 'standard' integrals over the spatial momenta. In what follows, we will review a well-known method for converting such *Matsubara sums* to integrals [57, 5], which conveniently also separates the thermal and nonthermal contributions.

We start by considering a sum $T\sum_{\omega_n;l} f(\omega_n)$ for $f : \mathbb{C} \to \mathbb{C}$ an a priori arbitrary function, with $l \in \{B, F\}$ indicating whether one sums over fermionic or bosonic modes[2].

We define an auxiliary function

$$\nu_l : \mathbb{C} \to \mathbb{C}, \quad x \mapsto (-1)^l i n_l(ix), \tag{2.11}$$

where $n_l(x) = (\exp(\beta x) - (-1)^l)^{-1}$ is the Bose or Fermi distribution function and we define $(-1)^B \equiv 1, (-1)^F \equiv -1$. Now, we see right away that ν_l is meromorphic with poles (only) at the Matsubara frequencies of appropriate grading ω_n, and furthermore can observe that at these poles $\mathrm{Res}(\nu_l, x = \omega_n) = T$. If we now further suppose that f is also meromorphic with *no* poles on the real axis, a simple exercise in analysis shows us that we are able to construct a curve $\Gamma_\delta = \cup_{\omega_n} C_\delta(\omega_n)$ with $\delta > 0$ chosen so that for each $n \in \mathbb{Z}$ only a single pole is enclosed within each of the circles $C_\delta(\omega_n)$ and write, by Cauchy's theorem,

$$T\sum_{\omega_n;l} f(\omega_n) = \frac{2\pi i}{2\pi i}\sum_{\omega_n,l} \mathrm{Res}(f(x)\nu_l(x), x = \omega_n) = \int_{\Gamma_\delta} f(x)\nu_l(x)\frac{\mathrm{d}x}{2\pi i}. \tag{2.12}$$

This is already an integral representation, but a more convenient form is obtained by further deforming Γ_δ into a long counterclockwise rectangle running along the real axis, with the long sides above and below it by

[2] An alternative, perhaps more common, notation is to write $\sum_{\{\omega_n\}}$ for fermionic Matsubara sums. This is also used later in the Thesis, particularly in the context of sum-integrals.

a small amount[3] of $\epsilon > 0$. The small strips at infinity vanish since f is regular on the reals, and, substituting ν_l, we are left with

$$T\sum_{\omega_n;l} f(\omega_n) = (-1)^l \left(\int_{-\infty-i\epsilon}^{\infty-i\epsilon} f(x) n_l(ix) \frac{\mathrm{d}x}{2\pi} + \int_{+\infty+i\epsilon}^{-\infty+i\epsilon} f(x) n_l(ix) \right) \frac{\mathrm{d}x}{2\pi}. \tag{2.13}$$

Changing $x \mapsto -x$ in the second variables, and using $-n_l(-x) = (-1)^l + n_l(x)$, we get the final form of our integral representation

$$T\sum_{\omega_n;l} f(\omega_n) = \int_{\mathbb{R}} f(x) \frac{\mathrm{d}x}{2\pi} + (-1)^l \int_{-\infty-i\epsilon}^{\infty-i\epsilon} \Big(f(x) + f(-x) \Big) n_l(ix) \frac{\mathrm{d}x}{2\pi}. \tag{2.14}$$

There are some noteworthy points about Eqn. (2.14). The first term represents $T = 0$ contributions, and we were able to set $\epsilon \to 0$ there by assuming f to be regular on the real axis. In addition, at least formally, we may immediately analytically continue the sum by setting $x \mapsto x - i\mu$ in order to obtain expressions at finite μ.

Occasionally, one runs into a situation where the criteria set for f — namely, regularity on the real axis — are not met, particularly for specific values of other parameters (such as three-momenta and masses) appearing in f. Often, this is a nonissue as long as each separate term of the series is well-defined. In that case, one can, for example, use arguments of uniform convergence to see that the sum must be continuous, or rely on the fact that the value of the sum on a null set of three-momenta is irrelevant if one is only interested in its integral over the said momenta, as is often the case. Slightly more care must be taken when approaching the zero-temperature limit if one wishes to use an integral representation (similar to) Eqn. (2.14), as certain summands (or, at the limit, integrands) might require principal value interpretations. For details, see Appendix C of [1].

To make use of the tools obtained here, we compute two simple examples of Matsubara *sum-integrals* appearing in perturbative computations

[3] To be precise, this distance is constructed to be smaller than 1) smallest the distance between the real axis and any poles of f, and 2) δ, that is, the distance needed to separate each circle around a Matsubara pole.

of the leading order free energy in Sec. 2.10 and Sec. 3.3. These are

$$B(T;d) \equiv \sum\!\!\!\!\!\!\int_{P} \ln P^2 \quad \text{and} \quad F(T,\mu;d) \equiv \sum\!\!\!\!\!\!\int_{\{Q\}} \ln Q^2 \tag{2.15}$$

where we have defined the sum-integral sign $\sum\!\!\!\!\!\!\int_P \equiv T\sum_{\omega_n}\int \frac{\mathrm{d}^d p}{(2\pi)^d}$ and use the braces $\{\}$ in the integration limits to indicate fermionic grading of the Matsubara sum in F. Note that the chemical potential is set to zero for B, as only fermions need to be considered at finite chemical potential for the purposes of QCD.

In both cases, it is useful to first differentiate under the summation sign. Starting with the bosonic integral and denoting weak equality up to dimensionally regulated spatial p-integration by $\approx$, we obtain

$$\begin{aligned} T\sum_{\omega_n} \ln P^2 &\approx 2T\int \mathrm{d}p\, p \sum_{\omega_n} \frac{1}{\omega_n^2 + p^2} \\ &\approx 2i\int \mathrm{d}p \int_{-\infty-i\epsilon}^{\infty-i\epsilon} \frac{\mathrm{d}x}{2\pi}\Big(\frac{1}{x+ip} - \frac{1}{x-ip}\Big) n_B(ix) \\ &\approx 2T\int \mathrm{d}p\, n_B(p) \approx 2T\ln\Big(1-\exp(-p/T)\Big), \end{aligned} \tag{2.16}$$

where scale-free vacuum integrals vanish in this massless case in dimensional regularisation. Next, performing the spatial integral, the angular parts are trivial and yield the standard measure of the $d-1$-sphere $\lambda(S^{d-1}) = 2\pi^{d/2}/\Gamma(d/2)$, while the radial integral is a simple Γ function after expanding the logarithm, and in the end we obtain

$$\begin{aligned} B(T;d) &= 2T\frac{\lambda(S^{d-1})}{(2\pi)^d}\int_{\mathbb{R}_+} \mathrm{d}p\, p^{d-1} \ln\Big(1-\exp(-p/T)\Big) \\ &= -2T^{d+1}\frac{\lambda(S^{d-1})}{(2\pi)^d}\Gamma(d)\sum_{n\in\mathbb{N}_+}\frac{1}{n^{d+1}} = -\frac{2\Gamma\left(\frac{1+d}{2}\right)}{\pi^{(1+d)/2}}\zeta(d+1)T^{d+1}, \end{aligned} \tag{2.17}$$

where ζ is the Riemann ζ function. The sum-integral is convergent for $\mathrm{Re}\, d > 0$; extension to a larger set of parameters is known as ζ regularisation in this context. The fermionic integral F is nearly identical, with the

major difference being the addition of a chemical potential and the Taylor expansion in the spatial integral, which requires more care. We get

$$T\sum_{\{\omega_n\}}\ln Q^2 \approx T\ln\Big(1+\exp(-[p-\mu]/T)\Big)+T\ln\Big(1-\exp(-[p+\mu]/T)\Big), \tag{2.18}$$

$$F(T,\mu;d)=\frac{2^{1-d}T^{d+1}}{\pi^{d/2}\Gamma(\frac{d}{2})}\left[\frac{(\mu/T)^{d+1}}{d(d+1)}-\Gamma(d)(1+(-1)^d)\mathrm{Li}_{d+1}(-e^{-\mu/T})\right.$$
$$\left.+\sum_{n\in\mathbb{N}_+}\frac{(-1)^{n+1}}{n^{d+1}}\Big\{\Gamma\Big(d,\frac{n\mu}{T}\Big)e^{n\mu/T}-(-1)^d\Gamma\Big(d,-\frac{n\mu}{T}\Big)e^{-n\mu/T}\Big\}\right]. \tag{2.19}$$

The last expression is readily evaluated for fixed d, which will be necessary in Sec. 2.10 for $d=2$ and Sec. 3.3 for $d=3$.

To close off this Section, we compute two additional sum-integrals appearing in perturbative computations in a way that does *not* use the integral representation derived earlier in this Section, but serve as further demonstrations of the ζ-regularisation technique. To wit, following [58] we first compute the fermionic integral

$$F_l^n(T,\mu;d)\equiv \sum\!\!\!\!\!\!\int_{\{Q\}}\frac{q_0^n}{(Q^2)^{l/2}}, \tag{2.20}$$

Instead of starting with the Matsubara sum, we perform the d- dimensional spatial integral first. Again, only the radial integral is nontrivial, and has the form of a simple B function, giving us an expression that can be summed with ease:

$$F_l^n(T,\mu;d)=\frac{T\mu(S^{d-1})}{(2\pi)^d}\frac{\Gamma(\frac{d}{2})\Gamma(\frac{l-d}{2})}{2\Gamma(\frac{l}{2})}\sum_{k\in\mathbb{Z}}\frac{(\pi T(2k+1)-i\mu)^n}{((\pi T(2k+1)-i\mu)^2)^{l/2-d/2}}$$
$$=T^{1+d+n-l}\frac{\pi^{d/2+n-l}}{2^{l-n}}\frac{\Gamma(\frac{l-d}{2})}{\Gamma(\frac{l}{2})}\times$$
$$\times\left(\zeta\Big[l-d-n,\frac{1}{2}-i\frac{\mu}{2\pi T}\Big]+(-1)^n\zeta\Big[l-d-n,\frac{1}{2}+i\frac{\mu}{2\pi T}\Big]\right), \tag{2.21}$$

where the two-argument ζ is the Hurwitz ζ function. As before, the final expression is defined also for values of $l - d - n$ for which the sum does not converge — for example, even when this quantity is negative.

An equivalent calculation for a bosonic momentum is of use at finite temperature. Setting the chemical potential to zero, the sum now results in the standard Riemann ζ function:

$$B_l^n(T;d) \equiv \sum\!\!\!\!\!\!\int_P \frac{p_0^n}{(P^2)^{l/2}} = T^{1+d+n-l} \frac{\pi^{d/2+n-l}}{2^{l-n-1}} \frac{\Gamma(\frac{l-d}{2})}{\Gamma(\frac{l}{2})} \zeta(l-d-n). \quad (2.22)$$

2.5 Tensor Structures in Thermal Field Theory

Both the compactification procedure associated with finite temperatures and the complex shift associated with finite densities single out the time direction — the rest frame of the thermal bath — from the spatial directions. This breaks the Lorentz symmetry, or in the Euclidean case the global SO(4) rotational symmetry, of the action, leaving only a spatial SO(3) rotation symmetry. This on the other hand affects calculations, for example by complicating the available tensor structures. With intact symmetry, the only constant tensors are the metric $g_{\alpha\beta}$ and the appropriately weighted Levi-Civita symbol $\sqrt{\det(g)}\varepsilon_{\alpha\beta\gamma\delta}$, but with the symmetry broken there is also the vector specifying the rest frame, conventionally defined as $N = (1, 0)$. As a result, expressions that only preserve the spatial SO(3) symmetry such as the spatial metric g_{ij} can appear.

As an example that will be used in Sec. 3.4, consider a rank two symmetric tensor field $T(P)$ depending on a single four-momentum P: In vacuum, it will admit a decomposition in the basis $\{g, P \otimes P\}$. However, the thermal basis is double in size, being given by $\{g, P \otimes P, P \otimes N + N \otimes P, N \otimes N\}$. As usual, further symmetries reduce the size of the basis. Supposing T to be transverse with respect to the four-momentum in the sense $T^{\alpha\beta}P_\beta = 0$, the remnant thermal basis is simply given by $\{g, N \otimes N\}$. A vitally important example is the gluon self-energy tensor $\Pi^{\alpha\beta}$ that has precisely these properties.

As this object will be used multiple times in the Thesis, it is worth commenting on this more. In particular, the transversality requirement

has intriguing and slightly nontrivial origins. It follows from the so-called Slavnov–Taylor identities, which relate n-point functions to each other. We will not go through the complete derivation; it can be achieved for example by explicitly constructing the BRST transformations mentioned in Sec. 1.6 (this is covered in detail in many textbooks, for example [46]). Applying the transformation to desired correlation functions then yields identities between correlation functions. In particular, applying it to the gluon propagator shows that the longitudinal part of the full propagator is given by the bare propagator. In other words, the self-energy corrections must be fully transverse. The Slavnov–Taylor identities are often seen as non-Abelian generalisations of the Ward–Takahashi identities, which are similar relations in QED. Indeed, the QED self-energy is likewise transverse, a fact which will be used in Sec. 2.10.

To continue with this specific (and useful) example, we will construct a convenient basis for a symmetric transverse tensor field of rank two. In order to do so, define three projection operators:

$$\mathbb{P}^D_{\alpha\beta}(P) = g_{\alpha\beta} - \frac{P_\alpha P_\beta}{P^2}, \tag{2.23}$$

$$\mathbb{P}^T_{\alpha\beta}(P) = g^i_\alpha g^j_\beta \Big(g_{ij} - \frac{p_i p_j}{p^2} \Big), \ \mathbb{P}^L(P) = \mathbb{P}^D(P) - \mathbb{P}^T(P). \tag{2.24}$$

It is easy to see that these are projections in the usual sense — symmetric and idempotent — and furthermore each is orthogonal to P, and $\mathbb{P}^T$ and $\mathbb{P}^L$ project onto mutually orthogonal subspaces. By defining $\overline{N} = \mathbb{P}^D(P)N$, the symmetric basis $\{g, P \otimes P, P \otimes N + N \otimes P, N \otimes N\}$ is seen to be equivalent to $\{\mathbb{P}^T(P), \mathbb{P}^L(P), P \otimes P, P \otimes \overline{N} + \overline{N} \otimes P\}$, which is more convenient: The basis for a symmetric and transverse $T(P)$ is now simply $\{\mathbb{P}^T(P), \mathbb{P}^L(P)\}$, and the tensor field admits an orthogonal decomposition

$$T(P) = \mathbb{P}^T(P)T^T(P) + \mathbb{P}^L(P)T^L(P). \tag{2.25}$$

Similar arguments and constructions are easy to extend to more complicated tensor structures, but in the end, the loss of complete Lorentz invariance will inevitably complicate matters. However, the explicit decomposition of Eqn. (2.25) will prove useful later in Sec. 3.4 in the context of Hard Thermal Loops.

2.6 Infrared Problems of Thermal Field Theories

From the point of view of perturbation theory, a particularly significant feature of thermal field theories that sets them apart from vacuum QFTs is their infrared behaviour. While it is well-known that the perturbative series of most physical QFTs in vacuum are merely asymptotic [59, 60] — in terms of Feynman graphs, the number of graphs grows factorially — they have been used extremely successfully to predict experimental results to very high accuracies, at least in theories such as QED that are weakly coupled.

However, at finite temperatures, a new problem arises. Even at relatively low orders in perturbation theory, naïve perturbative calculations encounter new uncancelled divergences. Ultraviolet (UV) divergences cancel in the usual way by means of renormalisation, as they should: In subtractive renormalisation, counterterms are constructed to remove them. What remains are leftover divergences that, in a typical context in a thermal equilibrium are most strongly associated with massless bosons: Without a mass to 'protect' them, it is easy to understand why the bosonic terms, and in particular their *Matsubara zero modes*, are particularly susceptible in the infrared (IR). In nature, gauge bosons are the prototypical particles with this characteristic.

For the rest of this Section we will mostly focus on QCD for concreteness, with other standard QFTs being in principle relatively simple extensions, although the details of the theory might affect the qualitative implications significantly. For QCD, the dynamics of gluons are of particular interest when studying the IR behaviour of the theory. In contrast, even at the massless limit the Matsubara modes of quarks always have a mass-like term πT protecting them in the IR. As such, fermions tend to cause less complications in the IR.

A transparent way to see that bosonic divergences are enhanced by thermal effects specifically is to consider the theory at high temperatures, and examine the way gluons contribute at different energy scales. The relevant scales are the *hard* scale πT, the *soft* scale $g_s T$, and the *ultrasoft* scale $g_s^2 T$, and the leading contributions to the free energy *from each scale* $\Omega_L \sim \int_{\mathbf{p}} p n_B(p)$ (that is, not necessarily leading order in the perturbative

expansion!) are given by

$$\Omega_L^{\text{hard}} \sim (\pi T)^4 n_B(\pi T) = \mathcal{O}(T^4), \tag{2.26}$$

$$\Omega_L^{\text{soft}} \sim (g_s T)^4 n_B(g_s T) = \mathcal{O}(g_s^3 T^4), \tag{2.27}$$

$$\Omega_L^{\text{ultrasoft}} \sim (g_s^2 T)^4 n_B(g_s^2 T) = \mathcal{O}(g_s^6 T^4). \tag{2.28}$$

For the two scales suppressed by powers of the coupling, we used the expansion $n_B(x) = T/x + \mathcal{O}(1)$ around $x = 0$. As mentioned, gluons are the most infrared-sensitive components of the QCD degrees of freedom, and we have only considered their contributions here. This is justified by repeating the analysis for the fermionic contributions $\Omega_L^F \sim \int_{\mathbf{p}} p n_F(p)$: While the behaviour of the distribution function n_F *is* qualitatively different at small and large scales, in contrast to the bosonic expansion it behaves as $n_F(x) \to 1/2$ as $x \to 0$. This much more benign behaviour will be important in Chapter 3, when analysing the cold dense regime.

The simple argument shows many interesting features. First, the soft, or *electric*, scale generates terms that are *fractional* in the coupling $\alpha_s = g_s^2/4\pi$, which are absent in the naïve diagrammatic expansion, an analytic (asymptotic) power series of α_s. The first such term is seen to be a $g_s^3 \sim \alpha_s^{3/2}$-contribution. The ultrasoft, or *magnetic*, scale is correspondingly seen to contribute starting at $\mathcal{O}(g_s^6)$.

Second, one can examine the way perturbative corrections arise in this fashion. The first correction from hard scales goes as $g_s^2 n_B(\pi T) = \mathcal{O}(g_s^2)$, showing that they are correctly described by standard perturbation theory. However, the corrections from soft scales are higher than one would naïvely expect, $g_s^2 n_B(g_s T) = \mathcal{O}(g_s)$, showing again how the odd powers of g_s arise. The last, and perhaps of the most fundamental importance, are the contributions from the ultrasoft scale: We see that $g_s^2 n_B(g_s^2 T) = \mathcal{O}(1)$ — these corrections are fundamentally nonperturbative, and cannot be captured by any perturbative computations. This is known as the *Linde problem* of QCD, after having been pointed out by Linde in [61], with the same observation made only slightly later by Gross, Pisarski, and Yaffe [62]. The short and more modern argument presented here is adapted from [56].

One can form some intuition to why perturbation theory breaks down by considering the physical situation: As discussed in Sec. 1.4, at sufficiently high energies (in this case, temperatures), the QCD degrees of freedom are quarks and gluons (see also the discussion on the phase diagram, Sec. 3.1). When interactions are considered, they effectively form a medium. Sufficiently energetic, hard, gluons are not affected by it at least to first approximation, propagating through it and only interacting through collisional interactions, those described by standard perturbation theory. However, less energetic, soft, gluons experience the effects of the medium and their behaviour is greatly modified in a way that is analogous to the screening in classical plasmas, and requires description of the medium effects. While this argument is insufficient for explaining the subtleties of the situation, it offers some physical insight to why a description beyond naïve perturbation theory is called for.

2.7 Addressing the Infrared Problems of QCD

In some cases, one can address the infrared divergences consistently with relatively simple prescriptions. The traditional approach is to take into account an infinite number of Feynman diagrams in a process known as *resummation*. By observing which diagrams are IR-sensitive and contribute at the same weak-coupling order, one can sum together an infinite number of individually divergent diagrams into a single contribution. For example, resumming gluon propagator terms in thermal QCD generates an effective term that acts as a screening mass, protecting the resummed propagator in the IR. However, the weak-coupling expansion in a resummed theory no longer matches with the number of loops. Owing to this, we will from now on refer to the strict expansion in Feynman diagrams, where there is a one-to-one correspondance with the weak coupling expansion and expansion in loop orders, as the naïve diagrammatic expansion. In thermal field theory, it suffers from infrared problems, while the proper weak-coupling expansion does not.

A more modern version of the resummation method makes use of the fact that only the soft gluons interacting with the medium require resummation. This lets one construct an effective theory using a so-called *Hard Thermal Loop* (HTL)-framework to use simplified versions of the struc-

tures such as self-energies of gluons to more easily address the IR dynamics of the soft sector. This approach works also at finite densities and lets one perform resummations beyond the naïve asymptotic series in g_s. It will be covered in much more detail in the next Chapter, particularly in Sec. 3.4.

At high temperatures, there is an approach for dealing with the divergences that arise in the soft sector that has proven particularly successful. As mentioned earlier, the zero modes of massless bosons, that is, *static* gauge fields A_a, are the source of the infrared sensitivity. Due to this restriction, the base space is reduced to being three-dimensional, and one can build a Wilsonian *dimensionally reduced* EFT of the static fields by integrating out the hard degrees of freedom [63, 64] — essentially performing a Kaluza–Klein reduction along the circle [65]. The spatial components A_i remain (now three-dimensional) standard Yang-Mills gauge fields in the EFT, but the temporal component A_0 now transforms as a scalar in the adjoint representation, which lets us construct the Lagrangian in the usual way by writing down every operator respecting the symmetries of the theory and performing matching calculations to obtain the Wilson coefficients. In QCD, this EFT is known as *Electrostatic QCD* (EQCD). This corresponds to an EFT of the soft modes, and, as such, will be the source of fractional powers of α_s in the expansion of the pressure.

As we saw in the previous Section, the perturbative expansion will eventually fail, requiring nonperturbative input. The physical source of this contribution is easy to understand in the dimensionally reduced framework: Since the temporal field A_0 is screened even in perturbation theory, it obtains an effective mass. Now, a massive scalar is easy to *also* integrate out from the theory, resulting in a three-dimensional *pure Yang-Mills theory* for the spatial gauge fields A_i. This EFT, known as *magnetostatic QCD* (MQCD), is the EFT of ultrasoft scales, and contains the nonperturbative information arising starting at $\mathcal{O}(g_s^6)$ for the hot pressure. While inaccessible by perturbation theory, the contributions have been evaluated using lattice simulations [66, 67, 68]. The nonperturbative contribution can be isolated to a single order in the expansion, but it is regardless a fundamental conceptual problem in the application of perturbation theory to thermal QCD. One should also note that, while a priori not obvious, the problem is absent in the Abelian gauge theory of

QED: The magnetic screening mass turns out to vanish at all orders in perturbation theory [69].

Finally, the Linde problem that has been outlined is not only restricted to non-Abelian theory, but also caused specifically by the presence of a finite temperature: At $T = 0$ but large μ, no such problems occur, and perturbation theory is in principle valid to arbitrarily high orders, although the asymptotic nature of the series might limit its usefulness. In fact, due to the absence of troublesome zero modes, the fractional powers of α_s do not appear at all at zero temperature. Having said that, infrared problems do still occur at $T = 0$ due to the interaction of soft gluons with the medium, and a simpler, dimensionally reduced description is no longer possible. In terms of the pressure, the remaining singularities lead to logarithms of the ratios of the energy scales, arising from dimensionless integrals, and are known to contribute to the pressure at both finite and zero temperatures. In addition, at the limit of small but finite temperatures, anomalous behaviour is known to occur in other quantities. Specifically, it has been known for QED plasma for a long time [70] that the specific heat has a $\mathcal{O}(T \ln T)$-term in the zero-temperature limit, breaking down a Fermi liquid description. More recently, the calculations have been extended to QCD and higher orders and argued to possibly affect the cooling of neutron stars [71], and similar observations have been made for a self-energy contribution [72].

The next Chapter will cover topics presented here for QCD in somewhat more detail, with the history of the computations of the pQCD pressure summarised in Sec. 3.3, and the logarithms of the pressure of cold dense quark matter being the theme of Sec. 3.5.

2.8 The Sign Problem

In Sec. 2.6 and Sec. 2.7, we saw how the Linde problem made calculations in pQCD and other perturbative non-Abelian gauge theories fundamentally impossible beyond a specific (low) order in perturbation theory. Beyond very small chemical potentials, most QFTs face a somewhat orthogonal problem: The so-called *sign problem*, making accurate lattice simulations at high chemical potentials unfeasible. While the concept has been mentioned before, for completeness let us state that lattice simula-

tions or *lattice field theories* refer to QFTs where the base space is changed from continuum to a discretised and finite lattice, rendering functional integrals finite-dimensional, well-defined, and something that may be evaluated numerically. There are numerous textbooks covering a basic introduction to lattice field theory, ranging from classics [73] to more recent literature [74].

The sign problem itself deserves further explanation. The reason for the problem is the way a finite chemical potential is introduced, as seen in Sec. 2.3: We start by replacing the Boltzmann measure with the Gibbs measure at finite density. From the point of view of path integrals, the action now becomes *complex*, in a way that generally cannot be addressed via a simple trick such as a Wick rotation. In lattice field theory, this is a major issue: A complex phase in the action causes increasingly rapid oscillations once exponentiated, which are numerically difficult to integrate over. More fundamentally, a complex action prohibits the use of *importance sampling*, a method of stochastic Monte Carlo integration used in lattice field theory. The method further emphasises the analogy between the Boltzmann measure and the functional integral kernel e^{-S}, using the latter as a probability measure for the purposes of stochastic sampling. Of course, this is no longer possible when S has become complex.

The problem is significant, and remains as one despite a number of attempts at solving it. Proposed solutions include reweighting the expectation values [75], analytically continuing the result from imaginary chemical potential [76, 77], attempting to obtain the Taylor coefficients at $\mu = 0$ [78, 79], complexifying the fields and using either complexified Langevin equations [80, 81, 82] or deforming the integral contours in the Lefschetz thimble approach [83, 84]. However, all come with their own issues; conceptual, numerical, or both, and have ultimately so far failed to solve the general problem.

The description of lattice field theory, the sign problem, and its proposed solutions given here is very brief, but since lattice field theory plays no notable role in any of the included Publications, we continue to omit a more comprehensive overview. However, *acknowledging* the problem is vital, as it is the main reason analytical methods, such as high-order pQCD much of this Thesis is dedicated to, are important for the study of dense QCD matter.

2.9 Dense Perturbation Theory: Cutting Rules

At exactly zero temperature, the Matsubara sums of thermal field theory become continuous integrals over the zero-component of the momentum. However, if one remains at finite chemical potentials, the results from the widely studied field of vacuum Feynman integrals cannot, a priori, be used directly, as for example Lorentz symmetry remains broken. In principle one could use the more widely available tools of finite-temperature methods for computing Matsubara sums and take the zero-temperature limit, but this is often unnecessarily complicated and riddled with subtleties.

Consider the simple sum-integral computed in Eqn. (2.21) as an example: While valid at any $T > 0, \mu > 0$, setting $T = 0$ in the ζ functions is not possible, and they must be expanded instead, which is tedious for larger values of the indices. However, the same integral can be computed directly at $T = 0$ with a continuous q_0-integral. Consider the $n = 0$ case $F_l^0(0, \mu; d)$ for simplicity.

$$F_l^0(0,\mu;d) = \int\limits_{\{Q\}} \frac{1}{Q^l} = \int\limits_{\mathbf{q}} \int\limits_{\mathbb{R}} \frac{\mathrm{d}q_0}{2\pi} \frac{1}{((q_0 - i\mu)^2 + q^2)^{l/2}}. \tag{2.29}$$

Residue calculus plays an important role at $T = 0$ as well, and applying standard contour methods we have

$$\begin{aligned} F_l^0(0,\mu;d) &= \int\limits_{\mathbf{q}} \int\limits_{\Sigma} \frac{\mathrm{d}z}{2\pi} \frac{1}{((z - i\mu)^2 + q^2)^{l/2}} \\ &= -i\frac{\lambda(S^{d-1})}{(2\pi)^d} \int\limits_{\mathbb{R}_+} \mathrm{d}q q^{d-1} \theta(q-\mu) \mathrm{Res}\left(\frac{1}{((z - i\mu)^2 + q^2)^{l/2}}, z = i(\mu - q) \right), \end{aligned} \tag{2.30}$$

where Σ is the standard semicircular contour around the lower half-plane, with its boundary vanishing by Jordan's lemma. One should note here that the Heaviside θ function — used to pick the poles contained within the contour — is analogous to the distribution functions seen in Sec. 2.4. Indeed, the zero-temperature limit of n_F is nothing but the θ function.

The residue can be evaluated analytically, and results in

$$\begin{aligned} &= \frac{\pi^{d/2-1/2}}{(2\pi)^d} \frac{\Gamma(\frac{l-1}{2})}{\Gamma(\frac{l}{2})\Gamma(\frac{d}{2})} \int\limits_{\mathbb{R}_+} \mathrm{d}q q^{d-l} \theta(q-\mu) \\ &= -\frac{\Gamma(\frac{l-1}{2})}{\Gamma(\frac{l}{2})\Gamma(\frac{d}{2})} \times \frac{\mu^{1+d-l}}{2^d \pi^{\frac{d+1}{2}} (1+d-l)}, \end{aligned} \tag{2.31}$$

where, in the last step, a scale-free contribution vanishing in dimensional regularisation was discarded using $\theta(x) = 1 - \theta(-x)$. As with the Matsubara sum in Eqn. (2.21), the final result is analytically continued to values for which the initial integral fails to converge.

Aside from the involved expansions of $T > 0$ results, T might act as a (partial) regulator of divergent integrals, and naïvely taking the cold limit of a $T > 0$ calculation might lead to T-dependent divergences. If the rest of the calculation is regularised with a different regulator, such as an ϵ-parameter of dimensional regularisation, this causes mixing of regulators, which requires additional care. A simple example is the bosonic sum-integral $\oint\!\!\!\!\!\!\sum_P (1/P^4 - 1/(P^2+M^2)^2)$. It is constructed in such a way that the UV-divergences cancel, which is easily seen in dimensional regularisation after extracting the finite-T part of the second term. That said, the difference also contains a term $\ln(T^2/M^2)$, divergent in the zero-temperature limit. If the integral is evaluated at $T = 0$ from the start, the first term vanishes in dimensional regularisation, so that the UV divergences no longer cancel: The $\ln T$ divergence manifests as a $1/\epsilon$-divergence of the second term at strict $T = 0$. Should one consider a finite-T integral similar to the original one but with both UV and IR divergences present, the two regimes would have different regulators.

Contour integration methods similar to those discussed in this Section can be applied for more complicated integrals. However, they also lead to a way of entirely side-stepping the problem and simplifying the computation of high-order integrals at finite density. We can achieve this by making use of a set of *zero-temperature cutting rules*, derived in [1], but used on a case-by-case basis before that, see [85]. The method lets one decompose a finite-density Feynman diagram into parts involving spatial integrals over *vacuum* n-point-functions, and make use the vast literature of vacuum integrals.

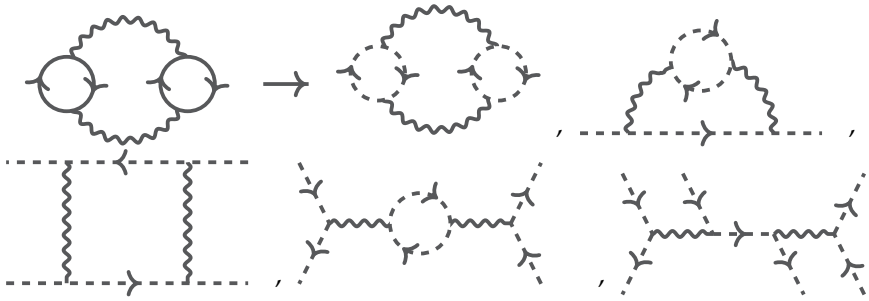

Figure 2.1: Generating cut diagrams from a 3-loop QCD diagram

The rules are easiest to present using a graphical representation: Given an L-loop n-point Feynman diagram $\mathcal{G}$ with (possibly no) real external momenta at finite chemical potential μ, one constructs each diagram that can be obtained from $\mathcal{G}$ by cutting any number $k \in \{0, \ldots, L\} \subset \mathbb{N}$ of the lines of $\mathcal{G}$ corresponding to finite-density propagators. A diagram formed in this way is termed a k-cut diagram, and corresponds to an $n + 2k$-point function. Each k-cut diagram is computed in vacuum, setting the chemical potential to zero, and afterwards evaluated with each *Euclidean* cut momenta $P = (p_0, \mathbf{p})$ set on-shell: $(p^0)^2 + E^2 = 0$ where E is the energy of the ith cut momentum, typically $E^2 = m^2 + p^2$ for a particle of mass m. Finally, the on-shell vacuum diagrams are integrated over $\mathbf{p} \in \mathbb{R}^d$ against the product of kernels $\prod_{i=0}^{k} -\theta(\mu - E_i)/(2E_i)$. The value of the diagram $\mathcal{G}$ is then the sum of all cut diagrams.

An explicit example of the graphical procedure applied to one of the fermionic 3-loop QCD diagrams, with quarks carrying the quark chemical potential (see Sec. 3.2), is shown in Fig. 2.1. In it, the standard QCD diagram is decomposed into a number of diagrams, with the dashed lines indicating quark propagators evaluated at zero chemical potential, and with each diagram on the RHS evaluated with the cut momenta (in this case, all external momenta) evaluated on-shell.

The rules can be proven by first writing down a generic diagram as a sum using every different admissible *momentum labelling* of the graph. Then, one notes that with specific choices of momenta, the zero-component

integrals are always particularly simple and they can be performed using standard residue calculus, in a manner analogous to the computation leading to Eqn. (2.31). Using the invariance of the graph with respect to the labellings and finally collecting the various terms into groups according to the number of cut momenta, rewriting terms as integrals when necessary to obtain the complete n-point functions allows one to obtain the form proposed by the rules. The proof is written out in detail in [1].

However, the said proof a priori assumes a simple scalar theory and no lines with identical momenta when it comes to the integral structure of the Feynman diagram. Relaxing both is possible, as is mentioned in the Publication, but requires some extra care, as the pole structure might be modified. More complicated QFTs, such as QCD, typically have momentum-dependent vertices that generate nontrivial numerator structure. In specific combinations, they can form contributions that cancel terms from the denominator, effectively removing poles and consequently also residue contributions. The opposite happens when distinct fermionic lines carry identical momenta, and higher-order poles appear in the zero-component integrals. There are ways around these issues, either by carefully examining them on a case-by-case basis, or, say, introducing mass derivatives to alter the order of the propagators, although the latter method requires care when it comes to convergence. In practical applications it does appear that such special cases are rare: For example, consider the 3-loop contributions to the QCD pressure used as an example earlier. Every diagram of naïve cold perturbation theory contributing at this order is shown in Fig. 3.4, and out of them only *one*, the diagram obtained as a part of the 'fermionic ring sum', displays higher-order poles.

While the use of the method in existing literature is largely confined in QCD, it is in principle generally applicable to any Euclidean QFT at finite density.

2.10 Nonperturbative Physics in $2+1$ Dimensions

While by far most of this Thesis focusses on perturbation theory, one of the included Publications [3] examines the *nonperturbative* aspects of QFT. This Section aims to give it context, motivate it, and summarise its essen-

tial parts. Although it was argued previously in Sec. 1.4 that at least in certain regimes, perturbation theory can make sense even in the context of a strongly coupled QFT such as QCD, it is unable to capture certain essential elements of these theories — as a prototypical example, confinement in the case of QCD is fundamentally nonperturbative.

For decades, lattice simulations have been the only nonexperimental method producing truly accurate information about nonperturbative physical QFTs, having produced impressive results regarding for example the critical properties [86, 87] and the hadron structure [40] of QCD. They have also greatly benefitted from the increased availability of computational power. Should one wish to study nonperturbative QFT without simulations, the options have been rather scarce. During the 21st century, *holography*, spearheaded by the famous AdS/CFT duality [88], has become a viable option for analytic studies. Using a conjectured correspondence between QFTs and higher-dimensional classical gravity allows one to study even the nonperturbative regimes of these theories [89]. While constructing the duals of realistic theories such as QCD appears extraordinarily challenging, the method can be useful for obtaining general, otherwise inaccessible, information.

However, holography and lattice are not the only options for studying nonperturbative QFTs. Nonperturbative or at least strongly coupled results can also be obtained for sufficiently simple theories using standard continuum methods. A common way to achieve this is to take the number of particle species to be large, in other words taking the large-N limit that was already mentioned in Sec. 1.4. Here, we consider an even more specialised large-N theories: In Sec. 1.8, CFTs were introduced as a special type of a field theory in which the coupling does not run. Here, this is taken to be a global property, not for example something valid only in the vicinity of a critical point. As a result, no Landau poles restricting the applicability scales of the theory appear. This is in contrast to a theory such as $3+1$-dimensional QED which, although well-described by the weak-coupling expansion, suffers from the Landau pole appear at a large energy scale. We also note that in the case of a $3+1$-dimensional base space, nontrivial renormalisation often complicates matters, but restricting ourselves to $2+1$ dimensions solves this issue. A theory combining these properties is quite special: Not only are we able to evaluate

quantities at both strong and weak couplings, the theory is essentially *finite* and we are able to apply it at *any* energy scales. In [3], we consider such a theory, a version of QED with a large number of fermions in $2+1$ dimensions, at finite temperature, where we indeed see explicitly that to NLO in large N_f there are no logarithmic divergences requiring renormalisation.

Before discussing the details, one should note that QED in $2+1$ dimensions at the limit of large N_f is, to the best of our knowledge, not representative of a physical theory. However, it should not be immediately discarded, as understanding simpler theories can often lead to a better grasp of more complicated ones: Indeed, $2+1$-dimensional QED was *not* first studied for its properties as a CFT, but rather as a simple model for explaining chiral symmetry breaking [90] (see also Sec. 3.1 for a short explanation of the concept). In addition, the (unfortunately nonconformal) model of QCD at large N_f in the more physical case of $3+1$ dimensions has seen some attention in the past, both at finite temperature [91] (see also erratum [92]) and at finite chemical potential [93].

To provide some context before the details of the QED calculation, it is useful to first mention an earlier related article [94] (note the erratum), where an $O(N)$-symmetric model with a sextic interaction, at large-N and likewise at finite temperature and $2+1$ dimensions, is considered, as well as the related $1+1$-dimensional examples [95, 96]. For our purposes, the former will do as means of explanation. The Euclidean Lagrangian is given by

$$\mathscr{L} = \frac{1}{2}\boldsymbol{\phi}_{,\alpha}\cdot\boldsymbol{\phi}^{,\alpha} + \frac{1}{2}m^2\boldsymbol{\phi}^2 + \frac{\lambda}{N}(\boldsymbol{\phi}^2)^3, \tag{2.32}$$

where $\boldsymbol{\phi}$ is an N-tuplet of scalar fields, m is their mass and λ the relevant coupling. The theory fulfills the requirements discussed earlier. Thermodynamic quantities can be computed exactly to leading order in N, and the relevant sum-integrals are finite in $2+1$ dimensions in dimensional regularisation. This is to be expected, as the theory is supposed to be well-defined at any couplings without any additional input. Of particular interest in this case is the entropy density of the theory. It can be evaluated with no assumptions on the coupling, and reads

$$s = -\frac{\partial\Omega}{\partial T} = \frac{NT^2}{4\pi}\left[\xi^2\ln\frac{1-e^{-\xi}}{(1-e^{\xi})^3} - 6\xi\mathrm{Li}_2(e^{\xi}) + 6\mathrm{Li}_3(e^{\xi})\right], \tag{2.33}$$

where the value of ξ is fixed (numerically) through

$$\frac{4\xi}{\sqrt{6\lambda}} = -\frac{\xi}{\pi} - \frac{2}{\pi}\ln(1-\exp^{-\xi}). \tag{2.34}$$

Together with the free energy Ω, the entropy density leads to a traceless stress-energy tensor, indicating conformality. Interestingly, Eqn. (2.33) conveys nontrivial information about the *strong-coupling limit*: Taking the strong-coupling limit $\lambda \to \infty$, one has $s/s_0 \to 4/5$ for s_0 the pressure of non-interacting theory. This resembles the famous CFT result of $s_{\mathrm{SYM}}/s_0 \to 3/4$ obtained using holographic methods for the so-called $\mathcal{N} = 4$ Super Yang–Mills theory [97]. In addition, the strong-coupling limit of the scalar theory is *also* valid for extended, non-sextic potentials which fail to be globally conformal, as explained in [94]. In fact, the form of the strong-coupling limit has been known since the 90s, having been pointed out in a large-N study of the *quartic* theory [98] as well as in the related large-N $O(N)$ vector model [99]. A relation of this form provides another reason for studying such simplified models: results from the simple case can generalise into nontrivial statements about more complicated models.

After this brief detour, we can finally consider the case of $2+1$-dimensional QED which is particularly relevant for this Thesis. The Lagrangian is nothing but the Abelian counterpart of Eqn. (1.6), with a dimensionless coupling $e^2 N_f/T$ for e the Abelian equivalent of the Yang–Mills coupling g_s, with massless fermions in order to avoid spoiling the conformality. The free energy can be obtained by considering all diagrams contributing to desired order in N_f. This idea resembles the Hard Thermal Loop resummation scheme discussed later in this Thesis (see Sec. 3.4), with an important difference: to next-to-leading order (NLO), one must consider the whole one-loop polarisation tensor of the gauge boson instead of the soft contributions only, as the complete information from the diagrams is needed for the resummation at arbitrary couplings. The polarisation tensor is finite in $2+1$ dimensions and can be written using a decomposition equivalent to that discussed in Sec. 2.5:

$$\begin{aligned}\Pi_{\alpha\beta}(P) = \Pi_A(P)\big(\mathbb{P}^D_{\alpha\beta}(P) - \mathbb{P}^D_{\alpha\gamma}(P)\mathbb{P}^D_{\beta\gamma}(P)N^\gamma N^\delta\big) \\ + \Pi_B(P)\mathbb{P}^D_{\alpha\gamma}(P)\mathbb{P}^D_{\beta\delta}(P)N^\gamma N^\delta,\end{aligned} \tag{2.35}$$

where the coefficient functions Π_A, Π_B read

$$\begin{aligned}\Pi_A(P) &= \frac{e^2 N_f}{T}\left[\frac{|P|\,T}{8} - \frac{4T^2}{p^2}\int\limits_{\mathbb{R}_+}\frac{\mathrm{d}k}{2\pi} n_F(kT)\times\right.\\ &\qquad\left.\times\left(p_0^2 + |P|\,\mathrm{Re}\frac{(ip_0+2kT)^2}{\sqrt{P^2-4k^2T^2-4ip_0kT}}\right)\right]\\ \Pi_B(P) &= \frac{e^2 N_f}{T}\left[\frac{|P|\,T}{8} + \frac{4T^2}{p^2}\int\limits_{\mathbb{R}_+}\frac{\mathrm{d}k}{2\pi} n_F(kT)\times\right.\\ &\qquad\left.\times\left(P^2 - |P|\,\mathrm{Re}\sqrt{P^2-4k^2T^2-4ip_0kT}\right)\right].\end{aligned} \tag{2.36}$$

Here, $|P| = \sqrt{P^2}$ for the Euclidean four-vector P. Moreover, we define the vacuum ($T \to 0$) part of the polarisation tensor $\Pi_V(P) = e^2 N_f\,|P|\,/8$.

Without additional assumptions, the integrals in Eqn. (2.36) do not appear to be analytically solvable, but are simple to evaluate numerically. Moving to the free energy, the LO contribution is trivial to evaluate: It is simply the fermionic vacuum term linear in N_f, obtained using Eqn. (2.19) and the definition of the free energy:

$$\Omega^{\mathrm{LO}}_{\mathrm{QED}_3} = -N_f \ln \mathrm{Det}(Q^2)^2 = -2N_f \sum\!\!\!\!\!\!\int_{\{Q\}} \ln Q^2 = -N_f \frac{3\zeta(3)}{2\pi} T^3. \tag{2.37}$$

The NLO term generated by gauge contributions requires numerics. Coming from photon and ghost contributions, it can be written as

$$\begin{aligned}\Omega^{\mathrm{NLO}}_{\mathrm{QED}_3} &= \frac{1}{2}\sum\!\!\!\!\!\!\int_P \ln\frac{(P^2+\Pi_A(P))(P^2+\Pi_B(P))}{P^2}\\ &= \sum\!\!\!\!\!\!\int_P \ln\left(|P| + \frac{\Pi_V(P)}{|P|}\right) + \frac{1}{2}\sum\!\!\!\!\!\!\int_P \ln\left(1 + \frac{\Pi_A(P)-\Pi_V(P)}{P^2+\Pi_V(P)}\right)\\ &\quad + \frac{1}{2}\sum\!\!\!\!\!\!\int_P \ln\left(1 + \frac{\Pi_B(P)-\Pi_V(P)}{P^2+\Pi_V(P)}\right),\end{aligned} \tag{2.38}$$

where last two terms containing Π_A, Π_B are rewritten in a way that renders them finite and allows for numerical evaluation.

Somewhat surprisingly, the first term associated with the vacuum contribution of the polarisation tensor contains not only a finite thermal component but also a seemingly divergent vacuum contribution

$$\Omega^{\text{vac}}_{\text{QED}_3} = \frac{1}{2} \int_P \ln \left(|P| + \frac{\Pi_V(P)}{|P|} \right). \tag{2.39}$$

However, by examining its structure carefully, one sees that terms naïvely of higher order in N_f can be used to resum the polarisation tensors, turning $\Omega^{\text{vac}}_{\text{QED}_3}$ into a finite contribution. They also result in a screened behaviour of the low-temperature (large coupling) polarisation tensors, which ought to be taken into account when computing the Π_A, Π_B contribution in this regime. Disregarding the vacuum terms, the results of the numerical evaluation, valid when $T \gg e^2 N_f / e^{N_f \pi^2/8}$, are shown in Fig 1. of [3].

A follow-up publication by Romatschke [100] considered the entropy density in this theory, pointing out an interesting interpretation. In the same large-coupling limit as the one considered for scalar theory, the degrees of freedom of the gauge bosons are seen to contribute *half* of the free entropy density, effectively 'fractionalising the photon', so that it cancels precisely against the ghost contribution. The article also offers similar interpretations in other theories.

Chapter 3

Thermal Quantum Chromodynamics

So far, we have constructed perturbative QCD in vacuum, and introduced thermal methods for general QFTs in equilibrium. In this Chapter, we combine the two, and delve deeper into the realm of thermal QCD, with a special focus on nonzero baryon density in the imaginary time formalism. After a brief discussion on the overarching themes, we review some details of perturbative Feynman diagram computations. The infrared problems covered in the previous Chapter are solved by constructing a Hard Thermal Loop effective theory for the soft degrees of freedom of QCD, and the results of one of the Publications are covered by explaining a method of extracting nonanalytic logarithmic terms of the pressure with the aid of Hard Thermal Loops.

3.1 The Phase Diagram of QCD

The thermodynamic properties of substances can be conveniently summarised by their phase diagram. For the phase diagram of QCD matter, usually known simply as the *phase diagram of QCD*, one often (but not always) considers two axes: temperature and some relevant chemical potential. The latter is usually chosen to be the quark chemical potential (or baryochemical potential), introduced in Sec. 2.3. Its nature will be further

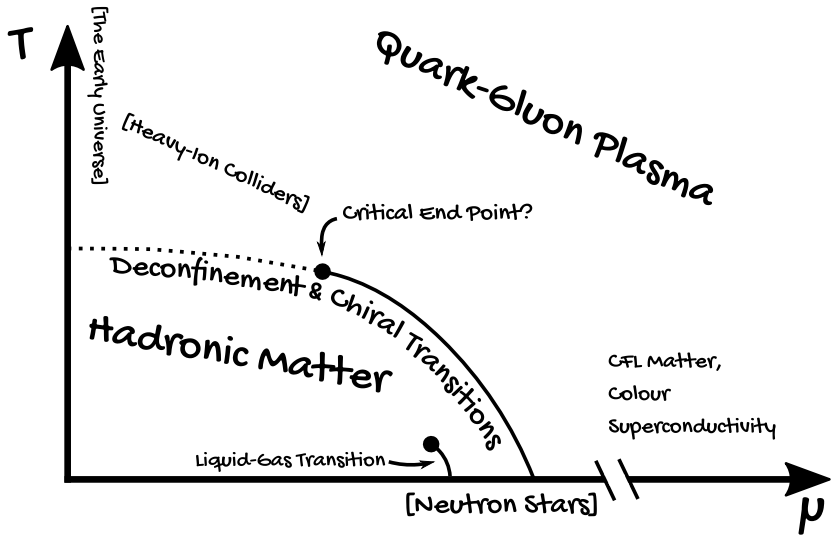

Figure 3.1: Sketch of a commonly conjectured form of the QCD phase diagram

expanded upon later in this Chapter. A sketch of the (conjectured) QCD phase diagram is shown in Fig. 3.1.

The most notable feature of the diagram is the division of the μ, T-plane to the high-energy deconfined phase and the low-energy confined phase. Our everyday world is set soundly in the latter, with the deconfined QCD matter — guark-gluon plasma (QGP) — being present only in extreme environments, particle accelerators being the only terrestrial example.

As covered in Sec. 1.4 and Sec. 2.8 respectively, the large value of the QCD coupling prevents perturbative first-principles computations at low energies, and the sign problem does the same for lattice simulations at large chemical potentials. The energy scales that are currently experimentally achievable are low compared to the enormous scales required for perturbative calculations to describe physics accurately. For this reason,

the most well-understood regime of the phase diagram is the $\mu = 0$-line, where lattice simulations encounter no real problems. The temperature increases as we ascend from origin along this line and confined hadronic matter eventually transitions into deconfined QGP. At zero density, the approximate critical temperature T_c of this transition has been evaluated to be from 150 to 160 MeV by different lattice collaborations [87, 86], with the exact value depending on the precise definitions used to obtain the transition temperature. The transition appears to be *crossover*, as neither lattice nor accelerator measurements have been able to observe discontinuities in any of the derivatives of the associated free energy.

Asymptotic freedom indicates that a transition to deconfined matter must happen also at small temperatures as sufficiently large chemical potentials are reached. While no reliable quantitative results derived from first principles are available, there are some qualitative hints based on the universality properties of field theories and effective models [101] that indicate that here, the confinement–deconfinement transition might be an ordinary first-order transition, as it is in the absence of quarks. Were this the case, it would suggest the existence of a *critical end point* of the first order transition line somewhere on the μ, T-plane. Pinpointing the location of this point is a major goal of lattice simulations [102] as well as experiments [103, 104].

Aside from the aforementioned phase transition line, the phase diagram is rather uneventful at large temperatures and/or small densities. The situation changes at larger densities and at most intermediate temperatures. Well within the confined regime, a low-temperature QCD system will, at sufficiently high densities, transition into a Fermi liquid. This *liquid–gas transition* of nuclear matter is a first-order transition line with a critical end point at approximately $\mu \sim 300\text{MeV}$, $T \sim 20\text{MeV}$ [105].

On the other hand, in the deconfined but low-temperature regime of the phase diagram, a number of different phases have been conjectured to occur. A well-established example is the *Colour-Flavour Locked* (CFL) phase, which sees the generation of a mass gap and the quarks pairing in a way analogous to the Cooper pairing of electrons in conventional superconductivity. This phase is known to be favoured with three quark flavours, in the limit of massless quarks [106]. Unfortunately, quantitive analysis of the effects of such phases reliant on pairing effects

is typically difficult in a pQCD context, as they are suppressed so heavily that their effect tends to be much smaller than other inaccuracies present in such calculations. The relevant scale for pairing effects is the *gap* Δ, which for colour superconductivity has been estimated to be approximately 100 MeV or smaller [107] — much less than the chemical potentials required for pQCD to be accurate at low temperatures. For example, compared to the results of the pQCD pressure computations performed and discussed in this Chapter, the effects pairing would have on the pressure are negligible in comparison to the error estimate obtained from varying the renormalisation scale. However, pairing effects do become relevant in the study of transport phenomena.

In sketching the QCD phase diagram, we have not separated the previously mentioned *confinement–deconfinement line* from the *Chiral symmetry restoration line*. The latter is associated with the chiral symmetry of QCD discussed briefly in Sec. 1.4. As already mentioned, the symmetry is spontaneously broken. This is due to the $\langle q\bar{q}\rangle$ condensate forming at low energies, where u and d are the only active quarks. The spontaneous symmetry breaking generates Goldstone bosons: pions, light composite particles which were also important for the historical development of QCD, as discussed in Sec. 1.3. Pions are not entirely massless, however, but acquire a small mass due the Dirac mass terms of the quarks also *explicitly* breaking the chiral symmetry. At sufficiently large energy scales, there is no condensate, and the symmetry is restored. The (T, μ) curve that determines this maps the chiral restoration line. In fact, the previously cited transition temperatures are estimated on the lattice by studying quantities such as susceptibilities related specifically to the chiral symmetry. In contrast, deconfinement is characterised by a change in the expectation value of the Polyakov loop, the holonomy of the gauge connection along a path on the imaginary-time interval $(0, \beta)$. In the absence of quarks, the loop is even a true order parameter of the center$(\mathrm{SU}(N_c))$ symmetry, but even in the presence of the quarks its variation can in principle be used as an indication of the transition.

The reason for not making the lines distinct is that the spontaneous breaking of the chiral symmetry appears to occur near the confinement–deconfinement transition. It is not known if they happen precisely at the same scales, as the transitions are known to split under certain condi-

tions [108]. In fact, large-N calculations suggest that at sufficiently high chemical potentials such a split happens and gives rise to a new phase of *quarkyonic* matter [109]. However, this split is still very much at the level of a conjecture for QCD with physical particle content, and as such is omitted from the phase diagram in Fig. 3.1. Additional complications in conclusively associating the two transitions is caused by the fact that pinpointing the location of a crossover transition is very much dependent on definitions.

Making use of the (seemingly) close proximity of the two transitions, building a chirally symmetric Wilsonian EFT using pions and the other low-lying hadronic states as the degrees of freedom provides a way to access a relatively large region of the parameter space. Importantly, this region is relevant for many experiments, and incorporates densities larger than those easily accessible by lattice methods. While not used within the works related to this Thesis, this EFT, the Chiral Effective Field Theory (χEFT), is an important low-energy counterpart to the first-principles pQCD approach valid at high energies.

In addition to the χEFT described above and pQCD that most of the works of this Thesis are based on, there are certainly other approaches to QCD at finite temperatures and, in particular, densities, including ones that do not rely on numerics. These include holographic methods, mentioned briefly in Sec. 2.10, which are able to probe strongly coupled field theories analytically and include finite-T and finite-μ effects by adding black hole geometries and modified gauge fields in the gravity dual respectively [89] as well as *Functional Renormalisation Group* (FRG) methods, which combine ideas of functional methods with the Wilsonian renormalisation group [110]. In particular, both have been applied to the study of dense quark matter and its applications [111, 112, 113, 114], which will be the focus of the next Section.

3.2 Applications of QCD at Finite Density

Even if our daily interactions with QCD have little contact with deconfined matter, there is a plethora of extreme applications requiring a solid understanding of thermal QCD effects at high energies. In the very early universe, the temperature greatly exceeded the QCD critical temperature,

and the decrease in temperature and the subsequent phase transitions in QCD as well as other parts of the Standard Model had great implications on the history of the universe [115].

The search for the high-temperature QGP phase was a major goal of late 20$^{\text{th}}$ century collider experiments. It was finally observed tentatively at the Super Proton Synchrotron (SPS) [36], and a few years later conclusively at the Relativistic Heavy Ion Collider (RHIC) [116], with heavy-ion collisions being an important source of precision measurements then, now, and in the future.

The aforementioned systems deal mostly with large temperatures and at most moderate net baryon number densities. This might change in the future: The Compressed Baryonic Matter (CBM) experiment at the Facility for Antiproton and Ion Research (FAIR) is hoping to observe the first-order deconfinement transition and search for the critical end point [103], and the Beam Energy Scan (BES)-II experiment at RHIC is currently exploring the high-density region with similar goals [104]. For now the most significant measurements giving insight on the properties of very dense strongly interacting matter are not terrestrial, but rather obtained by studying *neutron stars*.

Neutron stars are stellar remnants formed by supernova explosions of sufficiently massive stars, starting from approximately $8M_\odot$[1]. In comparison, the endpoint of the life cycles of lighter stars are white dwarfs, while sufficiently heavy ones collapse further into black holes. Here, however, we concentrate on neutron stars. They are kept together by neutron degeneracy pressure and strong interactions, and are consequently rather peculiar objects: While macroscopic, extended objects, the description of their properties intimately involves QCD, a theory that typically directly manifests in much smaller objects. To be more precise, the radius and mass of a neutron star are related by the TOV equations [117, 118, 119]

$$\begin{aligned} \frac{\mathrm{d}p}{\mathrm{d}r} &= -\frac{GM\mathcal{E}}{r^2}\left(1+\frac{p}{\mathcal{E}}\right)\frac{1+4\pi pr^3/M}{1-2GM/r}, \\ \frac{\mathrm{d}M}{\mathrm{d}r} &= 4\pi r^2\mathcal{E}. \end{aligned} \tag{3.1}$$

In Eqn. (3.1), M is the mass of the matter inside a star contained within

[1]Here $M_\odot$ is the solar mass or approximately 2×10^{30}kg.

a radius r. The equations are closed by a set equation of state — a relation between the pressure p and the energy (density) $\mathcal{E}$, both of them also depending on r. As described earlier in Sec. 1.5, for any equilibrium matter described by a Lagrangian field theory, the pressure is one of the basic physical quantities that can be calculated using thermal field theory.

The masses and radii obtained from the TOV equations, as well as directly observed, indicate that such remnants must truly be extraordinarily dense objects. The canonical mass of neutron stars is the so-called Chandrasekhar limit of $1.4M_\odot$, above which electron degeneracy pressure no longer suffices to keep the core of the progenitor star intact. The precise upper limit is not know, but stars as massive as $2M_\odot$ have been observed. The typical neutron star radius is of the order of 10 km. With densities this large, it has been suggested that their cores might very well accommodate deconfined *quark matter* exceeding the critical chemical potential near $T = 0$. At the same time, this means that low-energy methods such as χEFT become invalid deep inside neutron stars. This is one of the reasons pQCD studies of dense matter are particularly relevant: While the densities are not yet sufficiently large for pQCD alone to be reliable, it provides a complementary high-energy method of studying the equation of state, allowing for example the use of interpolative methods between the low- and high-energy results [120, 121, 122].

With these introductory astrophysical remarks out of the way, let us consider a neutron star as an environment for field theory calculations. We have already discussed the chemical potentials of QCD in Sec. 2.3 in the relevant case of three active quark flavours. In a prototypical neutron star environment, further constraints are set for the chemical potentials [123]. An important one is the assumption of chemically equilibrated matter. Weak interactions mediate a number of processes between the quarks, electrons and neutrinos, the simplest of which are β decay and electron capture,

$$n \leftrightharpoons p + e^- + \overline{\nu}_e, \quad p + e^- \leftrightharpoons n + \nu_e, \tag{3.2}$$

where $n, p, e^-, \overset{(-)}{\nu}_e$ are the neutron, proton, electron and the electron (anti) neutrino respectively. More generally, weak interactions allow for a similar process transforming the up quark into a strange quark. Neglecting the neutrino contribution, enforcing the reactions to occur in equilibrium

leads to the following relation between the chemical potentials of the electron μ_e and the three lightest quarks μ_u, μ_d, mu_s:

$$\mu \equiv \mu_d = \mu_u + \mu_e = \mu_s. \tag{3.3}$$

A second constraint is that the matter neutron stars are made of ought to be overall electrically neutral to a good approximation.

$$n_e = n_Q = \frac{2}{3}n_u - \frac{1}{3}n_d - \frac{1}{3}n_s, \tag{3.4}$$

where n_i are the densities $-\partial\Omega/\partial\mu_i$. Together, the constraints fix the chemical potential needed to describe equilibrium neutron stars. Note that often the baryochemical potential $\mu_B = 3\mu$ is used instead of the quark chemical potential μ.

The recent history of neutron star measurements has seen significant advances: The detection of particularly heavy $2M_\odot$ neutron stars [124] affecting many models, the increased precision of radius measurements [125], and lastly, the advent of gravitational wave astronomy, also constraining the characteristic parameters of neutron stars [126].

In particular with the latter, one must take into account possible generalisations to usual assumptions needed for accurate descriptions. Neutron stars in equilibrium are generally relatively cold, with temperatures estimated to reach at most a few hundred eV [127]. This allows one to use zero-temperature methods to a good approximation in many computations. However, gravitational wave observations come from neutron star collisions, which may exhibit significantly larger larger temperatures. Besides the usual thermal effects, the assumptions made above might not hold: At sufficiently high temperatures, it has been shown that the standard β equilibrium no longer holds [128] and as such generalisations to the above will be necessary.

3.3 Low-Order Results in Thermal pQCD

While both this Chapter as well as two of the included Publications are largely focussed on QCD at finite density, we will start recounting established results at finite density *and* temperature, as there is little complication in doing so at lower orders. Unless otherwise stated, massless quarks are assumed — this approximation is reasonable in the high energy

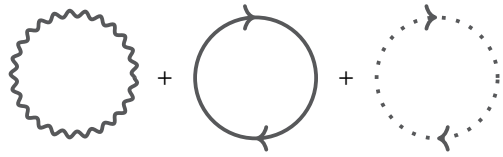

Figure 3.2: LO Feynman diagrams of the free energy of QCD

scales required for the perturbative expansion to be valid. The values $N_c = 3$ and $d_A = 8$ are fixed in physical QCD, but the number of quark flavours N_f depends on the situation. While QCD describes six flavours, for example in neutron star environments the densities are not expected to be large enough to activate the charm quark, and as such we would set $N_f = 3$ when studying them. However, as explained in Sec. 1.4, we keep all of these values arbitrary. This costs us very little and allows for possible generalisations and extensions.

To start with, the LO free energy is simply the negative logarithm of the non-interacting partition function. Using both Sec. 1.5 and Sec. 1.7, as well as the integrals Eqn. (2.19) and Eqn. (2.17), and writing $Q_i = (q_0 + i\mu_i, \mathbf{q})$, we get

$$\begin{aligned}
\Omega_{\mathrm{QCD}}^{\mathrm{LO}} &= -\ln \frac{\mathrm{Det}\partial\!\!\!/^{N_c N_f}\mathrm{Det}(-\Delta)^{d_A}}{\sqrt{\mathrm{Det}\big(-\delta^\beta_\alpha\Delta + (1-\xi^{-1})\partial^\alpha\partial_\beta\big)^{d_A}}} \\
&= \frac{d_A}{2}\Big(d\sum\!\!\!\!\!\!\int_P \ln P^2 + \sum\!\!\!\!\!\!\int_P \ln\frac{P^2}{\xi}\Big) - 2N_c\sum_{i=1}^{N_f}\sum\!\!\!\!\!\!\int_{\{Q_i\}}\ln Q_i^2 - d_A\sum\!\!\!\!\!\!\int_P \ln P^2 \\
&\overset{d=3}{=} -\frac{\pi^2}{45}\Big(d_A + \frac{7}{4}N_cN_f\Big)T^4 - \frac{1}{12\pi^2}N_c\sum_{i=1}^{N_f}\Big(\mu_i^2 + 2T^2\Big)\mu_i^2.
\end{aligned} \tag{3.5}$$

The contributions are often depicted in a graphical form, in the way shown in Fig. 3.2, although at LO this is somewhat misleading.

At higher orders, Feynman diagrams do become a valuable bookkeeping tool. The NLO diagrams can be seen in Fig. 3.3, and their con-

tribution is easily evaluated with the Feynman rules of Sec. 1.7. At this point, we move to Feynman gauge and fix $\xi = 1$, as it simplifies the integrals considerably — the pressure is a physical quantity, so it cannot depend on the choice of the gauge and we are free to do this. In Feynman gauge, the NLO pressure reads

$$\begin{aligned}
\Omega_{\rm QCD}^{\rm NLO} = &\frac{1}{12}\sum\!\!\!\!\!\!\int_{KP} \left(\Gamma_{AAA}\right)^{\alpha\beta\gamma}_{abc}(P,-K,K-P)\left(\Gamma_{AAA}\right)^{\alpha'\beta'\gamma'}_{a'b'c'}(-P,K,P-K)\times \\
&\times G^{aa'}_{\alpha\alpha'}(P)\,G^{bb'}_{\beta\beta'}(K)\,G^{cc'}_{\gamma\gamma'}(P-K) - \frac{1}{2}\sum\!\!\!\!\!\!\int_{\{QR\}} G^{cc'}_{\gamma\gamma'}(Q-R)\times \\
&\times \mathrm{Tr}\Bigg[\left(\Gamma_{\bar\psi A\psi}\right)^{IJ\gamma}_{f_1f_2c}(Q,-R,R-Q)\,S^{f_1f_1'}_{II'}(Q)\times \\
&\times \left(\Gamma_{\bar\psi A\psi}\right)^{J'I'\gamma'}_{f_2'f_1'c'}(R,-Q,-R+Q)\,S^{f_2f_2'}_{JJ'}(R)\Bigg] \\
&-\frac{1}{2}\sum\!\!\!\!\!\!\int_{KP}\left(\Gamma_{\bar\eta A\eta}\right)^{\gamma}_{abc}(P,-K,K-P)\left(\Gamma_{\bar\eta A\eta}\right)^{\gamma'}_{c'}(-P,K,-K+P)\times \\
&\times C^{aa'}(P)\,C^{bb'}(K)\,G^{cc'}_{\gamma\gamma'}(P-K) \\
&+\frac{1}{8}\sum\!\!\!\!\!\!\int_{KP} G^{ab}_{\alpha\beta}(P)\left(\Gamma_{AAAA}\right)^{\alpha\beta\gamma\delta}_{abcd}(P,P,K,K)\,G^{cd}_{\gamma\delta}(K)
\end{aligned} \tag{3.6}$$

$$\begin{aligned}
=&\frac{g_s^2}{4}d_A(d-1)\Bigg\{N_c(d-1)\left(\sum\!\!\!\!\!\!\int_P\frac{1}{P^2}\right)^2 \\
&-\frac{d_C}{2}\sum_{i=1}^{N_f}\left[2\left(\sum\!\!\!\!\!\!\int_P\frac{1}{P^2}\right)\left(\sum\!\!\!\!\!\!\int_{\{Q_i\}}\frac{1}{Q_i^2}\right)-\left(\sum\!\!\!\!\!\!\int_{\{Q_i\}}\frac{1}{Q_i^2}\right)^2\right]\Bigg\},
\end{aligned}$$

where the notation $d_C = 2^{\lfloor (d+1)/2\rfloor}$ was introduced for the number of generators of the Clifford algebra $\mathcal{C}\ell(1,d)$. The integrals factorise in this gauge, and the remaining 'master integrals' are simple special cases of

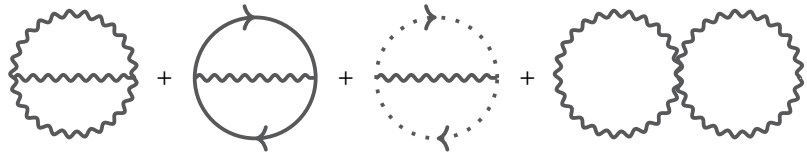

Figure 3.3: NLO Feynman diagrams of the free energy of QCD

Eqn. (2.22) and Eqn. (2.21). Inserting them,

$$\begin{aligned}\Omega_{\mathrm{QCD}}^{\mathrm{NLO}} = \frac{g_s^2}{16\pi^{4-d}} d_A (d-1)\Gamma^2(1-d/2)\Bigg(& (d-1)N_c\zeta^2(2-d) \\ & - \frac{d_C}{2}\sum_{i=1}^{N_f}\Bigg[\zeta(2-d)\left\{\zeta\Big(2-d,\frac{1}{2}-i\frac{\mu_i}{2\pi T}\Big)+\zeta\Big(2-d,\frac{1}{2}+i\frac{\mu_i}{2\pi T}\Big)\right\} \\ & - \frac{1}{4}\left\{\zeta\Big(2-d,\frac{1}{2}-i\frac{\mu}{2\pi T}\Big)+\zeta\Big(2-d,\frac{1}{2}+i\frac{\mu}{2\pi T}\Big)\right\}^2\Bigg]\Bigg) T^{2d-2} \\ & \overset{d=3}{=} \frac{g_s^2}{144} d_A\left[\Big(N_c+\frac{5}{4}N_f\Big)T^4+\frac{9}{4\pi^4}\sum_{i=1}^{N_f}\Big(\mu_i^2+2\pi^2T^2\Big)\mu_i^2\right].\end{aligned} \tag{3.7}$$

At vanishing chemical potentials or temperatures the expression reads:

$$\Omega_{\mathrm{QCD}}^{\mathrm{NLO}}|_{\mu=0,d=3} = \frac{g_s^2}{144} d_A\Big(N_c+\frac{5}{4}N_f\Big)T^4,\ \Omega_{\mathrm{QCD}}^{\mathrm{NLO}}|_{T=0,d=3} = \frac{g_s^2}{64\pi^4} d_A\sum_{i=1}^{N_f}\mu_i^4, \tag{3.8}$$

where the latter, getting contributions only from the very last term on the final line of Eqn. (3.6), can be obtained either by taking the limit of ζ functions or simply with Eqn. (2.31).

It is worth noting that so far the result is completely convergent aside from vacuum terms that vanish in dimensional regularisation, and no renormalisation is needed. This is generally not true, and just as the IR divergences start to arise, the coupling g_s (as well as other renormalisation-

dependent parameters, such as possible quark masses) must generally speaking be UV-renormalised.

However, NLO is as far as the naïve expansion gets us: As discussed in Sec. 2.6, beyond NLO one encounters IR divergences caused by the soft modes, which must be properly accounted for. At finite temperatures, this was argued to lead to fractional nonanalytic terms, starting with $\mathcal{O}(\alpha_s^{3/2})$. The low-order terms are known, starting with [129]. Having said that, as briefly covered in Sec. 2.7, they are convenient to handle in the framework of dimensionally reduced effective theories, and this description is qualitatively quite different from the description required at finite μ. For this reason, it will not be covered here, those interested can follow procedure from a number of sources, such as [130, 131].

As we reasoned in Sec. 2.7, the fractional terms are not the only divergences arising from the soft sector: Starting with $\mathcal{O}(\alpha_s^2 \ln \alpha_s)$ one encounters *logarithmic* terms that can be computed by resumming a class of diagrams. These terms have been known for a long time, computed by Freedman & McLerran at $T = 0$ [132, 133, 134] and by Toimela at finite temperature [135], but the more modern derivation makes use of the HTL effective theory, which will be introduced in the next Section, and the computation is postponed until Sec. 3.5. The same description can also be used to obtain the fractional terms, although for this part we will omit the details.

Of course, aside from the soft contributions from dimensional reduction and/or HTL resummation, one must compute the hard diagrams associated with the naïve Feynman expansion to obtain the full NNLO ($\mathcal{O}(\alpha_s^2)$) result. All of the three-loop diagrams contributing at this order are shown in Fig. 3.4 and Fig. 3.5, with the latter pure gauge contribution vanishing at zero temperature.

The evaluation of the diagrams is tedious, but in principle straightforward, with two important integral structures being the polarisation functions $\Pi_B(K) = \fint_P P^{-2}(P-K)^{-2}$ and $\Pi_F(P) = \fint_{\{Q\}} Q^{-2}(P-Q)^{-2}$, which can be evaluated using Fourier transforms. The finite-temperature computations were first performed in [136, 137], while the generalisation to both finite temperatures and densities can be found in [58]. While we will omit the details, the diagrammatics will prove useful when studying the logarithms of higher-order terms.

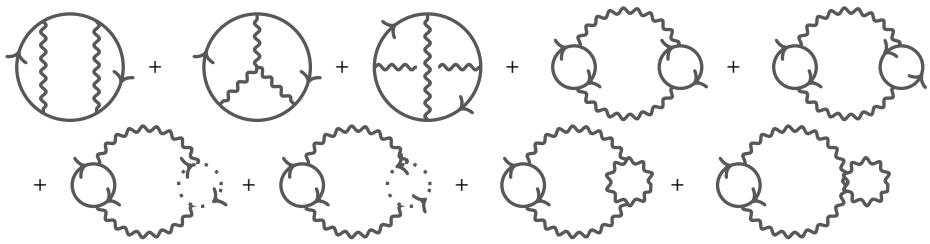

Figure 3.4: NNLO fermionic Feynman diagrams of the free energy of QCD

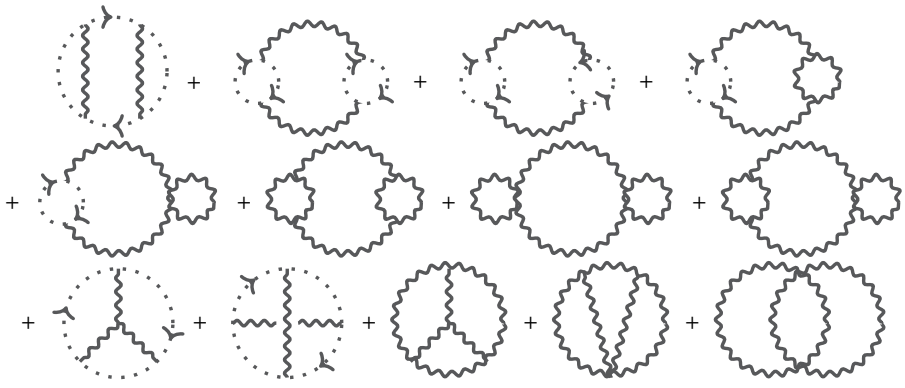

Figure 3.5: NNLO gauge Feynman diagrams of the free energy of QCD

At finite temperatures, the next two orders are $\mathcal{O}(\alpha_s^{5/2})$ and $\mathcal{O}(\alpha_s^3 \ln \alpha_s)$, and both are known; see [138, 139] respectively. In Sec. 2.6, we saw that the latter is the very final coefficient that can be obtained within perturbation theory, with the analytic $\mathcal{O}(\alpha_s^3)$ coefficient requiring MQCD lattice simulations due to the Linde problem. Again, the fractional term is absent at zero temperature, but at finite densities, one can obtain *doubly* logarithmic terms, and the term following $\mathcal{O}(\alpha_s^2)$ in the expansion is $\mathcal{O}(\alpha_s^3 \ln^2 \alpha_s)$. It was computed in [2], and will be discussed in more detail in Sec. 3.5. Additional contributions, such as the effects of finite quark mass corrections have also been considered, in [85] for $T = 0$ and in [140] for $\mu = 0$.

Of course, in both hot and cold cases, the asymptotic expansion of the QCD pressure is only valid at very high energy scales, and comparing it with data and other models requires some control over the uncertainty. In this context, the uncertainty bands are conventionally estimated by varying the renormalisation scale — as the energy is decreased, the variations become larger. To give some idea of the magnitudes of the required scales, such estimates set the uncertainties to 24% at $\mu \sim 0.9\,\mathrm{GeV}$ for the $T = 0$ pressure [120], while agreement with lattice results can be achieved with as low temperatures as $T \sim 350\,\mathrm{MeV}$ for the $\mu = 0$ pressure using NNLO pQCD results [141]. However, the convergence of the strict pQCD series is typically extremely poor anywhere near physical scales, and to improve it, various resummation and improvement schemes are used. For example, the previously cited [141] observes improved convergence after the EQCD contributions are *not* truncated according to strict EFT conventions. Along similar lines, including effects from quark mass thresholds has proven useful for convergence [140], as has using HTL-reorganised perturbation theory [142, 143], obtained by treating the HTL mass parameters introduced in the next Section as the expansion parameters. There have also been many attempts at studying the nonperturbative aspects of QFTs in general using resummation methods and their generalisations. These include methods based on *resurgence theory*, a set of results from mathematics that lets one extract non-perturbative information from the asymptotic perturbation series; see [144] as an example.

3.4 The Hard Thermal Loop Effective Theory

The concept of Hard Thermal Loops was mentioned in Sec. 2.7 as a way to alleviate the IR problems prominent in thermal field theories. The framework was developed rapidly from late 80s to early 90s, with Pisarski and collaborators [145, 146, 147] as well as Taylor and collaborators [148, 149, 150] contributing some of the most significant advancements. We are now ready to give the HTL theory a more thorough overview. While the method can, at least to first nontrivial order, be formulated as a Lagrangian EFT, we will postpone that to the end of the Section and discuss HTL quantities in a more intuitive way at first. It should also be mentioned that while the motivation to discuss HTLs in this Thesis arises largely from its usefulness at finite density, where the paradigm of dimensional reduction no longer applies, many of its applications as well as its historical development were largely motivated by the desire to perform analytical continuation of the imaginary-time formalism to Minkowskian space.

To build intuition, one should recall the discussion in the last paragraph of Sec. 2.6: We know that it is necessary to account for the IR divergences not associated with a lower-dimensional field theory by some means, for example resummation. However, energetic, hard, degrees of freedom require no resummation, and can be treated with standard perturbation theory, only the IR-sensitive soft degrees of freedom must be resummed. The resummed soft modes experience screening by the medium, effectively giving them a mass, and importantly, the screening is caused *by the hard modes*, with 'soft–soft' screening being suppressed. Alternatively, thinking in terms of Feynman diagrams, diagrams with external soft momenta are screened by interacting with loops with hard momenta. It is due to the appearance of such hard loop momenta that this effective treatment is often known as *Hard Thermal Loop* (HTL)-theory. At finite density, the term *Hard Dense Loop* (HDL) is occasionally used, but here the more common abbreviation HTL is used regardless of the setting.

As has been already noted for example in Sec. 2.6, as a massless boson the gluon is the most IR-sensitive field in QCD. It is due to this that soft gluons require careful resummation. While in the static limit

Figure 3.6: Resumming the propagator with self-energy insertions

of the imaginary-time formalism, quarks are protected in the IR by the πT-contribution in the odd Matsubara modes, this is no longer generally true after analytic continuation to real time. This is why soft quarks, those whose frequencies and momenta of $\mathcal{O}(g_s T, g_s \mu)$ after analytic continuation to real time, should in general be resummed in a similar way. Having said that, one should note that as chemical potential protects the quarks in the IR in any case, power-counting arguments can often be invoked to leave quarks unresummed in the cold dense regime. The resummation of quarks arises in a particularly natural way in the Lagrangian formulation, which is presented at the end of this Section. In this context, it appears as a separate term in the Lagrangian very analogous to that representing soft gluons.

In practice, the above description can be formulated as resumming soft propagators dressed with HTL self-energies, correcting the vertex functions containing soft fields appropriately, and addressing any remaining fields with naïve perturbation theory. As such, the first step is to resum the propagator. The standard procedure for this is to sum a geometric series of insertions of strongly connected (one-particle irreducible, or 1PI) self-energies Π, as seen in Fig. 3.6

$$G^{ab}_{\alpha\beta}(P) = \delta^{ab}\left(\frac{\mathbb{P}^T_{\alpha\beta}(P)}{P^2 + \Pi_T(P)} + \frac{\mathbb{P}^L_{\alpha\beta}(P)}{P^2 + \Pi_L(P)} + \xi\frac{P_\alpha P_\beta}{P^4}\right). \tag{3.9}$$

We now see conclusively why the soft fields must be resummed: The self-energy tensor is $\mathcal{O}(g_s^2)$ even for soft external momenta, while the bare propagators are of $1/P^2 = \mathcal{O}(g_s^{-2})$ in the soft regime. Hence, the powers of g_s cancel with the bare lines inserted next to the self-energy tensor. Thus, *each term* in the summation seen in Fig. 3.6 contributes starting at the same order. A posteriori, this can also seen from the resummed Eqn. (3.9): It cannot be expanded in small g_s when the momentum is soft.

Figure 3.7: One-loop gluon propagator

The tensor structure in Eqn. (3.9) is valid whenever Slavnov–Taylor identities (generalised Ward – Takahashi identities) enforcing transversality of the self-energy $\Pi^{\alpha\beta}P_\alpha = 0$ hold, as this leads to the decomposition given in Eqn. (2.25). The final term $\propto P^\alpha P^\beta$ is the only term not transverse with respect to the four-momenta, and due to the Slavnov–Taylor identity it is not modified beyond LO. The scalar-valued functions $\Pi_T(P), \Pi_L(P)$ are obtained by writing down the self-energy and projecting out the appropriate coefficient. In practice, the 1PI self-energy diagrams can usually be evaluated to only a fixed order. For (leading order) HTL-resummed QCD, the one-loop diagrams shown in Fig. 3.7 for the gluon propagator suffice. Since we are attempting to construct a theory for the limit of small external momentum P, the result simplifies from the complicated full one-loop result. In order to compute the limit, a useful trick is to expand differences $\|\mathbf{q} - \mathbf{p}\| \approx q - \mathbf{p}\cdot\mathbf{v}$, with $\mathbf{v} = \mathbf{q}/q$ being the velocities of the particles ´in the loops' [5]. The limit leads to a remarkable simplification, as the full $3+1$-dimensional (sum-)integral contributions to the self-energy factorise as follows:

1. a 'kinematic' part depending only on the four-dimensional angle $\Phi_P : \cot\Phi_P = p^0/p$ arising from the angular integral, and
2. an effective mass m_E, a momentum-independent part associated with the integrals F_2^0, B_2^0 found in Eqn. (2.22) and Eqn. (2.21) arising from the radial integral.

The derivation is particularly simple in the $T = 0$-limit, where only the first diagram of Fig. 3.7 contributes.

Explicitly,

$$\Pi_T(\Phi_P) = -\frac{m_E^2}{d-1}\csc^2\Phi_P\left[\int_{S^{d-1}}\Omega_{\mathbf{v}}\frac{ip_0}{P\cdot V} + \cos^2\Phi_P\right], \tag{3.10}$$

$$\Pi_L(\Phi_P) = m_E^2 \csc^2 \Phi_P \left[1 + \int\limits_{S^{d-1}} \Omega_{\mathbf{v}} \frac{ip_0}{P \cdot V}\right], \tag{3.11}$$

where we have introduced a light-like complex vector $V = (-i, \mathbf{v})$ with $\mathbf{v}$ a unit vector on $\mathbb{R}^d$, and write $\Omega_{\mathbf{v}}$ for the normalised angular measure on the sphere S^{d-1}: $\Omega_{\mathbf{v}}(S^{d-1}) = 1$. The integral can be performed explicitly and becomes simple in $d = 3$:

$$\begin{aligned}\int\limits_{S^{d-1}} \Omega_{\mathbf{v}} \frac{ip_0}{P \cdot V} &= \frac{\lambda(S^{d-2})}{\lambda(S^{d-1})} \int\limits_{-1}^{1} \mathrm{d}z (1-z^2)^{\frac{d-3}{2}} \frac{i\cos(\Phi_P)}{-i\cos(\Phi_P) + \sin(\Phi_P) z} \\ &= -{}_2F_1\Big(\frac{1}{2}, 1; \frac{d}{2}; -\tan^2\Phi_P\Big) \overset{d=3}{=} -\Phi_P \cot \Phi_P,\end{aligned} \tag{3.12}$$

where the very last equality requires $\Phi_P \in (0, \frac{\pi}{2})$ — for quantities such as the self-energy, this can be enforced due to reflection symmetry. The form of Eqn. (3.10) and Eqn. (3.11) shows that the leading contributions to $\Pi(P)$ are indeed $\mathcal{O}(g_s^2)$ even in the soft regime.

Generalisations of the integral in Eqn. (3.12) to other integrals with a single external momentum can be obtained in a straightforward manner with the same parametrisation at the expense of more complicated hypergeometric functions. A rather general case reads

$$\begin{aligned}\int\limits_{S^{d-1}} \Omega_{\mathbf{v}} \frac{(\mathbf{p}\cdot\mathbf{v})^n}{(P\cdot V)^m} = \frac{\Gamma(\frac{d}{2}) p^n}{2\sqrt{\pi}(-ip_0)^m} \Bigg[&(1 + (-1)^n) \frac{\Gamma(\frac{1+n}{2})}{\Gamma(\frac{d+n}{2})} \times \\ &\times {}_3F_2\Big(\frac{1+m}{2}, \frac{m}{2}, \frac{1+n}{2}, \frac{1}{2}, \frac{d+n}{2}; -\tan^2\Phi_P\Big) \\ &- im\tan\Phi_P (1 - (-1)^n) \frac{\Gamma(\frac{2+n}{2})}{\Gamma(\frac{d+n+1}{2})} \times \\ &\times {}_3F_2\Big(\frac{1+m}{2}, \frac{2+m}{2}, \frac{2+n}{2}, \frac{3}{2}, \frac{d+1+n}{2}; -\tan^2\Phi_P\Big)\Bigg].\end{aligned} \tag{3.13}$$

Such generalisations are useful in more complicated HTL calculations, including those involving the HTL vertices discussed later in this Section.

The effective mass appearing in Eqn. (3.11) and Eqn. (3.10) reads[57]

$$\begin{aligned} m_E^2 &= (d-1)g_s^2\Big((d-1)N_c B_2^0(T;d) - 2\sum_{i=1}^{N_f} F_2^0(T,\mu_i;d)\Big) \\ &\overset{d=3}{=} g_s^2\Big(\frac{N_c}{3}T^2 + \frac{N_f}{6}T^2 + \frac{1}{2\pi^2}\sum_{i=1}^{N_f}\mu_i^2\Big) \end{aligned} \tag{3.14}$$

and the self-energy is seen to obey the trace-identity

$$\delta_{\alpha\beta}\Pi^{\alpha\beta}(P) = (d-1)\Pi_T(P) + \Pi_L(P) = m_E^2 \tag{3.15}$$

in any dimension d. This confirms the sensibility of calling m_E an effective mass, as Eqn. (3.15) essentially generates the NLO dispersion relation of the gluons.

Note that the coefficients in Eqn. (3.10) & Eqn. (3.11) are given in Euclidean space — the often-seen Minkowskian version is immediately obtained by first moving back to the standard p^0, p-coordinates, and subsequently performing an analytic continuation to Minkowskian four-momenta. While the Debye screening mass is present in the limit of a vanishing zero-component of the momentum in both the Euclidean and the Minkowskian self-energies, in the latter one can also observe the existence of *plasma oscillations* in the limit of vanishing spatial momentum but finite (Minkowskian) frequency, giving a dispersion relation $\omega_p^2 = m_E^2/3$ for both the transverse and longitudinal components.

With the gluon propagator HTL-resummed, we next consider the vertex functions needed when the external momenta are not hard. They can be obtained in an identical fashion as limits of loop corrections to bare vertices in the limit of soft external momenta. Note, however, that they seemingly contain a 'truncated' one-loop correction in comparison to the resummed propagators. This is sufficient, as when any soft lines are already assumed to be fully resummed, further 1PI insertions would simply be absorbed into them. The expressions for the vertices are standard, and found in textbooks [151], but are typically written in Minkowski space; the Euclidean quantities shown here are from an upcoming work [152].

The three-gluon vertex, defined only for $R = -P - K$, reads

$$
\begin{aligned}
(\Gamma^{\mathrm{HTL}}_{AAA})^{\alpha\beta\gamma}_{abc}(P,K,R) &= igf^{abc}\left((\Gamma_{AAA})^{\alpha\beta\gamma}_{abc}(P,K,R) + m_E^2 T^{\alpha\beta\gamma}(P,K,R)\right),\\
T^{\alpha\beta\gamma}(P,K,R) &= \int\limits_{S^{d-1}} \Omega_{\mathbf{v}} \frac{V^\alpha V^\beta V^\gamma}{P\cdot V}\left[\frac{ik_0}{K\cdot V} - \frac{ir_0}{R\cdot V}\right].
\end{aligned}
\tag{3.16}
$$

For the four-gluon vertex, we consider only a special case relevant for two-loop resummed diagrams (NNNLO calculations in pQCD) with constrained external momenta and a partial contraction in colour indices:

$$
\begin{aligned}
\delta^{cd}(\Gamma^{\mathrm{HTL}}_{AAAA})^{\alpha\beta\gamma\delta}_{acdb}(P,K,-K,-P) &= (\Gamma_{AAAA})^{\alpha\beta\gamma\delta}_{acdb}(P,K,-K,-P)\delta^{cd}\\
&\quad - 2g_s^2 f^{cd}{}_a f_{cdb} m_E^2 T^{\alpha\beta\gamma\delta}(P,K,-K,-P),\\
T^{\alpha\beta\gamma\delta}(P,K,-K,-P) &= \int\limits_{S^{d-1}} \Omega_{\mathbf{v}} \frac{V^\alpha V^\beta V^\gamma V^\delta}{(P+K)\cdot V (P-K)\cdot V}\left[\frac{ik_0}{K\cdot V} - \frac{ip_0}{P\cdot V}\right].
\end{aligned}
\tag{3.17}
$$

In its full generality, the four-gluon vertex structure is considerably less compact. The bare vertices Γ_{AAA} and Γ_{AAAA} are found in Eqn. (1.21) and Eqn. (1.23). As already argued, the vertex corrections appear as linear corrections in m_E^2.

In addition, the form of the vertices can be related to the self-energy when considering an alternative representation for the HTL self-energy: We have

$$
\begin{aligned}
\Pi^{\alpha\beta}(P) &= \mathbb{P}_T^{\alpha\beta}(P)\Pi_T(P) + \mathbb{P}_L^{\alpha\beta}(P)\Pi_L(P)\\
&= m_E^2 \int \Omega_{\mathbf{v}} \left[\delta^{\alpha 0}\delta^{\beta 0} - V^\alpha V^\beta \frac{ip_0}{P\cdot V}\right].
\end{aligned}
\tag{3.18}
$$

However, unlike the coefficients of the self-energy, the angular integrals over $\mathbf{v}$-vectors generally admit no simple analytic evaluation for the integrals appearing in the vertices on their own.

Luckily, the vertex structures can often be simplified in practical calculations using various symmetry properties. We see immediately that the vertex corrections are symmetric tensors and traceless with respect to any pair of indices. It is likewise an easy check to see that the above four-gluon vertex is symmetric under permutations of the two arguments, and the three-gluon vertex is symmetric under *cyclic* permutations of its arguments.

The *modified Ward* (or Slavnov–Taylor) *identities* are a set of slightly more subtle, but perhaps even more useful identities obtained by contracting the three- and four-gluon vertices with four-momenta:

$$m_E^2 P_\alpha T^{\alpha\beta\gamma}(P,K,R) = \Pi^{\beta\gamma}(R) - \Pi^{\beta\gamma}(K), \tag{3.19}$$

$$2P_\alpha T^{\alpha\beta\gamma\delta}(P,K,-K,-P) = T^{\beta\gamma\delta}(K-P,P-K) - T^{\beta\gamma\delta}(-P-K,K,P), \tag{3.20}$$

with further identities obtained by repeated contractions and the symmetry properties. Relations such as the ones seen above result from the Slavnov–Taylor identities discussed in Sec. 2.5, generally speaking relating contracted n-point functions with $n-1$-point functions. They are a necessary condition for gauge invariance to remain in the HTL theory, and in fact an alternative way for constructing the HTLs follows by *requiring* the identities (and appropriate symmetries) and working backwards to obtain their form using the self-energy [147].

As a consequence of the relationship between the contracted vertices and the self-energies, fully contracted expressions can often be reduced to the analytically known HTL self-energy. For example, in the soft two-loop HTL pressure shown in Fig. 3.9, the only exceptions to this are the contraction of two three-gluon corrections with each other as well as a handful of terms containing the zero-components of the vertex corrections. This is an example of a situation where integrals of the form Eqn. (3.13) are useful to an extent, although generally speaking numerical methods will be necessary. With all first-order HTL corrections listed, it is also worth noting that they are all gauge-invariant [153].

To end this Section, we will briefly discuss alternative ways to construct the HTL theory. As hinted in the lede, HTLs can also be obtained

from an effective Lagrangian [154]. Constructed by assuming a structure containing the effective mass m_E^2 as well as two instances of the field-energy tensor F, symmetries such as gauge invariance, and the generation of gluonic HTL amplitudes, one has

$$\mathcal{L}_g = \frac{m_E^2}{2}\mathrm{Tr}\int\limits_{S^{d-1}} \Omega_{\mathbf{v}} F^{\alpha\beta}\frac{V^\beta V^\gamma}{(V\cdot D_A)^2}F^{\gamma\alpha}, \tag{3.21}$$

where D_A is the adjoint covariant derivative. An analogous improvement term can also be written down for quarks; it is

$$\mathcal{L}_q = m_q^2\int\limits_{S^{d-1}} \Omega_{\mathbf{v}}\overline{\psi}\frac{\not{V}}{(V\cdot D_F)}\psi, \tag{3.22}$$

with D_F now the derivative in the fundamental representation and m_q a mass parameter analogous to m_E reading $m_q^2 = d_A g_s^2(T^2+\mu^2/\pi^2)/8$ in $d=3$. This term will generate not only a resummed quark propagator as well as a HTL-corrected quark-gluon vertex, but also an effective vertex of two gluons and two quarks, not present in the unresummed theory.

The Lagrangian formalism is used particularly commonly in the HTL perturbation theory (HTLpt) approach to Hard Thermal Loops, serving as a way to completely reorganise perturbation theory in terms of the mass parameters. While not a first-principles method, it has shown significant improvements in certain convergence properties of the perturbative expansions, effectively resumming parts of the expansion.

A downside of the Lagrangian approach, and to an extent of HTLs in general, is the difficulty in extending it to higher orders. In standard Wilsonian EFTs, including the DR models discussed briefly in Sec. 2.7, extending the formalism to *higher-dimensional operators* suppressed by the scale is a standard procedure [155, 156, 157], even if it often makes computations considerably more cumbersome. However, for HTL this has only been achieved in certain special cases [158]. Even beyond the addition of such higher-dimensional opeartors, at finite μ one is able to add term directly proportional to μ that is *not* suppressed by any small scales [159]. The operator is odd under charge conjugation — hence the requirement for finite μ — and will not effect the computation of the free energy, but is nevertheless a leading-order term omitted from the standard HTL

Lagrangian. Lastly, the HTL Lagrangian terms also have a somewhat undesirable property: They are non-local, due to the D^{-1}-type operator.

There is yet another way to derive the HTL self-energy and, as a consequence of gauge invariance, the HTL vertex functions. This is to solve the non-Abelian equivalent of the Vlasov equations. While we will not cover this approach in detail (for that, see [160]), the result gives confidence that we have been doing something sensible: The Vlasov equations describe how particle distributions evolve in a plasma. If HTL theory arises as a solution to Vlasov equations for the soft modes, then it appears reasonable to say that we are indeed describing the medium effects to some approximation.

Generally speaking, HTL is the correct first-order approximation for the behaviour in the soft sector, with corrections arising both in the coupling as well as powers of the soft momenta. Due to the difficulty involved with these corrections, in calculations such as the NNNLO pressure of cold dense QCD most of the rest of this Introduction is dedicated to, it has turned out to be more beneficial to use one-loop HTL in higher-order diagrammatic calculations rather than higher-order HTL self-energies and vertices with possibly less complex diagrams. In such situations, power counting allows one to ensure that sufficient order in the expansion parameter is reached.

After reading this Thesis, or possibly already at this point, the astute reader will have noticed that half of its title is misleading — strictly speaking, Hard Thermal Loops appear in this introductory Part alone, not in any of the included Publications. However, the nearly-equivalent concept of hard *dense* loops is vital in [2], and in [3] the formalism and the machinery required for the relevant resummations draws inspiration from HTL computations.

As a last note to finish the Section, a reader interested in more detail is advised to read the classic review [161].

3.5 Logarithms of the Cold Dense Pressure

With the HTL theory developed in the previous Chapter as a way to properly account for the soft momenta, we are equipped to deal with the IR divergences discussed in Sec. 2.6. For simplicity, we focus on the physics

of cold and dense QCD for now, and are able to cure IR problems with HTL resummation of soft gluons. In this regime, we would not even be able to use dimensional reduction, as the theory has no three-dimensional effective sector. While we lack this simple effective description there is a simplification in that terms of fractional order in α_s are not generated in the perturbative small-coupling expansion of the pressure. Regardless, the pressure is *not* analytic, containing terms of $\mathcal{O}(g_s^k \ln^m g_s)$. The logarithmic terms, particularly the *leading logarithm* at each order, can be extracted in a considerably easier way than the corresponding full perturbative order by observing their sources with some care.

To begin with, recall that any logarithms must arise from *ratios* of physical scales. However, in the $T = 0$ theory, there are only two scales: The soft scale $\mathcal{O}(g_s\mu)$,which can be described with using HTL, and the hard scale $\mathcal{O}(\mu)$ associated with the naïve diagrammatic expansion. Notably, there is no analogue to the ultrasoft scale: Since pure gauge terms vanish as scale-free at $T = 0$, leading contributions to the pressure at each scale are given by $\Omega_L \sim \int_{\mathbf{p}} p n_F(p)$ instead. As we saw in Sec. 2.6, the fermionic distribution function is constant at small arguments, rather than (divergent and) dynamically dependent on the momentum. As such a would-be ultrasoft scale $g_s^2\mu$ (or any smaller scales) does not exist. In addition, logarithms originate from interpolating integrals containing terms of the form $\int_{\Lambda_{\mathrm{UV}}}^{\Lambda_{\mathrm{IR}}} \mathrm{d}P/P = \ln(\Lambda_{\mathrm{UV}}/\Lambda_{\mathrm{IR}})$. Additionally, these must be bosonic: Corresponding integrals with fermionic momenta are protected in the IR by the chemical potentials, and will not give rise to a logarithm of the coupling. However, for bosonic momenta we obtain precisely the logarithm we are looking for when the effective cutoffs $\Lambda_{\mathrm{UV}} = \mathcal{O}(\mu)$ and $\Lambda_{\mathrm{IR}} = \mathcal{O}(g_s\mu)$, as now the integral goes as $-\ln(g_s) + \mathcal{O}(1)$. We call the momenta P that lie in this interpolating domain $g_s\mu < P < \mu$ *semisoft*, following [2].

Next, we observe that the semisoft momenta have special and useful properties from the point of view of resummation. They are softer than hard momenta, and thus cannot be described entirely by the same order of naïve perturbation theory as the corresponding hard momenta. As they are not hard, their interactions with the medium must be accounted for, in this case using the HTL prescription. At the same time their scales are greater than that of the effective HTL mass $m_E \propto g_s\mu$ — the defin-

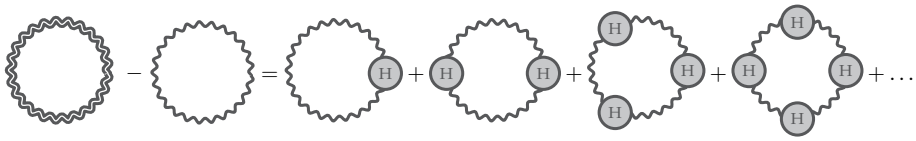

Figure 3.8: Gluonic ring-sum: Source of $\mathcal{O}(g_s^4 \ln g_s)$

ing scale of soft momenta — which in practical calculations means that expressions such as the HTL-resummed propagator of Eqn. (3.9) can be *expanded* to finite loop order.

While such expanded integrals would normally vanish in dimensional regularisation, in the computation of the logarithms they are assigned a finite value due to the cutoff procedure described in the above paragraph: In order to obtain the combination of resummed-but-expanded momenta, we have already restricted ourselves to the specific momentum regime of semisoft momenta, and are able to set the cutoffs. In particular any logarithms can be extracted by picking the terms of the expansion containing $\int \mathrm{d}^4P/P^4$ for P a semisoft momentum.

Now, the method to extract the N^kLO — k orders beyond LO — leading logarithm is straightforward. From simple power-counting, one sees that at this order, the appropriate soft contributions are given by the set of $k-1$-loop HTL-resummed (and vertex-corrected) QCD diagrams: They contribute at $\mathcal{O}(g_s^{2k} \ln^n g_s)$. The nonanalytic contributions can be examined by looking at the resummed and/or HTL-corrected gluonic quantities. The maximal number of logarithms arises when *each* of the $k-1$ loop momenta flowing in the resummed $k-1$-loop yields a logarithm. Hence, the leading logarithm is $\mathcal{O}(g_s^{2k} \ln^{k-1} g_s)$, and given by extracting only the parts of the resummed but expanded diagrams containing terms of the form $\int \mathrm{d}^4P/P^4$ are included, with each loop momentum being semisoft.

For $k = 1$, this results in the well-known *gluonic ring sum* shown in Fig. 3.8, which has been vacuum-subtracted, and with the shaded blobs indicating self-energy insertions that we are able to HTL-approximate. The ring sum can be written out in a simple way using the results of the previous Section — note in particular that the trace in what follows is

extraordinarily simple in Feynman gauge:

$$\begin{aligned}\Omega^{\text{HTL ring}} &= -\frac{1}{2}\sum_{n\in\mathbb{N}_+}\frac{(-1)^n}{n}\int_P \operatorname{Tr}\Big[\Pi_{\text{HTL}}(P)G_0(P)\Big]^n \\ &= -\frac{d_A}{2}\sum_{n\in\mathbb{N}_+}\frac{(-1)^n}{n}\int_P\Big[(d-1)\Big(\frac{\Pi_T(P)}{P^2}\Big)^n+\Big(\frac{\Pi_L(P)}{P^2}\Big)^n\Big] \\ &= \frac{d_A}{2}\int_P\Big[(d-1)\ln\Big(1+\frac{\Pi_T(P)}{P^2}\Big)+\ln\Big(1+\frac{\Pi_L(P)}{P^2}\Big)\Big].\end{aligned} \tag{3.23}$$

Above, Π_{HTL} denotes the HTL self-energy and G_0 the bare propagator with $\xi = 1$.

If we want to only extract the logarithmic term, the full resummation is not even necessary: Identifying the logarithm as a scale-free integral $\int \mathrm{d}P P^{-1}$ in the semisoft region, we obtain it in $d = 3$ dimensions as

$$\Omega_{\text{QCD}}^{\text{NNLO},\ln g_s} = \Omega^{\text{HTL ring}}|_{\ln g_s} = -\frac{d_A}{4}\int_P\frac{2\Pi_T^2(P)+\Pi_L^2(P)}{P^4} = \frac{d_A}{(8\pi)^2}m_E^4\ln g_s. \tag{3.24}$$

The integral over $2\Pi_T^2+\Pi_L^2$ is not entirely trivial, but gives a remarkably simple result. Here, it is worth emphasising that this is indeed the complete logarithmic $\mathcal{O}(g_s^4\ln g_s)$ term at zero temperature. While the term has been known for a long time [132, 133, 134], the first computations were cumbersome and made use of the full one-loop self-energy, instead of the HTL self-energy sufficient for studying the soft momenta contributing to this term. Indeed, it is only due to the development of the HTL theory that a simpler computation became possible [162].

For $k = 2$, the HTL diagrams contributing to logarithmic terms at NNNLO are shown in Fig. 3.9, with the shaded gluonic vertices being HTL-corrected. Starting with the leading logarithm, we can immediately discard the second diagram, as it does not have enough dimensionless integrals, and cannot contribute to the leading logarithm. Regardless, the ghost-diagram must be included: While unresummed, the ghost lines can still contribute appropriate logarithm-generating integrals $\int \mathrm{d}^4P/P^4$.

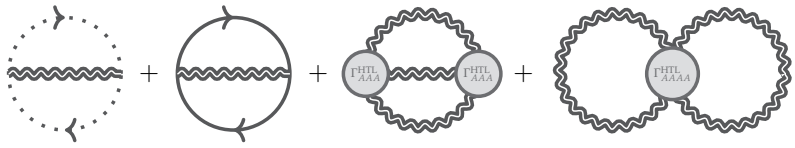

Figure 3.9: Two-loop resummed HTL diagrams: Source of $\mathcal{O}(g_s^6 \ln^2 g_s)$, $\mathcal{O}(g_s^6 \ln g_s)$

The observation that only semisoft lines contribute logarithms simplifies matters considerably, and together with dimensional analysis — the logarithmic terms of the pressure must have a coefficient of m_E^4 in front of them, as this is the only dimensionful parameter — we may expand the lines analogously to Eqn. (3.24), obtaining the diagrams of Fig. 3.10. The last step required to compute the leading logarithm is to observe that the terms contributing to it must be *well-separated* in order for two logarithms to be produced. While conceptually identical, the vertex structures in particular cause the computation to become technically considerably more involved than the NNLO equivalent. One may make use of existing literature on HTL perturbation theory [163, 164] to extract the necessary components and perform the computation, which was the method used in [2]. The result is, again, remarkably simple, and reads

$$\Omega_{\mathrm{QCD}}^{\mathrm{NNNLO},\ln^2 g_s} = \Omega^{2-\text{loop HTL}}\big|_{\ln^2 g_s} = \frac{N_c d_A}{(4\pi)^4}\frac{11}{24} g_s^2 m_E^4 \ln^2 g_s. \tag{3.25}$$

Adding this term to the known $\mathcal{O}(g^4)$ pressure shows only a small change, shown in Fig 2. of [2], indicating that the asymptotic expansion is still under control at NNNLO[2].

Regardless of the method, the intermediate steps are, despite being straightforward, somewhat lengthy, and we omit them here. In the process one can also see that not all of the a priori expected expanded diagrams of Fig. 3.10 contribute: Importantly, the rather nontrivial term with two HTL-vertex corrections turns out to contain no leading logarithms.

[2]We choose to use this abbreviation following [2]. On occasion, one encounters *LL* for 'leading log' in similar contexts instead.

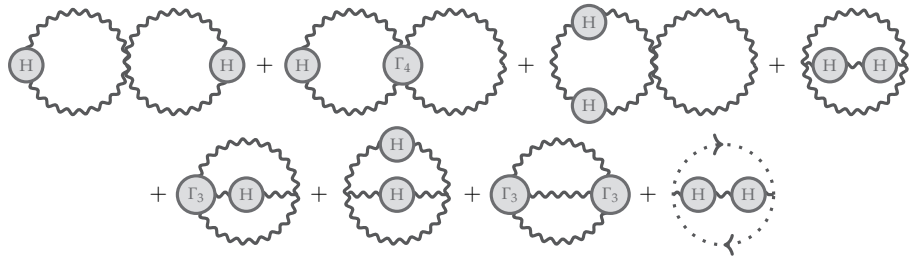

Figure 3.10: UV expansion of Fig. 3.9: Source of $\mathcal{O}(g_s^6 \ln^2 g_s)$

In addition, a rather interesting point was observed in [2]: For the leading logarithm, it suffices to replace the complicated structure of the HTL self-energy with their on-shell limits. This corresponds to setting $\Pi_T \to m_E^2/2$, $\Pi_L \to 0$, and matches with the particle content of the theory, leaving two massive transverse polarisations and one massless longitudinal polarisation. While this is currently at the level of a conjecture, it explains the simplicity of the results of integrals such as Eqn. (3.24).

To end the discussion of this Section, we note that while the expression given here were computed in a fixed gauge, the logarithmic terms are independent parts of the expansion of the pressure, and must therefore be gauge-invariant. In the NNLO case it is straightforward to confirm that the ξ-parameter drops out, and for the NNNLO case the two-loop HTL pressure has been explicitly confirmed to be gauge invariant [163].

Chapter 4

Summary and Outlook

We are nearing the end of the introductory Part, and at this point it is worth briefly reviewing what has been achieved. Over the course of the past three Chapters, we have introduced a number of tools required to understand the thermal properties of the theory of strong interactions, Quantum Chromodynamics, in an equilibrium setting. These have ranged from very fundamental matters such as the concept of gauge theories to more refined constructions, for example the HTL theory used to understand the behaviour of low-energy modes in gauge theories.

The original research performed for this Thesis largely focussed on pQCD in a cold, dense setting. Some basic methods of complex analysis applied to thermal field theory were explained and a set of zero-temperature, finite-density cutting rules making use of them was introduced. The derivation, based on [1], and its implications were discussed in Sec. 2.9. The rules aim to simplify high-order calculations by reducing them to integrals over vacuum n-point functions. This bridges the somewhat considerable gap between the much-studied vacuum Feynman integrals and likewise well-developed tools of finite-temperature Feynman sum-integrals compared to the methods used at zero temperature but finite density.

The cold dense regime of QCD was the main focus of the penultimate Chapter of the introductory Part. Especially significant was the introduction of an effective HTL resummation description of the soft degrees of freedom in Sec. 3.4, needed to properly account for the IR problems in-

nate to thermal field theories. Together with a novel method for extracting nonanalytic logarithmic terms in the weak-coupling expansion of the pressure it is possible to obtain the first NNNLO coefficient in the expansion of the cold dense pressure, reviewed in Sec. 3.5 and first obtained in [2].

In addition to the study cold dense physics, there was a short foray into studying strongly coupled theories. In Sec. 2.10 we covered why certain QFTs — in particular, certain CFTs in $2+1$ dimensions — are quite extraordinary: They are well-defined at any scales without a need for renormalisation. Furthermore, taking the large-N limit, one is able to evaluate many quantities of interest in such theories at *any* values of the coupling. Seemingly different from the main focus, such studies still make use of resummation methods akin to the HTL theory. Notably, this required neither holography nor lattice simulations, which are the commonly encountered frameworks for studying theories at strong coupling. While we briefly covered some results for a number of theories, the most central feature was QED in $2+1$ dimensions at large-N_f, the focus of the included Publication [3].

4.1 Future Work

We now turn our eyes to the future. Our understanding of any part of physics is rarely if ever truly complete and the topics covered here are no exception.

A better understanding of strongly coupled field theories, especially without relying on numerical lattice methods, is one of the major goals of current theoretical physics. As such, any progress towards it is important. The hope is that methods similar to those used to understand $2+1$-dimensional QED could be applied to at least slightly more realistic and physical models or at least used to gain insight on them.

In the realm of cold and dense matter, it would be interesting if methods from QCD such as the cutting rules or an analogy of HTL could be applied to other theories. Even within QCD, neutron stars remain poorly understood. As an example, the study of transport coefficients is a possible future research direction, requiring deviation from the in-equilibrium imaginary-time formalism used in this Thesis. In addition, going beyond

the cold approximation has practical uses. While this has been studied to some extent in the context of neutron stars relevant for cold dense matter [162], an improved understanding of temperature effects would be particularly beneficial now, as gravitational wave measurements from collisions involving neutron stars have become a reality.

It should also also be emphasised that not only does the identification of logarithms as discussed in Sec. 3.5 work at arbitrary orders, in general at $T = 0$ perturbation theory suffers from no known fundamental obstacles such as the Linde problem in Sec. 2.6. Hence, (resummed) perturbation theory requires no nonperturbative input at *any order*, as long as the corrections to the associated asymptotic series remain small, and computing further corrections is a sensible course of action in the future. In particular, computing leading logarithms in the way discussed earlier is a relatively straightforward matter.

Having said that, for now the most obvious continuation of the research carried out for this Thesis is completing the NNNLO evaluation of the cold dense pressure. The identification of logarithms as scale-free semisoft integrals paves way for the computation of more complicated logarithmic terms, and starting at NNNLO one must also compute *subleading* logarithms, which is currently being worked on [152].

To finish the introduction, we will go over the remaining steps required to compute the complete NNNLO pressure. Before elaborating what the computation of subleading logarithms actually entails, we observe that the process discussed so far essentially corresponds to writing down the IR theory at appropriate order, and taking its UV limit in order to obtain the description at semisoft momenta. At NNNLO, this is of course nothing but the expansion of Fig. 3.10. However, one could in principle also take the opposite limit, starting from the UV theory and bringing it to its IR limit, which at NNNLO would correspond to considering the IR divergences of the IR sensitive subset of four-loop diagrams.

For subleading logarithms, only a subset of the loop momenta must be semisoft: As many as there are to be logarithms. This means that the remaining momenta can be anything else: soft, semisoft or hard, and because the descriptions for the two are distinct, they must be considered separately.

To elucidate, consider the first subleading logarithm, the $\mathcal{O}(g_s^6 \ln g_s)$-

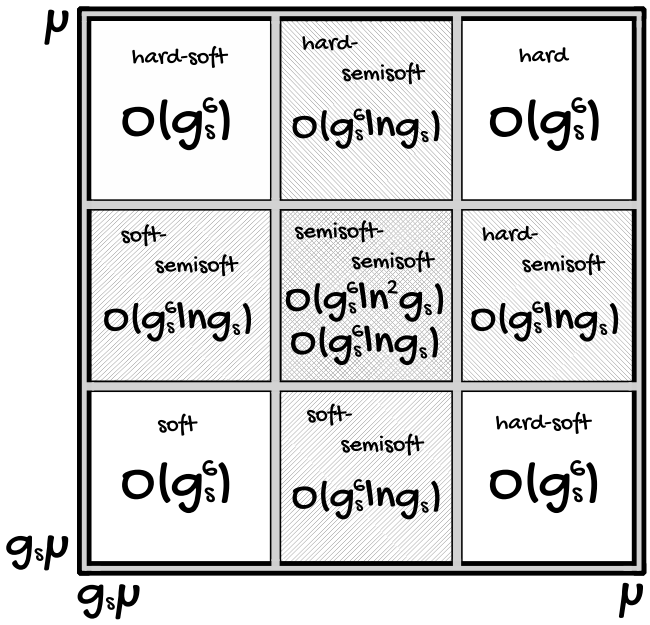

Figure 4.1: Momentum regions contributing to the NNNLO pressure

term appearing at NNNLO. The regions contributing at this order, and in particular to the logarithms, are shown in Fig. 4.1, and we see three distinct contributions:

1. *Hard-semisoft* logarithms, arising from the three-loop diagrams of Fig. 3.4 after adding a single resummed and expanded semisoft gluonic line,

2. *Soft-semisoft* logarithms, arising from the two-loop HTL diagrams of Fig. 3.9 after setting one of the loop momenta semisoft and expanding appropriate lines,

3. *Semisoft-semisoft* logarithms, arising from the same terms of Fig. 3.10 as the double logarithm, but as a subleading contribution of terms that are *not* well-separated.

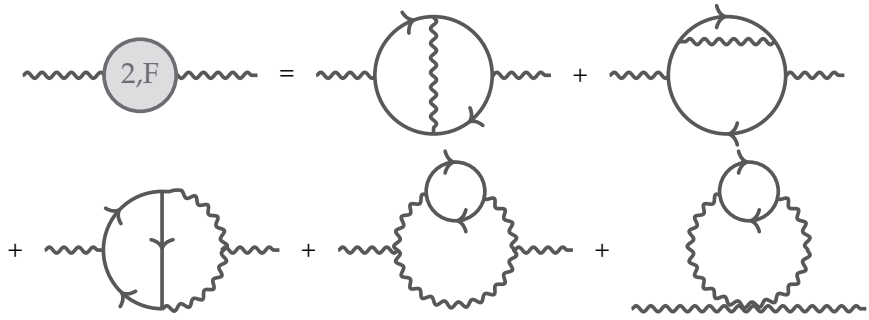

Figure 4.2: Fermionic contributions to the two-loop gluon self-energy

The first contribution can be obtained by treating the semisoft lines as before, leading to the computation of the HTL limit of the (fermionic part of the) two-loop gluon self-energy shown in Fig. 4.2, or alternatively to the computation of modified vacuum two-loop integrals after extracting the logarithmic contributions.

The second and last contributions can, at least using the 'UV limit of the soft theory' description used in [2] and Sec. 3.5, be obtained in a relatively straightforward manner by again extracting the logarithmic integrals and computing the remaining integrals — although with the latter using numerics becomes inevitable.

In addition to the logarithms, one can of course also compute the analytic $\mathcal{O}(g_s^6)$ contributions to the pressure. Again, these involve multiple sources:

1. The soft contributions arise from the two-loop HTL diagrams of Fig. 3.9 without expanding, and after removing the logarithmic divergences,

2. The hard contributions arise from naïve four-loop perturbative diagrams.

The former are currently being worked on alongside with the logarithmic contributions. Computing full four-loop diagrams required for the latter seems like a daunting prospect at the time of writing, but there is

hope that novel techniques for evaluating high-order diagrams — such as the zero-temperature cutting rules — might open up the possibility of performing these calculations.

Bibliography

[1] I. Ghisoiu, T. Gorda, A. Kurkela, P. Romatschke, S. Säppi, and A. Vuorinen, "On high-order perturbative calculations at finite density," *Nucl. Phys. B*, vol. 915, pp. 102–118, 2017.

[2] T. Gorda, A. Kurkela, P. Romatschke, S. Säppi, and A. Vuorinen, "Next-to-Next-to-Next-to-Leading Order Pressure of Cold Quark Matter: Leading Logarithm," *Phys. Rev. Lett.*, vol. 121, no. 20, p. 202701, 2018.

[3] P. Romatschke and S. Säppi, "Thermal free energy of large Nf QED in 2+1 dimensions from weak to strong coupling," *Phys. Rev. D*, vol. 100, p. 073009, 2019.

[4] J. Baez and J. Muniain, *Gauge Fields, Knots and Gravity*. 7 1995.

[5] M. Laine and A. Vuorinen, *Basics of Thermal Field Theory*, vol. 925. Springer, 2016.

[6] C.-N. Yang and R. L. Mills, "Conservation of Isotopic Spin and Isotopic Gauge Invariance," *Phys. Rev.*, vol. 96, pp. 191–195, 1954.

[7] R. Aldrovandi and J. Pereira, "Existence of Lagrangians for the Yang-Mills Equations," *Rept. Math. Phys.*, vol. 26, p. 237, 1988.

[8] B. Ioffe, "Axial anomaly: The Modern status," *Int. J. Mod. Phys. A*, vol. 21, pp. 6249–6266, 2006.

[9] B. Graner, Y. Chen, E. Lindahl, and B. Heckel, "Reduced Limit on the Permanent Electric Dipole Moment of Hg199," *Phys. Rev. Lett.*,

vol. 116, no. 16, p. 161601, 2016. [Erratum: Phys.Rev.Lett. 119, 119901 (2017)].

[10] P. Fileviez Perez and H. H. Patel, "The Electroweak Vacuum Angle," *Phys. Lett. B*, vol. 732, pp. 241–243, 2014.

[11] J. E. Kim and G. Carosi, "Axions and the Strong CP Problem," *Rev. Mod. Phys.*, vol. 82, pp. 557–602, 2010. [Erratum: Rev.Mod.Phys. 91, 049902 (2019)].

[12] E. Rutherford, "Collision of α particles with light atoms. IV. An anomalous effect in nitrogen," *Phil. Mag.*, vol. 90, no. sup1, pp. 31–37, 2010.

[13] J. Chadwick, "Possible Existence of a Neutron," *Nature*, vol. 129, p. 312, 1932.

[14] J. Chadwick, "The Existence of a Neutron," *Proc. Roy. Soc. Lond. A*, vol. A136, no. 830, pp. 692–708, 1932.

[15] C. Lattes, H. Muirhead, G. Occhialini, and C. Powell, "PROCESSES INVOLVING CHARGED MESONS," *Nature*, vol. 159, pp. 694–697, 1947.

[16] G. Rochester and C. Butler, "Evidence for the Existence of New Unstable Elementary Particles," *Nature*, vol. 160, pp. 855–857, 1947.

[17] V. D. Hopper and S. Biswas, "Evidence concerning the existence of the new unstable elementary neutral particle," *Phys. Rev.*, vol. 80, pp. 1099–1100, Dec 1950.

[18] H. Anderson, E. Fermi, E. Long, and D. Nagle, "Total Cross-sections of Positive Pions in Hydrogen," *Phys. Rev.*, vol. 85, p. 936, 1952.

[19] Y. Ne'eman, "Derivation of strong interactions from a gauge invariance," *Nucl. Phys.*, vol. 26, pp. 222–229, 1961.

[20] M. Gell-Mann, "The Eightfold Way: A Theory of strong interaction symmetry," 3 1961.

[21] M. Gell-Mann, "A Schematic Model of Baryons and Mesons," *Phys. Lett.*, vol. 8, pp. 214–215, 1964.

[22] G. Zweig, "An SU(3) model for strong interaction symmetry and its breaking. Version 1," 1 1964.

[23] J. Joyce, *Finnegan's Wake*. Faber and Faber, 1939.

[24] S. Glashow, J. Iliopoulos, and L. Maiani, "Weak Interactions with Lepton-Hadron Symmetry," *Phys. Rev. D*, vol. 2, pp. 1285–1292, 1970.

[25] J. Aubert *et al.*, "Experimental Observation of a Heavy Particle J," *Phys. Rev. Lett.*, vol. 33, pp. 1404–1406, 1974.

[26] J. Augustin *et al.*, "Discovery of a Narrow Resonance in e^+e^- Annihilation," *Phys. Rev. Lett.*, vol. 33, pp. 1406–1408, 1974.

[27] M. Kobayashi and T. Maskawa, "CP Violation in the Renormalizable Theory of Weak Interaction," *Prog. Theor. Phys.*, vol. 49, pp. 652–657, 1973.

[28] S. Herb *et al.*, "Observation of a Dimuon Resonance at 9.5-GeV in 400-GeV Proton-Nucleus Collisions," *Phys. Rev. Lett.*, vol. 39, pp. 252–255, 1977.

[29] S. Abachi *et al.*, "Observation of the top quark," *Phys. Rev. Lett.*, vol. 74, pp. 2632–2637, 1995.

[30] F. Abe *et al.*, "Observation of top quark production in $\bar{p}p$ collisions," *Phys. Rev. Lett.*, vol. 74, pp. 2626–2631, 1995.

[31] M. Tanabashi *et al.*, "Review of particle physics," *Phys. Rev. D*, vol. 98, p. 030001, Aug 2018.

[32] D. J. Gross and F. Wilczek, "Ultraviolet Behavior of Nonabelian Gauge Theories," *Phys. Rev. Lett.*, vol. 30, pp. 1343–1346, 1973.

[33] H. Politzer, "Reliable Perturbative Results for Strong Interactions?," *Phys. Rev. Lett.*, vol. 30, pp. 1346–1349, 1973.

[34] E. D. Bloom *et al.*, "High-Energy Inelastic e-p Scattering at 6-Degrees and 10-Degrees," *Phys. Rev. Lett.*, vol. 23, pp. 930–934, 1969.

[35] J. Ellis, "The Discovery of the Gluon," *Int.J.Mod.Phys.A*, vol. 29, no. 31, p. 1430072, 2015.

[36] U. W. Heinz and M. Jacob, "Evidence for a new state of matter: An Assessment of the results from the CERN lead beam program," Jan. 2000. arXiv:nucl-th/0002042.

[37] G. S. Bali, "QCD forces and heavy quark bound states," *Phys. Rept.*, vol. 343, pp. 1–136, 2001.

[38] K. D. Lane, "An Introduction to technicolor," in *Theoretical Advanced Study Institute (TASI 93) in Elementary Particle Physics: The Building Blocks of Creation - From Microfermius to Megaparsecs*, pp. 381–408, 6 1993.

[39] W. de Boer, "Grand unified theories and supersymmetry in particle physics and cosmology," *Prog. Part. Nucl. Phys.*, vol. 33, pp. 201–302, 1994.

[40] N. Ukita *et al.*, "Light hadron spectrum with 2+1 flavor dynamical O(a)-improved Wilson quarks," *PoS*, vol. LATTICE2007, p. 138, 2007.

[41] N. Cabibbo and G. Parisi, "Exponential Hadronic Spectrum and Quark Liberation," *Phys. Lett. B*, vol. 59, pp. 67–69, 1975.

[42] J. C. Collins and M. Perry, "Superdense Matter: Neutrons Or Asymptotically Free Quarks?," *Phys. Rev. Lett.*, vol. 34, p. 1353, 1975.

[43] J. Zinn-Justin, *Quantum Field Theory and Critical Phenomena; 4th ed.* Internat. Ser. Mono. Phys., Oxford: Clarendon Press, 2002.

[44] M. E. Peskin and D. V. Schroeder, *An Introduction to quantum field theory*. Reading, USA: Addison-Wesley, 1995.

[45] L. Faddeev and V. Popov, "Feynman Diagrams for the Yang-Mills Field," *Phys. Lett. B*, vol. 25, pp. 29–30, 1967.

[46] S. Pokorski, *Gauge Field Theories*. Cambridge Monographs on Mathematical Physics, Cambridge University Press, 2 ed., 2000.

[47] N. Vandersickel and D. Zwanziger, "The Gribov problem and QCD dynamics," *Phys. Rept.*, vol. 520, pp. 175–251, 2012.

[48] G. Wick, "The Evaluation of the Collision Matrix," *Phys. Rev.*, vol. 80, pp. 268–272, 1950.

[49] F. Herzog, B. Ruijl, T. Ueda, J. Vermaseren, and A. Vogt, "The five-loop beta function of Yang-Mills theory with fermions," *JHEP*, vol. 02, p. 090, 2017.

[50] S. Narison, *QCD as a Theory of Hadrons: From Partons to Confinement*, vol. 17. Cambridge University Press, 7 2007.

[51] T. Matsubara, "A New approach to quantum statistical mechanics," *Prog. Theor. Phys.*, vol. 14, pp. 351–378, 1955.

[52] R. Kubo, "Statistical mechanical theory of irreversible processes. 1. General theory and simple applications in magnetic and conduction problems," *J. Phys. Soc. Jap.*, vol. 12, pp. 570–586, 1957.

[53] P. C. Martin and J. S. Schwinger, "Theory of many particle systems. 1.," *Phys. Rev.*, vol. 115, pp. 1342–1373, 1959.

[54] E. A. Calzetta and B.-L. B. Hu, *Nonequilibrium Quantum Field Theory*. Cambridge Monographs on Mathematical Physics, Cambridge University Press, 9 2008.

[55] J. Berges, "Introduction to nonequilibrium quantum field theory," *AIP Conf. Proc.*, vol. 739, no. 1, pp. 3–62, 2004.

[56] J. Ghiglieri, A. Kurkela, M. Strickland, and A. Vuorinen, "Perturbative Thermal QCD: Formalism and Applications," Feb 2020. arXiv:hep-ph/2002.10188.

[57] J. Kapusta and C. Gale, *Finite-temperature field theory: Principles and applications*. Cambridge Monographs on Mathematical Physics, Cambridge University Press, 2006.

[58] A. Vuorinen, "The Pressure of QCD at finite temperatures and chemical potentials," *Phys. Rev. D*, vol. 68, p. 054017, 2003.

[59] F. Dyson, "Divergence of perturbation theory in quantum electrodynamics," *Phys. Rev.*, vol. 85, pp. 631–632, 1952.

[60] L. Lipatov, "Divergence of the Perturbation Theory Series and the Quasiclassical Theory," *Sov. Phys. JETP*, vol. 45, pp. 216–223, 1977.

[61] A. D. Linde, "Infrared Problem in Thermodynamics of the Yang-Mills Gas," *Phys. Lett. B*, vol. 96, pp. 289–292, 1980.

[62] D. J. Gross, R. D. Pisarski, and L. G. Yaffe, "QCD and Instantons at Finite Temperature," *Rev. Mod. Phys.*, vol. 53, p. 43, 1981.

[63] P. H. Ginsparg, "First Order and Second Order Phase Transitions in Gauge Theories at Finite Temperature," *Nucl. Phys. B*, vol. 170, pp. 388–408, 1980.

[64] T. Appelquist and R. D. Pisarski, "High-Temperature Yang-Mills Theories and Three-Dimensional Quantum Chromodynamics," *Phys. Rev. D*, vol. 23, p. 2305, 1981.

[65] A. N. Jourjine, "Quantum Field Theory in Infinite Temperature Limit," *Annals Phys.*, vol. 155, p. 305, 1984.

[66] A. Hietanen, K. Kajantie, M. Laine, K. Rummukainen, and Y. Schroder, "Plaquette expectation value and gluon condensate in three dimensions," *JHEP*, vol. 01, p. 013, 2005.

[67] A. Hietanen, K. Kajantie, M. Laine, K. Rummukainen, and Y. Schroder, "Non-perturbative plaquette in 3-D pure SU(3)," *PoS*, vol. LAT2005, p. 174, 2006.

[68] F. Di Renzo, M. Laine, V. Miccio, Y. Schroder, and C. Torrero, "The Leading non-perturbative coefficient in the weak-coupling expansion of hot QCD pressure," *JHEP*, vol. 07, p. 026, 2006.

[69] J.-P. Blaizot, E. Iancu, and R. R. Parwani, "On the screening of static electromagnetic fields in hot QED plasmas," *Phys. Rev. D*, vol. 52, pp. 2543–2562, 1995.

[70] T. Holstein, R. Norton, and P. Pincus, "de Haas-van Alphen Effect and the Specific Heat of an Electron Gas," *Phys. Rev. B*, vol. 8, pp. 2649–2656, 1973.

[71] A. Gerhold, A. Ipp, and A. Rebhan, "Non-Fermi-liquid specific heat of normal degenerate quark matter," *Phys. Rev. D*, vol. 70, p. 105015, 2004.

[72] A. Gerhold and A. Rebhan, "Fermionic dispersion relations in ultradegenerate relativistic plasmas beyond leading logarithmic order," *Phys. Rev. D*, vol. 71, p. 085010, 2005.

[73] M. Creutz, *Quarks, gluons and lattices*. Cambridge Monographs on Mathematical Physics, Cambridge, UK: Cambridge Univ. Press, 6 1985.

[74] C. Gattringer and C. B. Lang, *Quantum chromodynamics on the lattice*, vol. 788. Berlin: Springer, 2010.

[75] Z. Fodor and S. Katz, "A New method to study lattice QCD at finite temperature and chemical potential," *Phys. Lett. B*, vol. 534, pp. 87–92, 2002.

[76] P. de Forcrand and O. Philipsen, "The QCD phase diagram for small densities from imaginary chemical potential," *Nucl. Phys. B*, vol. 642, pp. 290–306, 2002.

[77] R. Bellwied, S. Borsanyi, Z. Fodor, J. Günther, S. Katz, C. Ratti, and K. Szabo, "The QCD phase diagram from analytic continuation," *Phys. Lett. B*, vol. 751, pp. 559–564, 2015.

[78] C. Allton, S. Ejiri, S. Hands, O. Kaczmarek, F. Karsch, E. Laermann, C. Schmidt, and L. Scorzato, "The QCD thermal phase transition in the presence of a small chemical potential," *Phys. Rev. D*, vol. 66, p. 074507, 2002.

[79] S. Sharma, "The QCD Equation of state and critical end-point estimates at $\mathcal{O}(\mu_B^6)$," *Nucl. Phys. A*, vol. 967, pp. 728–731, 2017.

[80] G. Parisi, "ON COMPLEX PROBABILITIES," *Phys. Lett. B*, vol. 131, pp. 393–395, 1983.

[81] G. Aarts, L. Bongiovanni, E. Seiler, D. Sexty, and I.-O. Stamatescu, "Controlling complex Langevin dynamics at finite density," *Eur. Phys. J. A*, vol. 49, p. 89, 2013.

[82] D. Sexty, "Simulating full QCD at nonzero density using the complex Langevin equation," *Phys. Lett. B*, vol. 729, pp. 108–111, 2014.

[83] E. Witten, "Analytic Continuation Of Chern-Simons Theory," *AMS/IP Stud. Adv. Math.*, vol. 50, pp. 347–446, 2011.

[84] M. Cristoforetti, F. Di Renzo, A. Mukherjee, and L. Scorzato, "Monte Carlo simulations on the Lefschetz thimble: Taming the sign problem," *Phys. Rev. D*, vol. 88, no. 5, p. 051501, 2013.

[85] A. Kurkela, P. Romatschke, and A. Vuorinen, "Cold Quark Matter," *Phys. Rev. D*, vol. 81, p. 105021, 2010.

[86] S. Borsanyi, Z. Fodor, C. Hoelbling, S. D. Katz, S. Krieg, and K. K. Szabo, "Full result for the QCD equation of state with 2+1 flavors," *Phys. Lett. B*, vol. 730, pp. 99–104, 2014.

[87] P. Steinbrecher, "The QCD crossover at zero and non-zero baryon densities from Lattice QCD," *Nucl. Phys. A*, vol. 982, pp. 847–850, 2019.

[88] J. M. Maldacena, "The Large N limit of superconformal field theories and supergravity," *Int. J. Theor. Phys.*, vol. 38, pp. 1113–1133, 1999.

[89] M. Ammon and J. Erdmenger, *Gauge/gravity duality: Foundations and applications*. Cambridge: Cambridge University Press, 4 2015.

[90] R. D. Pisarski, "Chiral Symmetry Breaking in Three-Dimensional Electrodynamics," *Phys. Rev. D*, vol. 29, p. 2423, 1984.

[91] G. D. Moore, "Pressure of hot QCD at large N(f)," *JHEP*, vol. 10, p. 055, 2002.

[92] A. Ipp, G. D. Moore, and A. Rebhan, "Comment on and erratum to 'Pressure of hot QCD at large N(f)'," *JHEP*, vol. 01, p. 037, 2003.

[93] A. Ipp and A. Rebhan, "Thermodynamics of large N(f) QCD at finite chemical potential," *JHEP*, vol. 06, p. 032, 2003.

[94] P. Romatschke, "Finite-Temperature Conformal Field Theory Results for All Couplings: O(N) Model in 2+1 Dimensions," *Phys. Rev. Lett.*, vol. 122, no. 23, p. 231603, 2019. [Erratum: Phys.Rev.Lett. 123, 209901 (2019)].

[95] P. Romatschke, "Simple non-perturbative resummation schemes beyond mean-field: case study for scalar ϕ^4 theory in 1+1 dimensions," *JHEP*, vol. 03, p. 149, 2019.

[96] P. Romatschke, "Simple non-perturbative resummation schemes beyond mean-field II: thermodynamics of scalar ϕ^4 theory in 1+1 dimensions at arbitrary coupling," *Mod. Phys. Lett. A*, vol. 35, no. 09, p. 2050054, 2020.

[97] S. S. Gubser, I. R. Klebanov, and A. A. Tseytlin, "Coupling constant dependence in the thermodynamics of N=4 supersymmetric Yang-Mills theory," *Nucl. Phys. B*, vol. 534, pp. 202–222, 1998.

[98] I. Drummond, R. Horgan, P. Landshoff, and A. Rebhan, "Foam diagram summation at finite temperature," *Nucl. Phys. B*, vol. 524, pp. 579–600, 1998.

[99] S. Sachdev, "Polylogarithm identities in a conformal field theory in three-dimensions," *Phys. Lett. B*, vol. 309, pp. 285–288, 1993.

[100] P. Romatschke, "Fractional Degrees of Freedom at Infinite Coupling in Large Nf QED in 2+1 Dimensions," *Phys. Rev. Lett.*, vol. 123, no. 24, p. 241602, 2019.

[101] K. Rajagopal, "Mapping the QCD phase diagram," *Nucl. Phys. A*, vol. 661, pp. 150–161, 1999.

[102] Z. Fodor, M. Giordano, J. N. Günther, K. Kapás, S. D. Katz, A. Pásztor, I. Portillo, C. Ratti, D. Sexty, and K. K. Szabó, "Trying to constrain the location of the QCD critical endpoint with lattice simulations," *Nucl. Phys. A*, vol. 982, pp. 843–846, 2019.

[103] S. Chattopdhyay, "Physics at high baryon density at FAIR," *J. Phys. G*, vol. 35, p. 104027, 2008.

[104] D. Tlusty, "The RHIC Beam Energy Scan Phase II: Physics and Upgrades," in *13th Conference on the Intersections of Particle and Nuclear Physics*, 10 2018.

[105] J. Elliott, P. Lake, L. Moretto, and L. Phair, "Determination of the coexistence curve, critical temperature, density, and pressure of bulk nuclear matter from fragment emission data," 2013.

[106] M. G. Alford, K. Rajagopal, and F. Wilczek, "Color flavor locking and chiral symmetry breaking in high density QCD," *Nucl. Phys. B*, vol. 537, pp. 443–458, 1999.

[107] M. G. Alford, A. Schmitt, K. Rajagopal, and T. Schäfer, "Color superconductivity in dense quark matter," *Rev. Mod. Phys.*, vol. 80, pp. 1455–1515, 2008.

[108] A. J. Mizher, M. Chernodub, and E. S. Fraga, "Phase diagram of hot QCD in an external magnetic field: possible splitting of deconfinement and chiral transitions," *Phys. Rev. D*, vol. 82, p. 105016, 2010.

[109] L. McLerran and R. D. Pisarski, "Phases of cold, dense quarks at large N(c)," *Nucl. Phys. A*, vol. 796, pp. 83–100, 2007.

[110] J. M. Pawlowski, "Aspects of the functional renormalisation group," *Annals Phys.*, vol. 322, pp. 2831–2915, 2007.

[111] C. Hoyos, D. Rodríguez Fernández, N. Jokela, and A. Vuorinen, "Holographic quark matter and neutron stars," *Phys. Rev. Lett.*, vol. 117, no. 3, p. 032501, 2016.

[112] N. Jokela, M. Järvinen, and J. Remes, "Holographic QCD in the Veneziano limit and neutron stars," *JHEP*, vol. 03, p. 041, 2019.

[113] M. Drews and W. Weise, "Functional renormalization group studies of nuclear and neutron matter," *Prog. Part. Nucl. Phys.*, vol. 93, pp. 69–107, 2017.

[114] M. Leonhardt, M. Pospiech, B. Schallmo, J. Braun, C. Drischler, K. Hebeler, and A. Schwenk, "Symmetric nuclear matter from the strong interaction," Jul 2019. arXiv:nucl-th/1907.05814.

[115] D. Boyanovsky, H. de Vega, and D. Schwarz, "Phase transitions in the early and the present universe," *Ann. Rev. Nucl. Part. Sci.*, vol. 56, pp. 441–500, 2006.

[116] T. Ludlam and S. Aronson, "Hunting the quark gluon plasma," Apr 2005. BNL Report BNL-73847-2005.

[117] R. C. Tolman, "On the Weight of Heat and Thermal Equilibrium in General Relativity," *Phys. Rev.*, vol. 35, pp. 904–924, 1930.

[118] J. Oppenheimer and G. Volkoff, "On Massive neutron cores," *Phys. Rev.*, vol. 55, pp. 374–381, 1939.

[119] R. C. Tolman, "Static solutions of Einstein's field equations for spheres of fluid," *Phys. Rev.*, vol. 55, pp. 364–373, 1939.

[120] E. Annala, T. Gorda, A. Kurkela, and A. Vuorinen, "Gravitational-wave constraints on the neutron-star-matter Equation of State," *Phys. Rev. Lett.*, vol. 120, no. 17, p. 172703, 2018.

[121] E. Annala, T. Gorda, A. Kurkela, J. Nättilä, and A. Vuorinen, "Constraining the properties of neutron-star matter with observations," *Mem. Soc. Ast. It.*, vol. 90, no. 1-2, p. 81, 2019.

[122] E. Annala, T. Gorda, A. Kurkela, J. Nättilä, and A. Vuorinen, "Evidence for quark-matter cores in massive neutron stars," *Nature Phys.*, 2020.

[123] H. Heiselberg, "Color superconducting quark matter in neutron stars," Dec 1999. arXiv:hep-ph/9912419.

[124] P. B. Demorest, T. Pennucci, S. Ransom, M. Roberts, and J. Hessels, "A two-solar-mass neutron star measured using shapiro delay," *nature*, vol. 467, no. 7319, pp. 1081–1083, 2010.

[125] C. D. Capano, I. Tews, S. M. Brown, B. Margalit, S. De, S. Kumar, D. A. Brown, B. Krishnan, and S. Reddy, "Stringent constraints on neutron-star radii from multimessenger observations and nuclear theory," *Nature Astron.*, vol. 4, no. 6, pp. 625–632, 2020.

[126] B. Abbott *et al.*, "GW170817: Measurements of neutron star radii and equation of state," *Phys. Rev. Lett.*, vol. 121, no. 16, p. 161101, 2018.

[127] O. Y. Gnedin, D. G. Yakovlev, and A. Y. Potekhin, "Thermal relaxation in young neutron stars," *Mon. Not. Roy. Astron. Soc.*, vol. 324, p. 725, 2001.

[128] M. G. Alford and S. P. Harris, "Beta equilibrium in neutron star mergers," *Phys. Rev. C*, vol. 98, no. 6, p. 065806, 2018.

[129] J. I. Kapusta, "Quantum Chromodynamics at High Temperature," *Nucl. Phys. B*, vol. 148, pp. 461–498, 1979.

[130] E. Braaten and A. Nieto, "Free energy of QCD at high temperature," *Phys. Rev. D*, vol. 53, pp. 3421–3437, 1996.

[131] K. Kajantie, M. Laine, K. Rummukainen, and M. E. Shaposhnikov, "Generic rules for high temperature dimensional reduction and their application to the standard model," *Nucl. Phys. B*, vol. 458, pp. 90–136, 1996.

[132] B. A. Freedman and L. D. McLerran, "Fermions and Gauge Vector Mesons at Finite Temperature and Density. 1. Formal Techniques," *Phys. Rev. D*, vol. 16, p. 1130, 1977.

[133] B. A. Freedman and L. D. McLerran, "Fermions and Gauge Vector Mesons at Finite Temperature and Density. 2. The Ground State Energy of a Relativistic electron Gas," *Phys. Rev. D*, vol. 16, p. 1147, 1977.

[134] B. A. Freedman and L. D. McLerran, "Fermions and Gauge Vector Mesons at Finite Temperature and Density. 3. The Ground State Energy of a Relativistic Quark Gas," *Phys. Rev. D*, vol. 16, p. 1169, 1977.

[135] T. Toimela, "The Next Term in the Thermodynamic Potential of QCD," *Phys. Lett. B*, vol. 124, pp. 407–409, 1983.

[136] P. B. Arnold and C.-X. Zhai, "The Three loop free energy for pure gauge QCD," *Phys. Rev. D*, vol. 50, pp. 7603–7623, 1994.

[137] P. B. Arnold and C.-X. Zhai, "The Three loop free energy for high temperature QED and QCD with fermions," *Phys. Rev. D*, vol. 51, pp. 1906–1918, 1995.

[138] C.-x. Zhai and B. M. Kastening, "The Free energy of hot gauge theories with fermions through g**5," *Phys. Rev. D*, vol. 52, pp. 7232–7246, 1995.

[139] K. Kajantie, M. Laine, K. Rummukainen, and Y. Schroder, "The Pressure of hot QCD up to g6 ln(1/g)," *Phys. Rev. D*, vol. 67, p. 105008, 2003.

[140] M. Laine and Y. Schroder, "Quark mass thresholds in QCD thermodynamics," *Phys. Rev. D*, vol. 73, p. 085009, 2006.

[141] J. Blaizot, E. Iancu, and A. Rebhan, "On the apparent convergence of perturbative QCD at high temperature," *Phys. Rev. D*, vol. 68, p. 025011, 2003.

[142] M. Strickland, J. O. Andersen, A. Bandyopadhyay, N. Haque, M. G. Mustafa, and N. Su, "Three loop HTL perturbation theory at finite temperature and chemical potential," *Nucl. Phys. A*, vol. 931, pp. 841–845, 2014.

[143] S. Mogliacci, J. O. Andersen, M. Strickland, N. Su, and A. Vuorinen, "Equation of State of hot and dense QCD: Resummed perturbation theory confronts lattice data," *JHEP*, vol. 12, p. 055, 2013.

[144] P. C. Argyres and M. Unsal, "The semi-classical expansion and resurgence in gauge theories: new perturbative, instanton, bion, and renormalon effects," *JHEP*, vol. 08, p. 063, 2012.

[145] R. D. Pisarski, "Scattering Amplitudes in Hot Gauge Theories," *Phys. Rev. Lett.*, vol. 63, p. 1129, 1989.

[146] E. Braaten and R. D. Pisarski, "Soft Amplitudes in Hot Gauge Theories: A General Analysis," *Nucl. Phys. B*, vol. 337, pp. 569–634, 1990.

[147] E. Braaten and R. D. Pisarski, "Deducing Hard Thermal Loops From Ward Identities," *Nucl. Phys. B*, vol. 339, pp. 310–324, 1990.

[148] J. Frenkel and J. Taylor, "High Temperature Limit of Thermal QCD," *Nucl. Phys. B*, vol. 334, pp. 199–216, 1990.

[149] J. Taylor and S. Wong, "The Effective Action of Hard Thermal Loops in QCD," *Nucl. Phys. B*, vol. 346, pp. 115–128, 1990.

[150] J. Frenkel and J. Taylor, "Hard thermal QCD, forward scattering and effective actions," *Nucl. Phys. B*, vol. 374, pp. 156–168, 1992.

[151] M. L. Bellac, *Thermal Field Theory*. Cambridge Monographs on Mathematical Physics, Cambridge University Press, 3 2011.

[152] T. Gorda, A. Kurkela, R. Paatelainen, S. Säppi, and A. Vuorinen, "In Preparation," 2020.

[153] A. Rebhan, "Thermal gauge field theories," *Lect. Notes Phys.*, vol. 583, pp. 161–208, 2002.

[154] E. Braaten and R. D. Pisarski, "Simple effective Lagrangian for hard thermal loops," *Phys. Rev. D*, vol. 45, no. 6, p. 1827, 1992.

[155] S. Chapman, "A New dimensionally reduced effective action for QCD at high temperature," *Phys. Rev. D*, vol. 50, pp. 5308–5313, 1994.

[156] A. Hietanen, K. Kajantie, M. Laine, K. Rummukainen, and Y. Schroder, "Three-dimensional physics and the pressure of hot QCD," *Phys. Rev. D*, vol. 79, p. 045018, 2009.

[157] M. Laine, P. Schicho, and Y. Schröder, "Soft thermal contributions to 3-loop gauge coupling," *JHEP*, vol. 05, p. 037, 2018.

[158] S. Carignano, M. E. Carrington, and J. Soto, "The HTL Lagrangian at NLO: the photon case," *Phys. Lett. B*, vol. 801, p. 135193, 2020.

[159] D. Bodeker and M. Laine, "Finite baryon density effects on gauge field dynamics," *JHEP*, vol. 09, p. 029, 2001.

[160] D. F. Litim and C. Manuel, "Semiclassical transport theory for non-Abelian plasmas," *Phys. Rept.*, vol. 364, pp. 451–539, 2002.

[161] J.-P. Blaizot and E. Iancu, "The Quark gluon plasma: Collective dynamics and hard thermal loops," *Phys. Rept.*, vol. 359, pp. 355–528, 2002.

[162] A. Kurkela and A. Vuorinen, "Cool quark matter," *Phys. Rev. Lett.*, vol. 117, no. 4, p. 042501, 2016.

[163] J. O. Andersen, E. Petitgirard, and M. Strickland, "Two loop HTL thermodynamics with quarks," *Phys. Rev. D*, vol. 70, p. 045001, 2004.

[164] J. O. Andersen, E. Braaten, E. Petitgirard, and M. Strickland, "HTL perturbation theory to two loops," *Phys. Rev. D*, vol. 66, p. 085016, 2002.